MASSACHUSETTS GENERAL HOSPITAL

HARVARD MEDICAL SCHOOL

Brain Circuitries in Basic and Clinical Neuroscience

Seventh International Conference on Creative Content Technologies, ComputerWorld 2015, March 24, 2015 - Nice, France

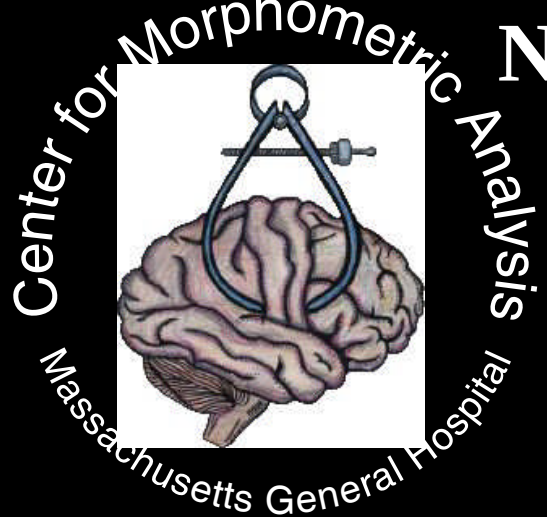

Nikos Makris, M.D., Ph.D.

Center for Morphometric Analysis

Departments of Psychiatry and Neurology

Massachusetts General Hospital

Harvard Medical School

Disclosures of Potential Conflicts

Source	Consultant	Advisory Board	Stock or Equity >$10,000	Speakers' Bureau	**Research Support**	Honorarium for this talk or meeting	Expenses related to this talk or meeting
NIA-NIMH (RO1) (Aging)					**X**		
MGH-MAC Core (Multiple Projects)					**X**		
NIH (R21) (Neurodegeneration-FTD)					**X**		
NIH (R21) (Neurodegeneration-FTD and ALS)					**X**		
NIH (R21) (Modeling Deep Brain Stimulation and MRI safety)					**X**		
Departmental					**X**		

Center for Morphometric Analysis (CMA)-MGH collaborating PIs

Marek Kubicki, M.D., Ph.D. (BWH/HMS)
Bradford Dickerson, M.D. (MGH/HMS)
Giorgio Bonmassar, Ph.D. (MGH/HMS)
Jill Goldstein, Ph.D. (BWH/HMS)
Larry Seidman, Ph.D.(BIDMC/MMHC/HMS)
Gordon Harris, Ph.D. (MGH/HMS)
Scott Rauch, M.D. (McLean/HMS)
Scott Lukas, Ph.D. (McLean/HMS)
Joseph Biederman, M.D. (MGH/HMS)
Marlene Oscar-Berman, Ph.D.(BUSM)
Deepak Pandya, M.D. (BUSM)
Douglas Rosene, Ph.D. (BUSM)
Martha Shenton, Ph.D. (BWH/HMS)
David Kennedy, Ph.D.(UMassMS)
David Caplan, M.D., Ph.D. (MGH/HMS)
Bruce Rosen, M.D., Ph.D. (MGH/HMS)
Helen Grant, M.D., Ph.D.(Children's//HMS)
Hans Breiter, M.D.(NWU)
Anne Blood, Ph.D. (MGH/HMS)

Harvard Medical School affiliated Hospitals

Massachusetts General Hospital (MGH)
Brigham and Women's Hospital (BWH)
McLean Hospital
Beth Israel Deaconess Medical Center (BIDMC)
Mass Mental Health Center (MMHC)
Children's Hospital

Center for Morphometric Analysis (CMA)-MGH Core

Nikos Makris, M.D., Ph.D. (Director)
Verne Caviness, M.D., Ph.D. (Founding Director)
George Papadimitriou, B.Sc. (Computer Science)
Lichen Liang, Ph.D. (MRI Engineering, Modeling)
Takeshi Takahashi, M.D., Ph.D. (Functional Conn.)
Isaac Ng, B.A. (RA)
Anni Zhu, B.A. (RA)
Yeetzou Kao (RA)

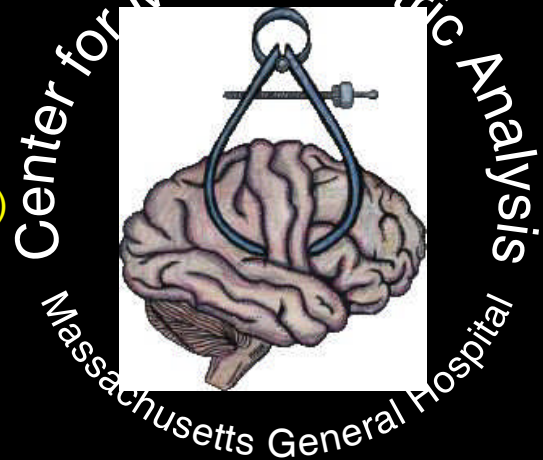

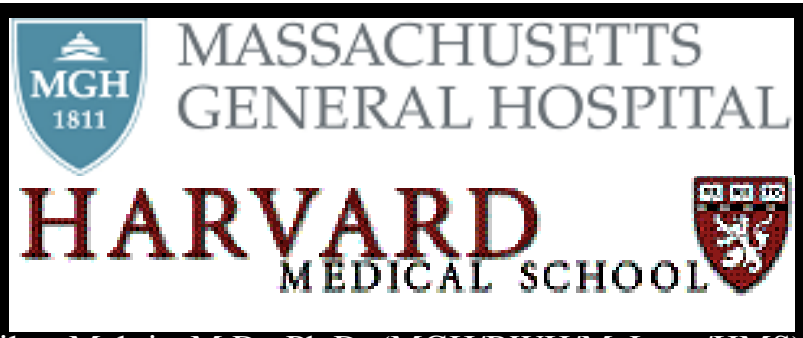


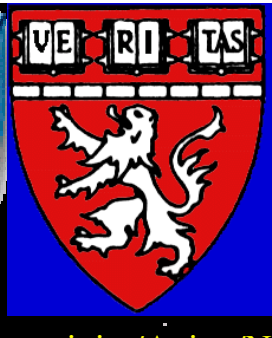

Nikos Makris, M.D., Ph.D. (MGH/BWH/McLean/HMS)	**Brain** Connectivity/Aging/Neurodegeneration/Addiction/ADHD/Stroke/ITD
Verne Caviness, M.D., Ph.D. (MGH/HMS)	Brain Development/Laptop Imaging Technology Development/Stroke
Marek Kubicki, M.D., Ph.D. (BWH/HMS)	Schizophrenia/Imaging Technology Development/Aging/Brain Connectivity
Bradford Dickerson, M.D. (MGH/HMS)	Neurodegeneration/Aging/ITD/Brain Connectivity
Giorgio Bonmassar, Ph.D. (MGH/HMS)	Technology Development/MRI Safety/Deep Brain Stimulation
Jill Goldstein, Ph.D. (BWH/HMS)	Stress Response/Sexual Dimorphisms/Aging/MDD/Schizophrenia
Larry Seidman, Ph.D.(BIDMC/MMHC/HMS)	Schizophrenia/MDD/BPD/ADHD/Resting State Brain Connectivity
Gordon Harris, Ph.D. (MGH/HMS)	3D Imaging Visualizations Technology Development/Alcohol Dependence
Scott Rauch, M.D. (McLean/HMS)	OCD/PTSD/Anxiety Disorder/Psychosurgery
Scott Lukas, Ph.D. (McLean/HMS)	Nicotine Dependence/Alcohol Dependence
Joseph Biederman, M.D. (MGH/HMS)	Attention Deficit/Hyperactivity Disorder (ADHD)/Bipolar Disorder (BPD)
Marlene Oscar-Berman, Ph.D.(BUSM)	Alcohol Dependence
Deepak Pandya, M.D. (BUSM)	Brain Connectivity
Douglas Rosene, Ph.D. (BUSM)	Aging in the Rhesus Monkey/Monkey Brain Connectivity
Martha Shenton, Ph.D. (BWH/HMS)	Traumatic Brain Injury/Imaging Technology Development
David Kennedy, Ph.D.(UMassMS)	Neuroinformatics/Imaging Databasing
David Caplan, M.D., Ph.D. (MGH/HMS)	Stroke/Aphasia Research
Bruce Rosen, M.D., Ph.D. (MGH/HMS)	Imaging Technology Development (ITD)/Program in Acupuncture Research
Helen Grant, M.D., Ph.D.(Children's//HMS)	Brain Development
Hans Breiter, M.D.(NWU)	Cocaine Dependence
Anne Blood, Ph.D. (MGH/HMS)	Dystonia Research

Some discoveries are breakthroughs in knowledge and others in technology

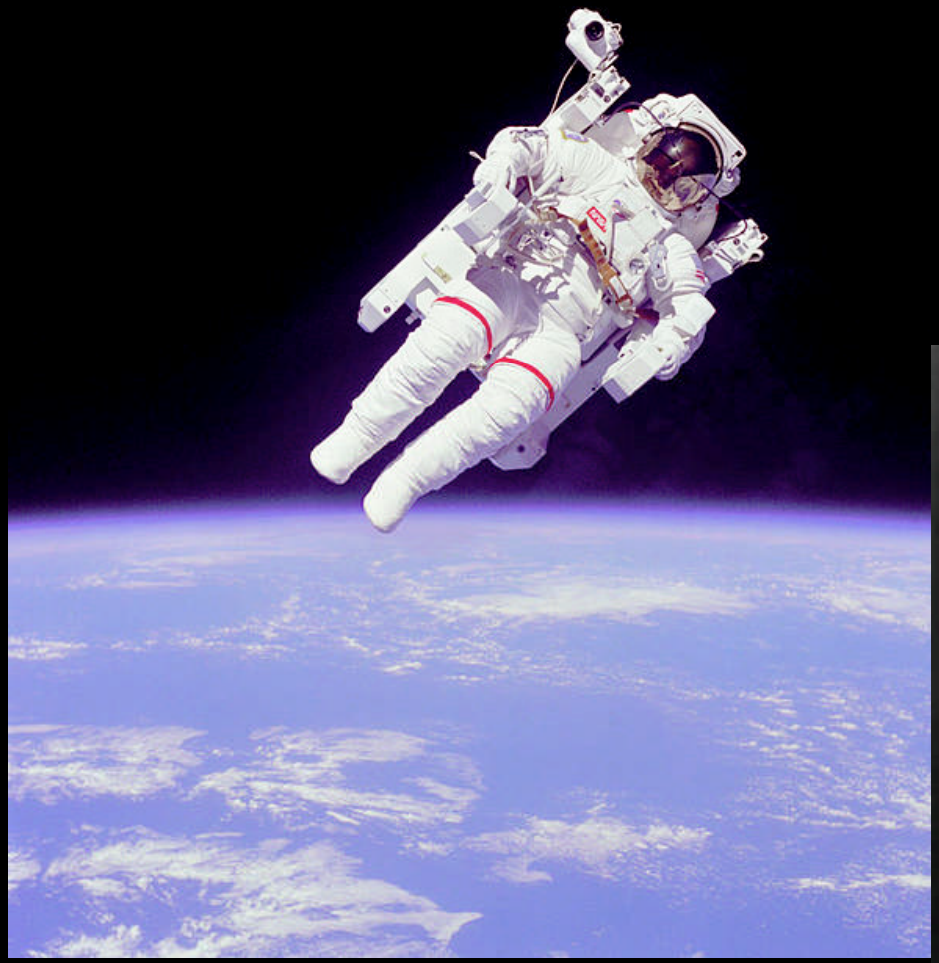

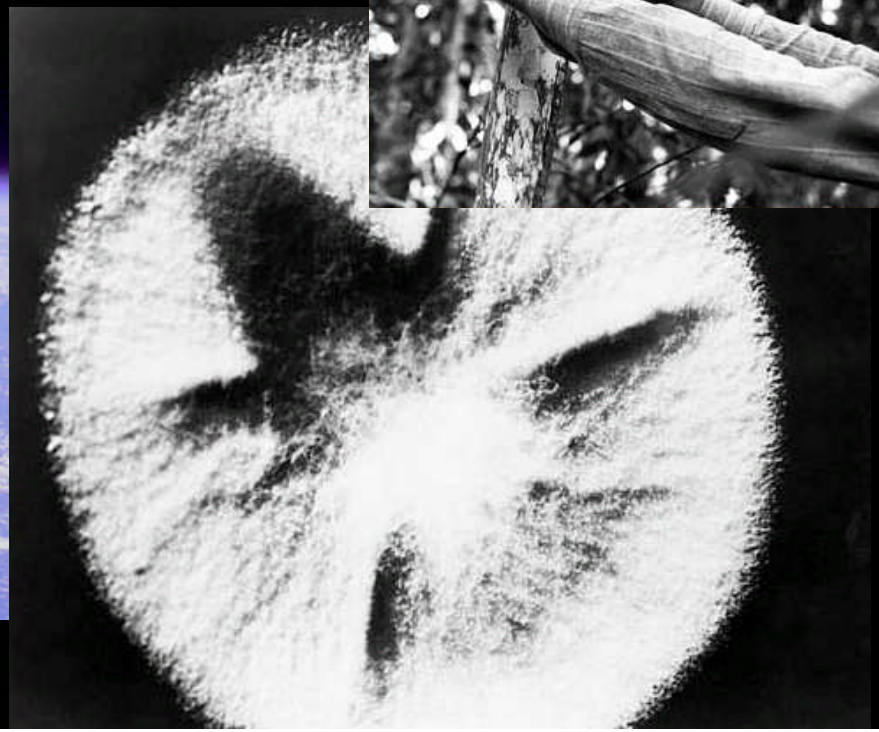

Importance of Technology in Scientific Discovery

(Hypothesis: Great Tools to see lead to Great Discoveries)

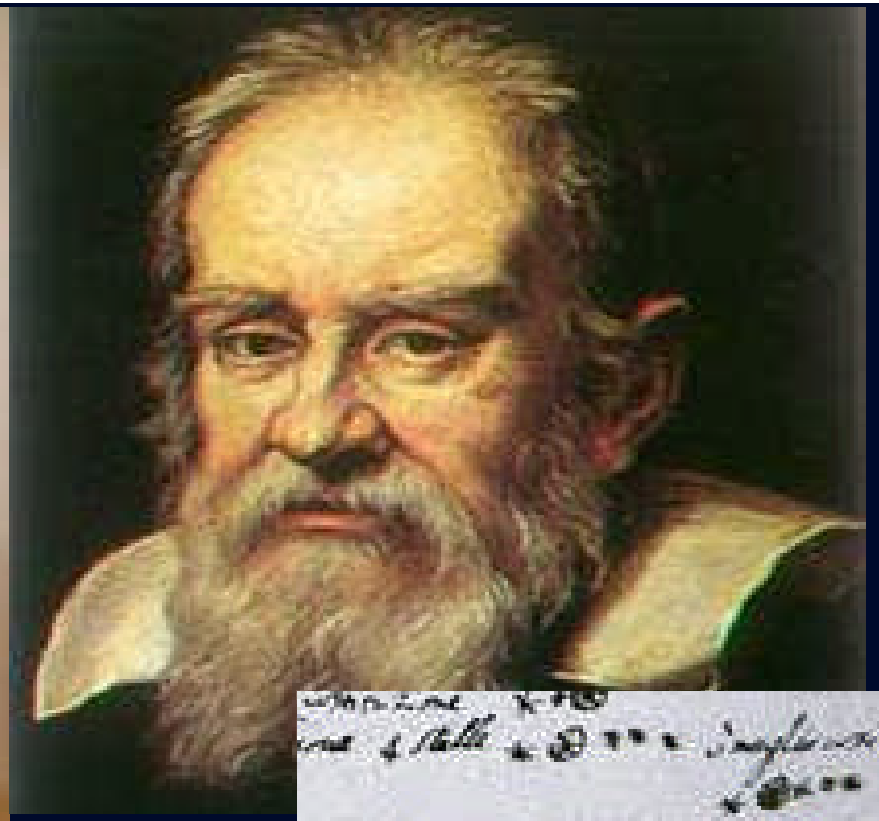

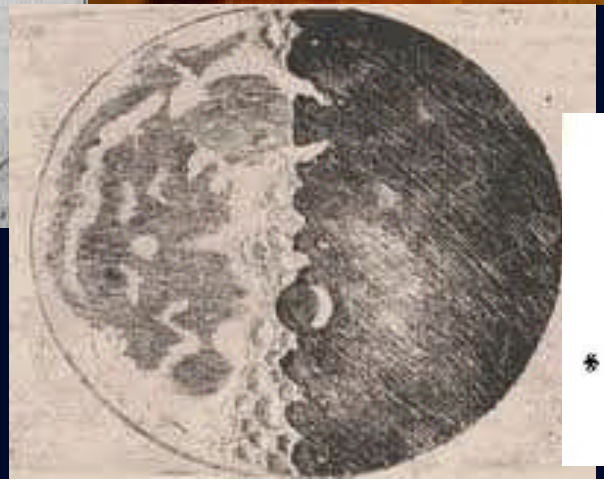

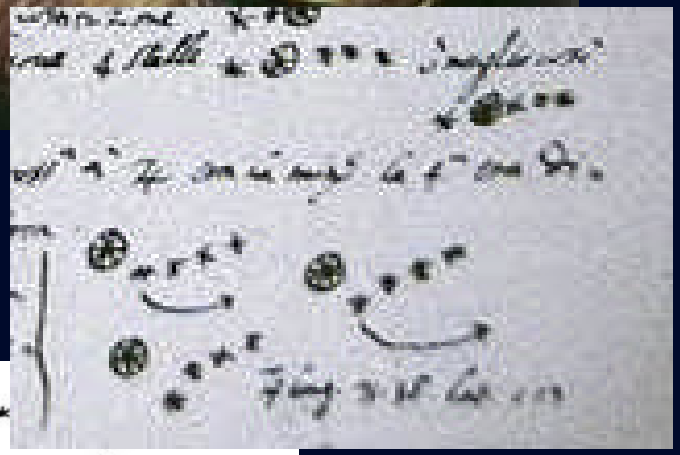

Courtesy of Dr. Bruce Rosen

Importance of Technology in Medicine and Neuroscience

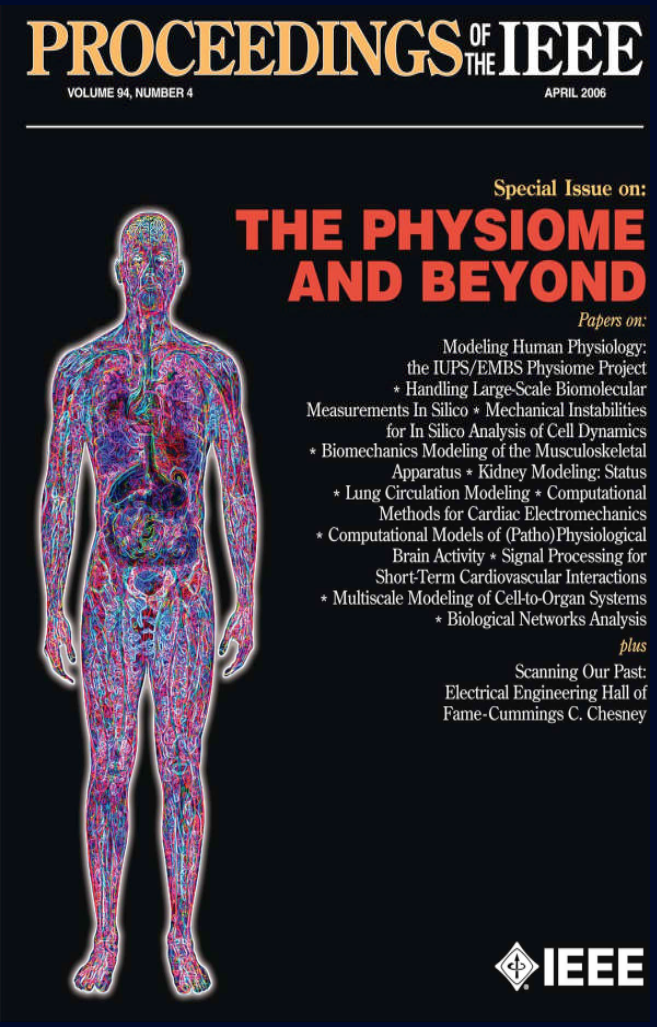

That our understating of the human brain has advanced more in the last two decades than in the rest of human history is a well-known fact.

This seems to be a consequence of **key technological discoveries** as has occurred in other fields of science in the course of history.

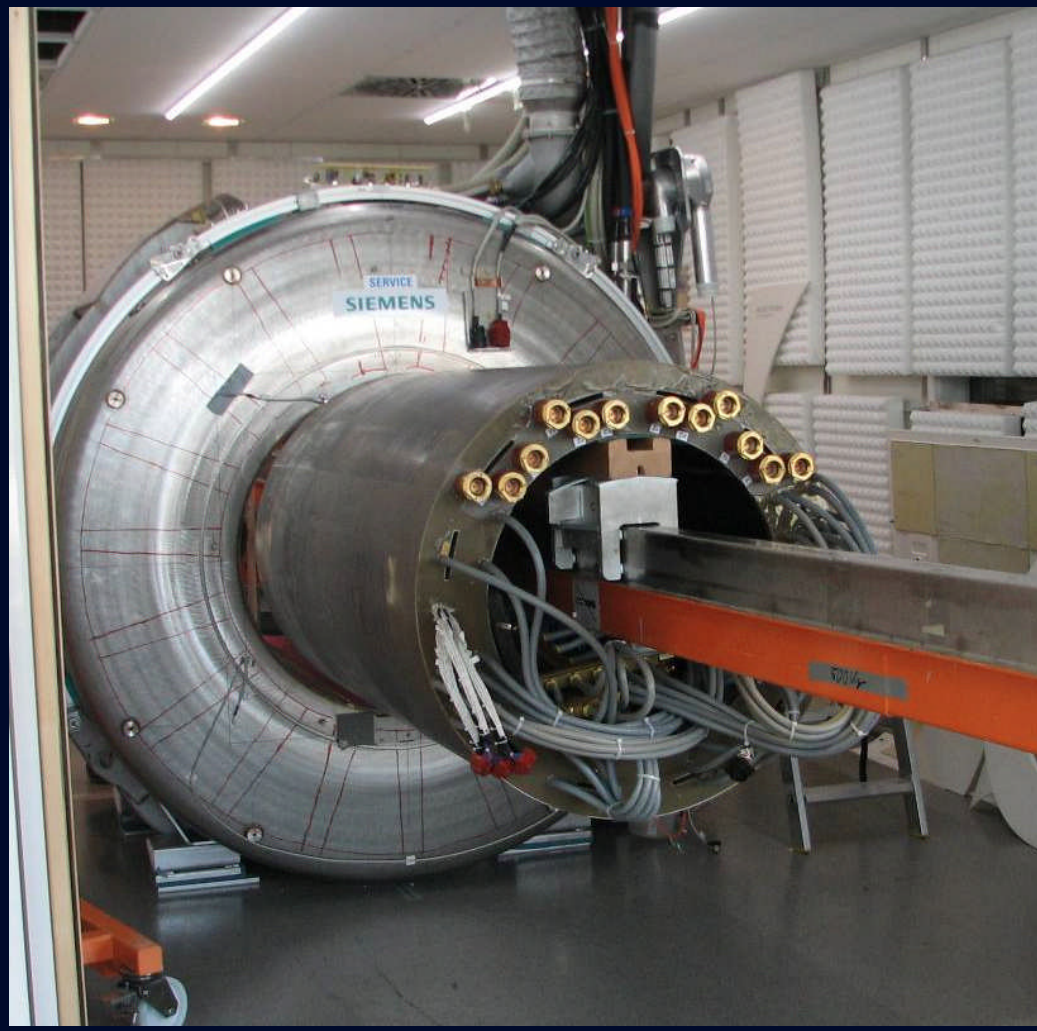

MRI was rated by general practitioners in the USA as the principal contributor to medical practice today over the last decade (i.e., 1991-2000) (Fuchs VR and Sox HC Jr. (2001) Physicians' Views Of The Relative Importance Of Thirty Medical Innovations, Health Affairs: Vol. 20, Number 5).

Modeling Human Anatomy and Physiology

(Integration across multiple levels of description is a major goal in medicine)

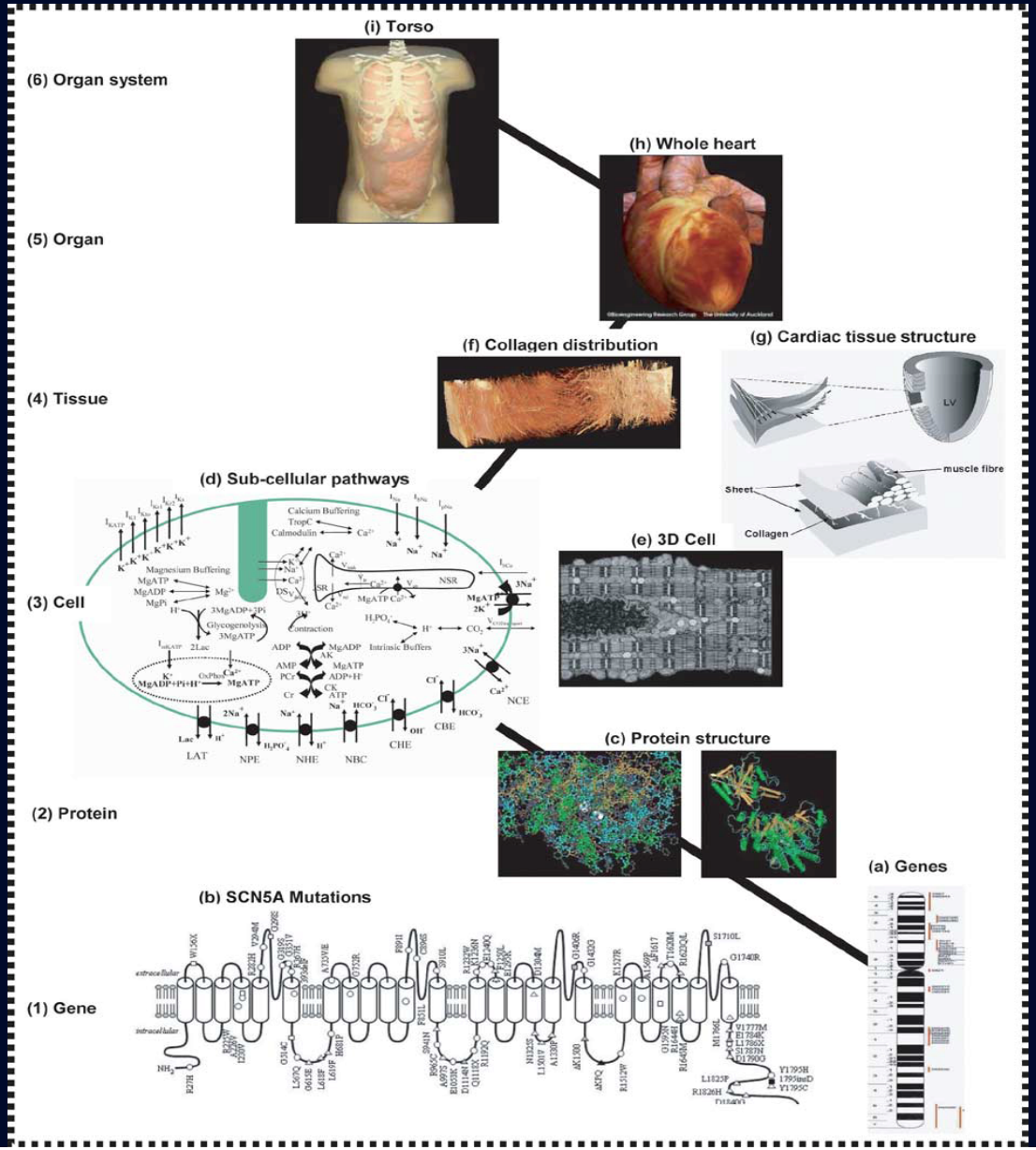

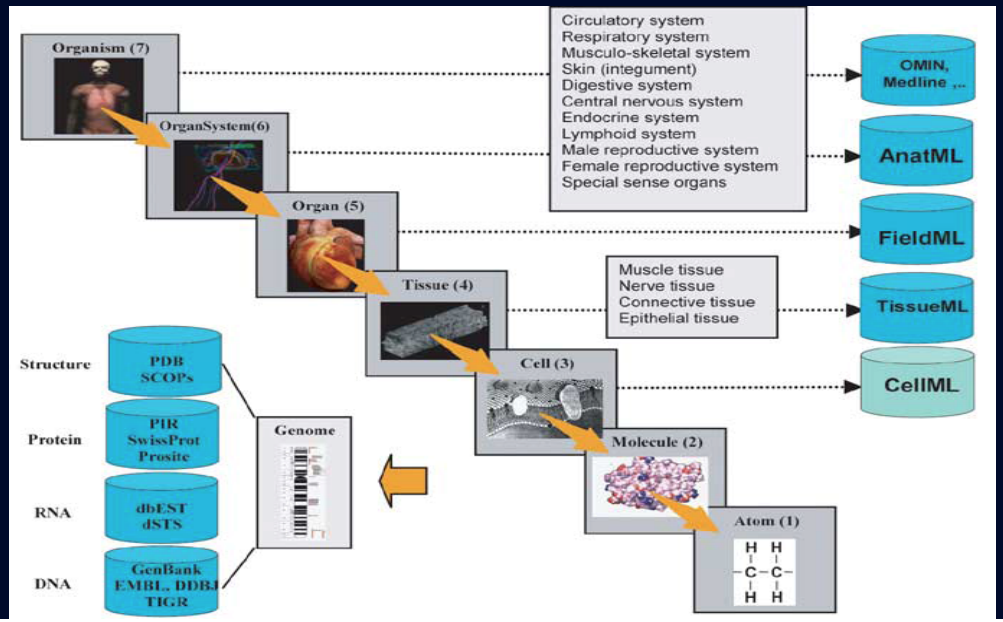

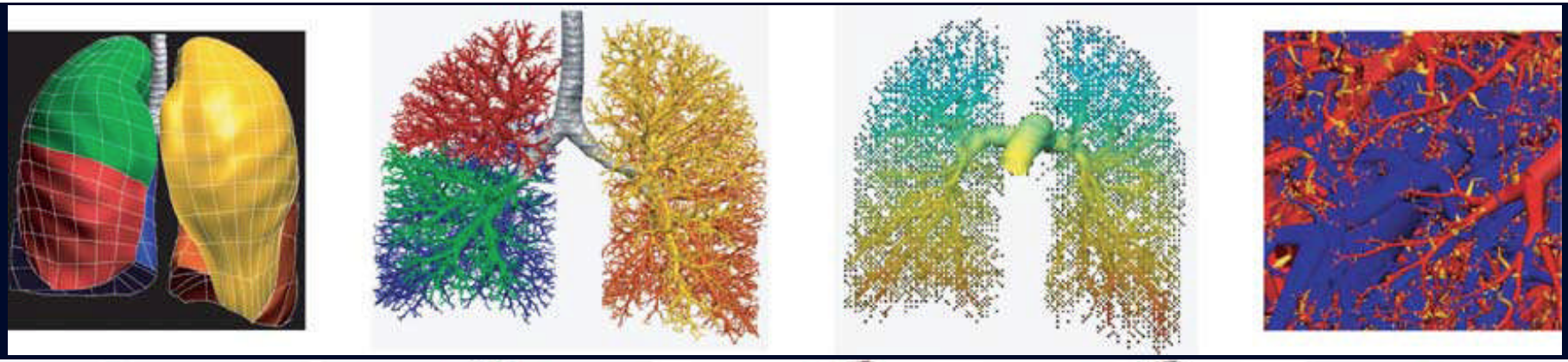

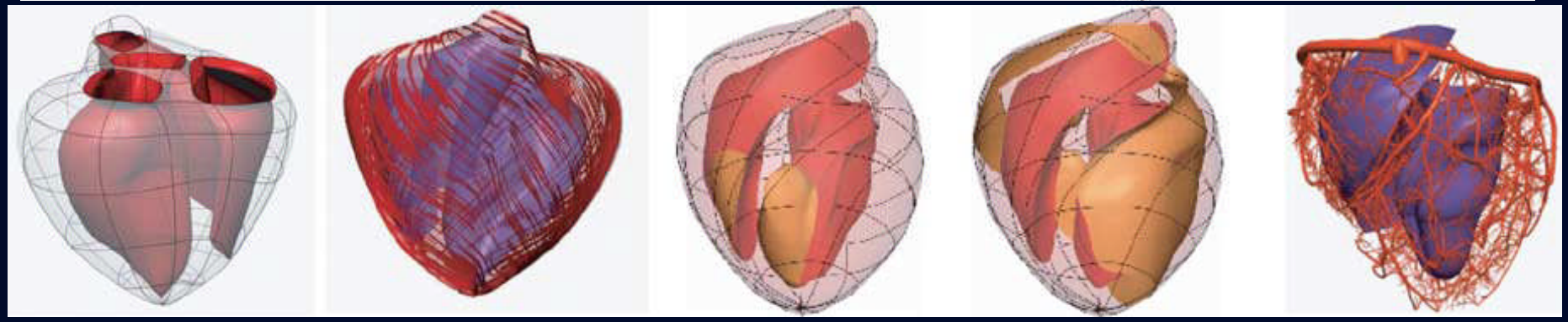

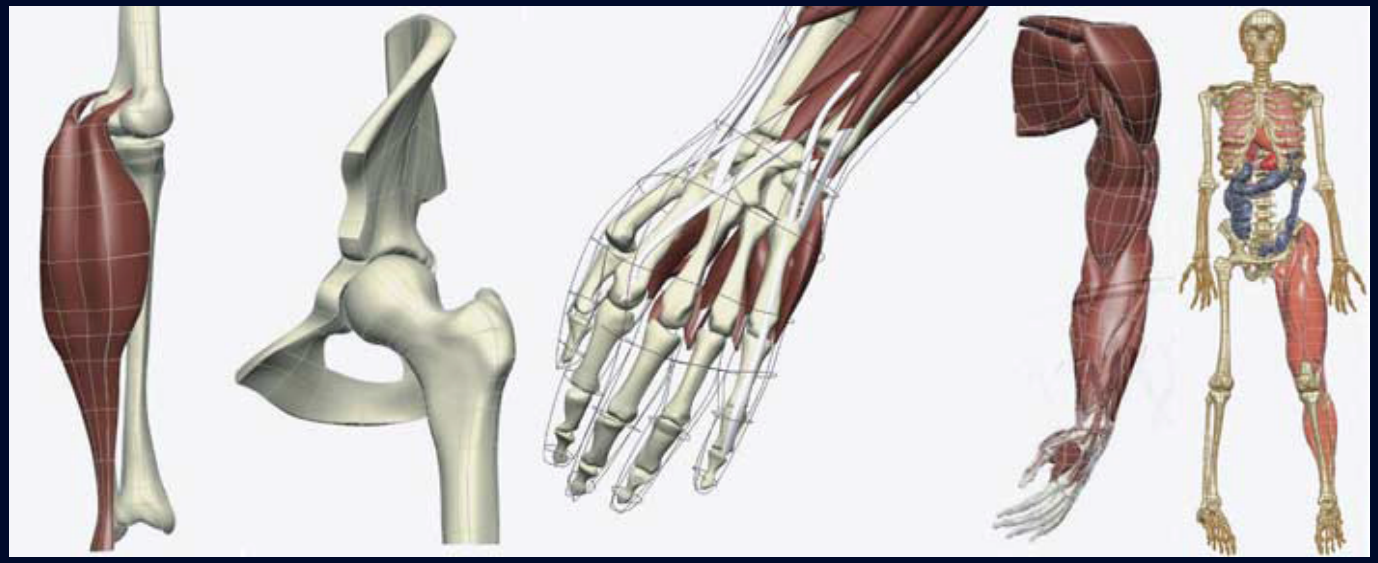

MRI-PET installations at MGH

Unique Instruments in New England

Nuclear Imaging two ways

Whole Body

Head-only

Courtesy of Dr. Bruce Rosen

Magnetic resonance imaging (MRI) technology had a critical role in understating the human brain.

Besides the great cultural and intellectual value of the accrued information and novel conceptualizations in brain science, **these advances had a tremendous impact on the way we are currently facing neurological and psychiatric diseases and the neurosurgical approaches we adopt for diagnosis, surgical planning and treatment.**

”Despite 4000 papers, not a single finding has changed routine clinical care in psychiatry”

But this will change, and the change will revolve around a new definition of psychiatric diseases as disorders of brain *circuitry* - that this will change our definition of the illnesses, and “our understanding of their causes, treatments, and preventions”

Paraphrasing Tom Insel, Director, National Institute of Mental Health

In Imaging Research, Brain Connectivity is done with Diffusion MRI

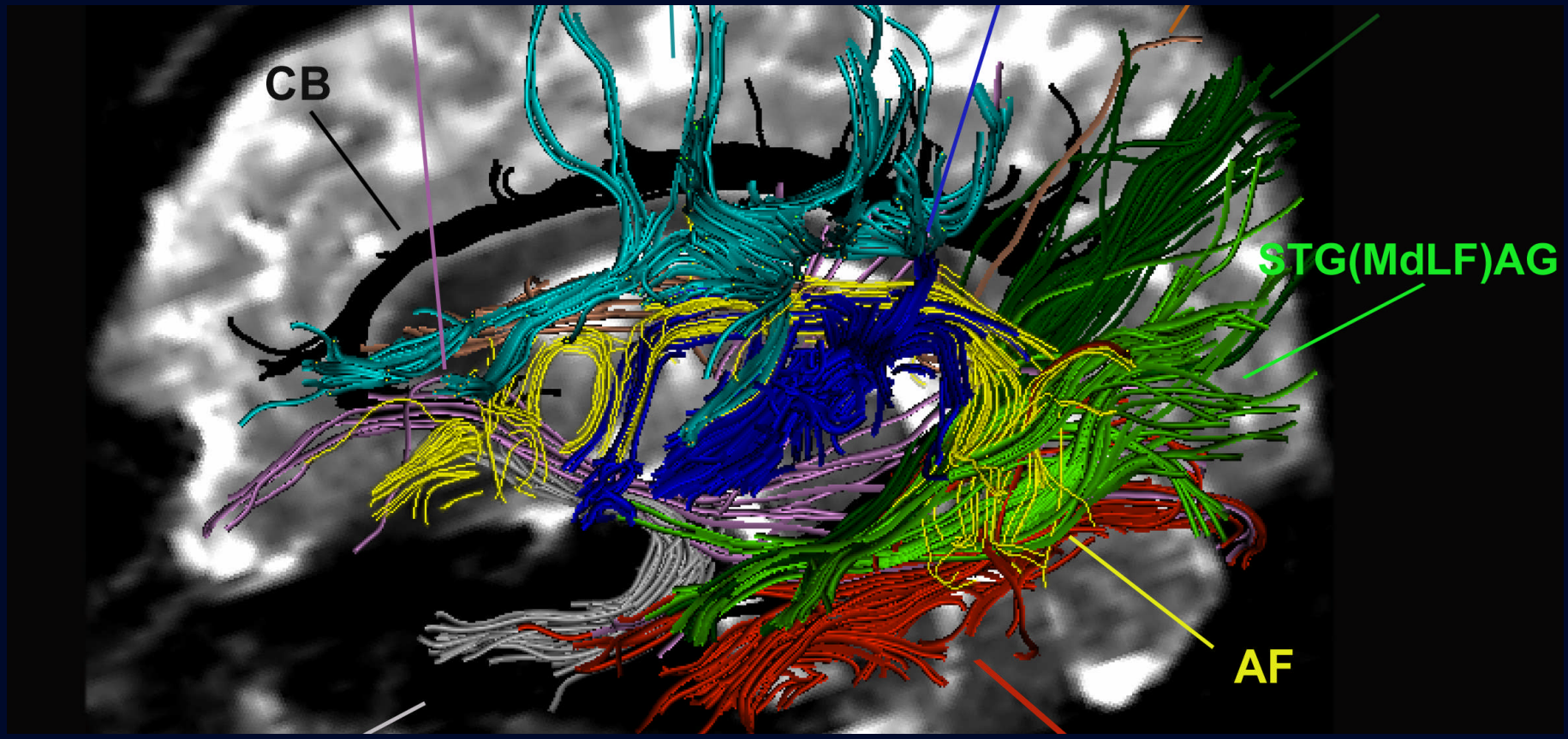

In astronomy, the way to sensitivity and resolution is mirror diameter

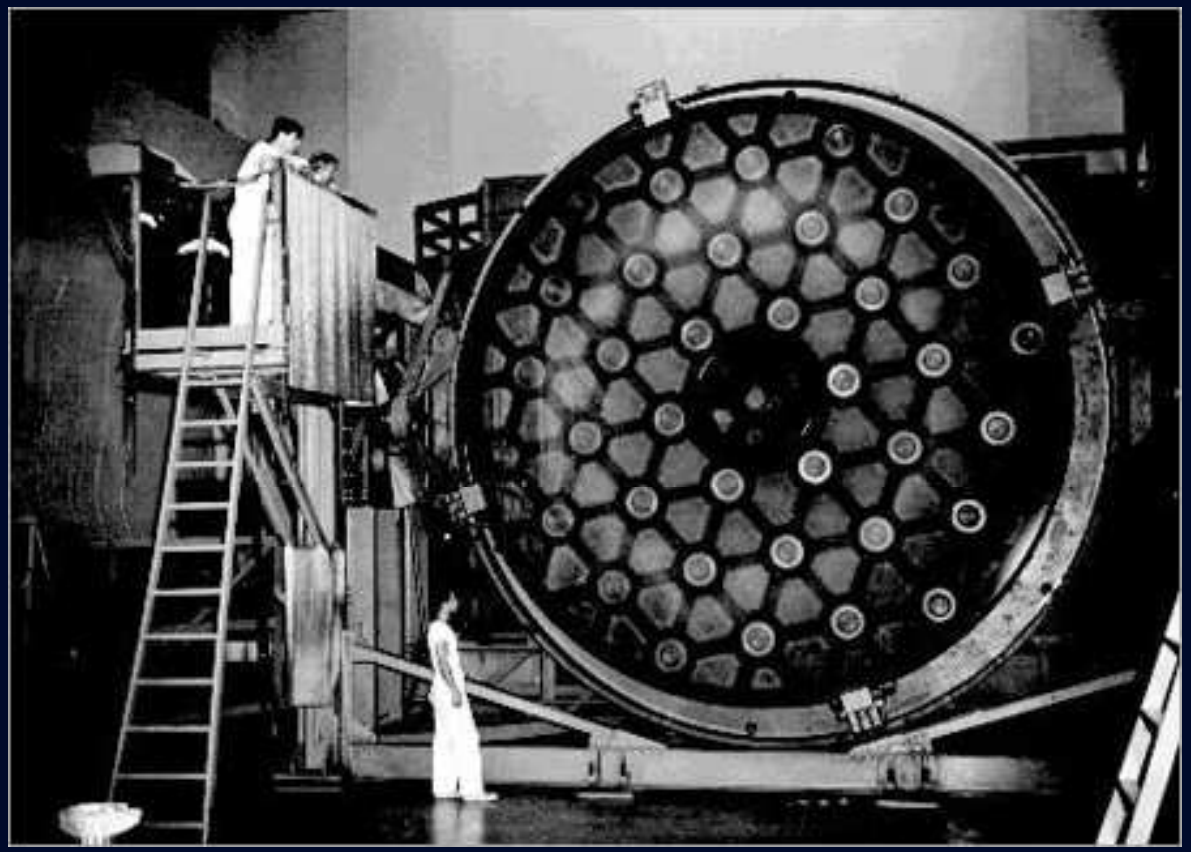

Corning 200" mirror for the Hale Telescope at Mt Palomar

Courtesy of Dr. Bruce Rosen

Human Connectome Project

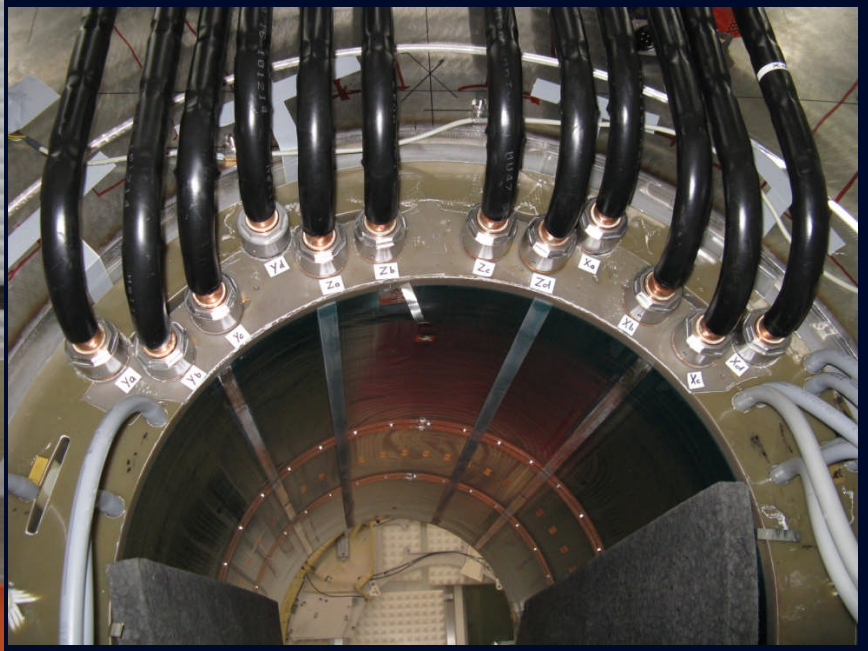

Gmax = 300mT/m
(7x Greater than conventional)

1.5 Ton gradient
24 MWatts peak power

In Diffusion MRI, the way to see micro-structure is gradient strength

Courtesy of Dr. Bruce Rosen

Human Connectome Project – NIH Neuroscience Blueprint

BRR PubMed Martinos Center File Drop Apple Yahoo! Google Maps YouTube News (262) Popular

The NIH Human Connectome Project

WU-Minn Consortium | Harvard/MGH-UCLA Consortium | Neuroscience Blueprint

About

The NIH Human Connectome Project is an ambitious effort to map the neural pathways that underlie human brain function. The overarching purpose of the Project is to acquire and share data about the structural and functional connectivity of the human brain. It will greatly advance the capabilities for imaging and analyzing brain connections, resulting in improved sensitivity, resolution, and utility, thereby accelerating progress in the emerging field of human connectomics.

Altogether, the Human Connectome Project will lead to major advances in our understanding of what makes us uniquely human and will set the stage for future studies of abnormal brain circuits in many neurological and psychiatric disorders.

Consortia

The sixteen institutes and centers of the NIH Blueprint for Neuroscience have funded two major grants that will take complementary approaches to deciphering the brain's amazingly complex wiring diagram.

The WU-Minn Project

The Harvard/MGH-UCLA Project

Courtesy of Dr. Bruce Rosen

Search the HCP

Search

powered by Google™

HCP In The News

Sporns' 'Networks of the Brain': a roadmap to new
Indiana University
The first of these projects is to develop a "virtual brain," a powerful computational model that can simulate brain function; and the second is called the Human Connectome Project, established to map the human brain's major connections. ...

Data Overload: Scientists Struggle to Streamline
LiveScience.com
The goal of the Human Connectome Project (HCP), for instance, is to map connections among neurons using evidence from brain-imaging studies and link the findings to behavioral tests and DNA samples from more than 1000 healthy adults. ...

Proposal unveiled for revamped Gateway Arch park
Reuters
No specifics were presented for how the money would be raised, but Walter Metcalf, an official of the foundation planning the project, said the cost would be $578.5 million. He said funding was in the "early stage" but would use federal, ...

Apple σημαίνει καινοτομία
SigmaLive
Το προηγούμενο έτος τα εργαστήρια της εταιρείας κατέθεσαν 2.537 αιτήσεις διπλωμάτων ευρεσιτεχνίας, ενώ στα νέα της εγχειρήματα συγκαταλέγεται το Human Connectome Project, μια απόπειρα να χαρτογραφηθούν οι συνδέσεις του ανθρώπινου εγκεφάλου. ...

powered by Google™

NIH HCP Initiative History

- Human Connectome Project grant published July 15, 2009. (RFA, Press Release)

Diffusion Imaging of Microstructure

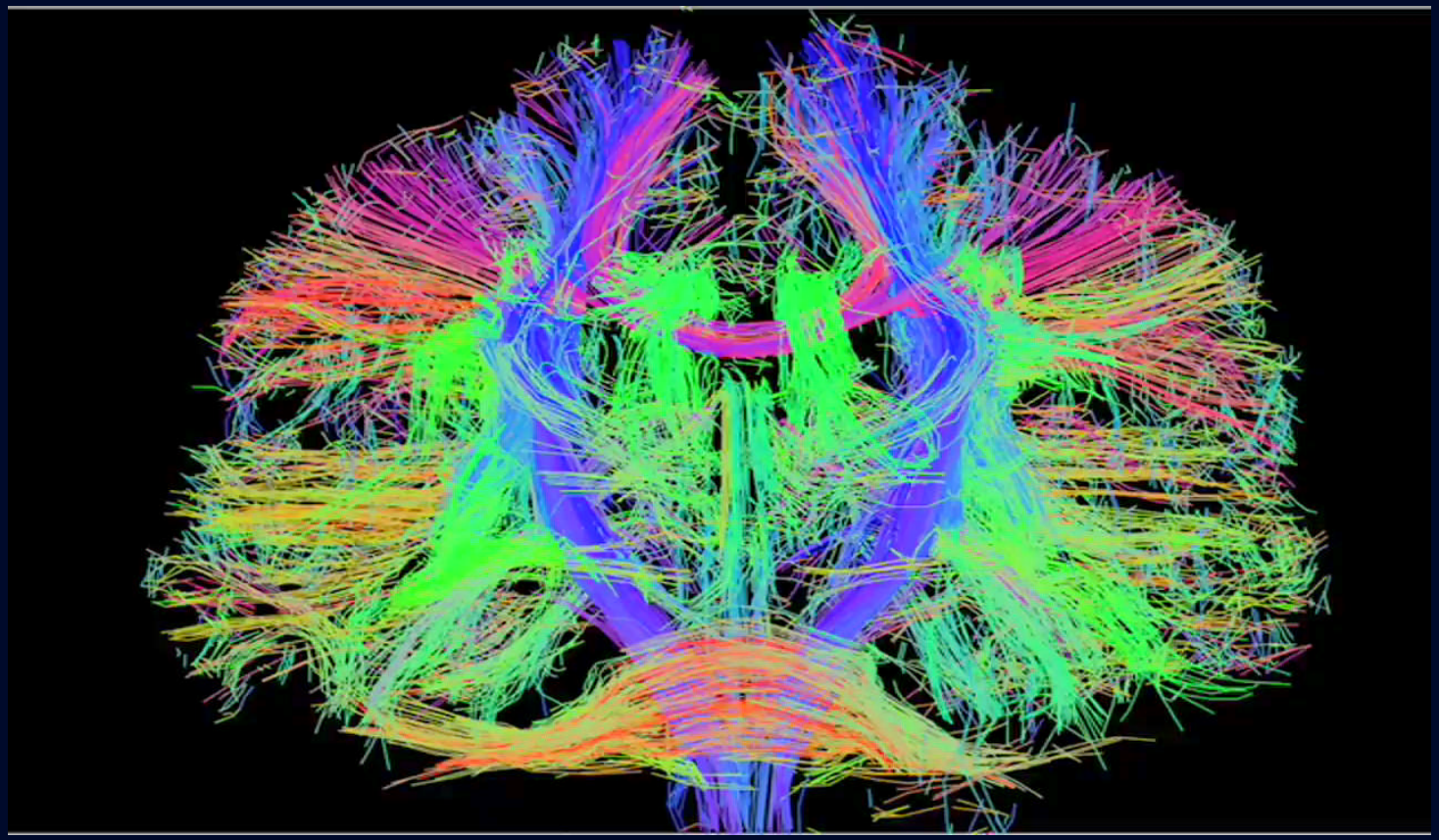

Courtesy of Dr. Bruce Rosen

Water Diffusion in the Brain has *Directionality*

Isotropic diffusion

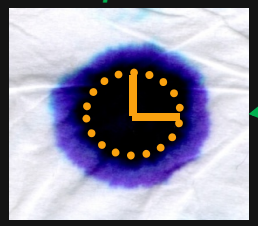

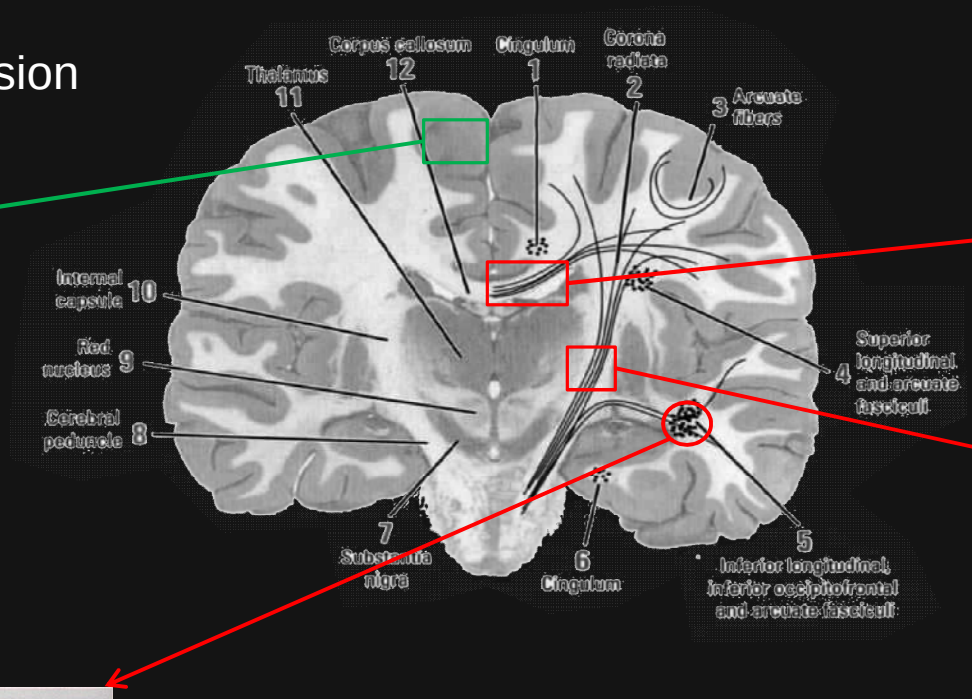

Anisotropic diffusion

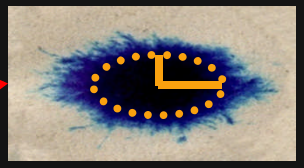

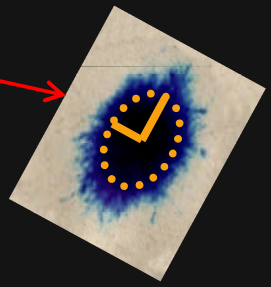

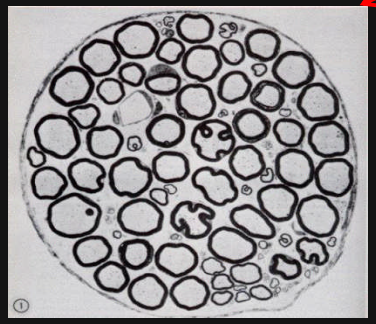

Possible sources of anisotropy:

- Axonal membranes of *densely packed axons hinder diffusion perpendicularly* to the fiber long axis.
- Myelin may also modulate anisotropy.

Diffusion Tensor Imaging

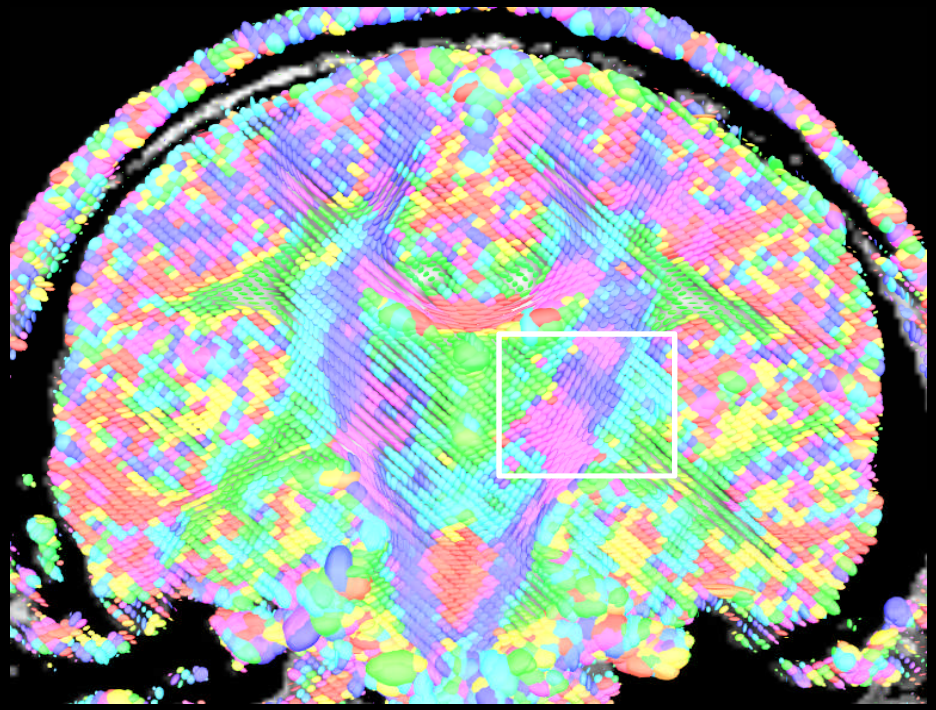

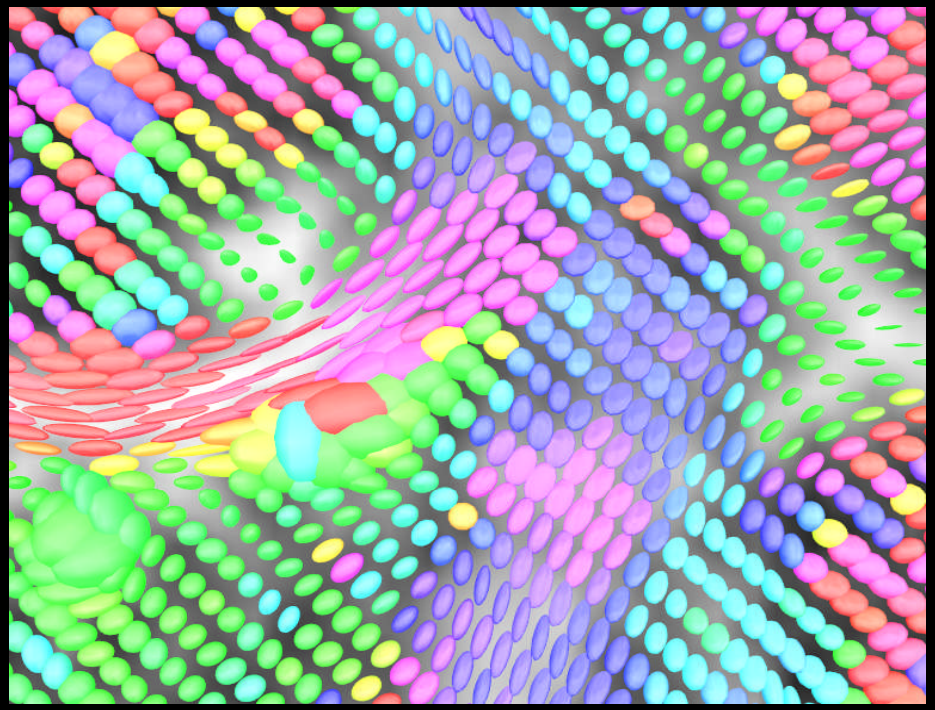

- At each location, the diffusion behavior of water is modeled as an ellipsoid.
- In medical imaging this ellipsoid is called a diffusion tensor.

From Tensors to Tracts

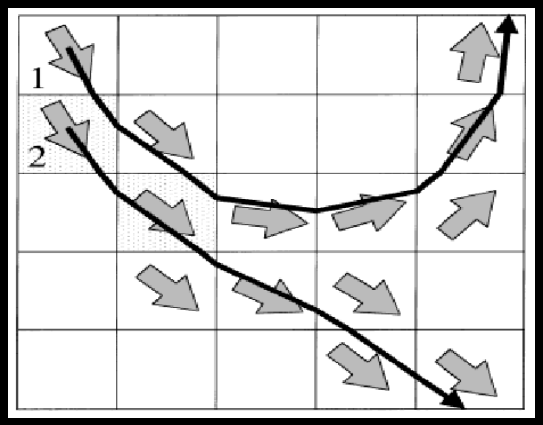

- Associate the major diffusion direction with the tangent to a curve.
- Estimate the curve from its tangents.

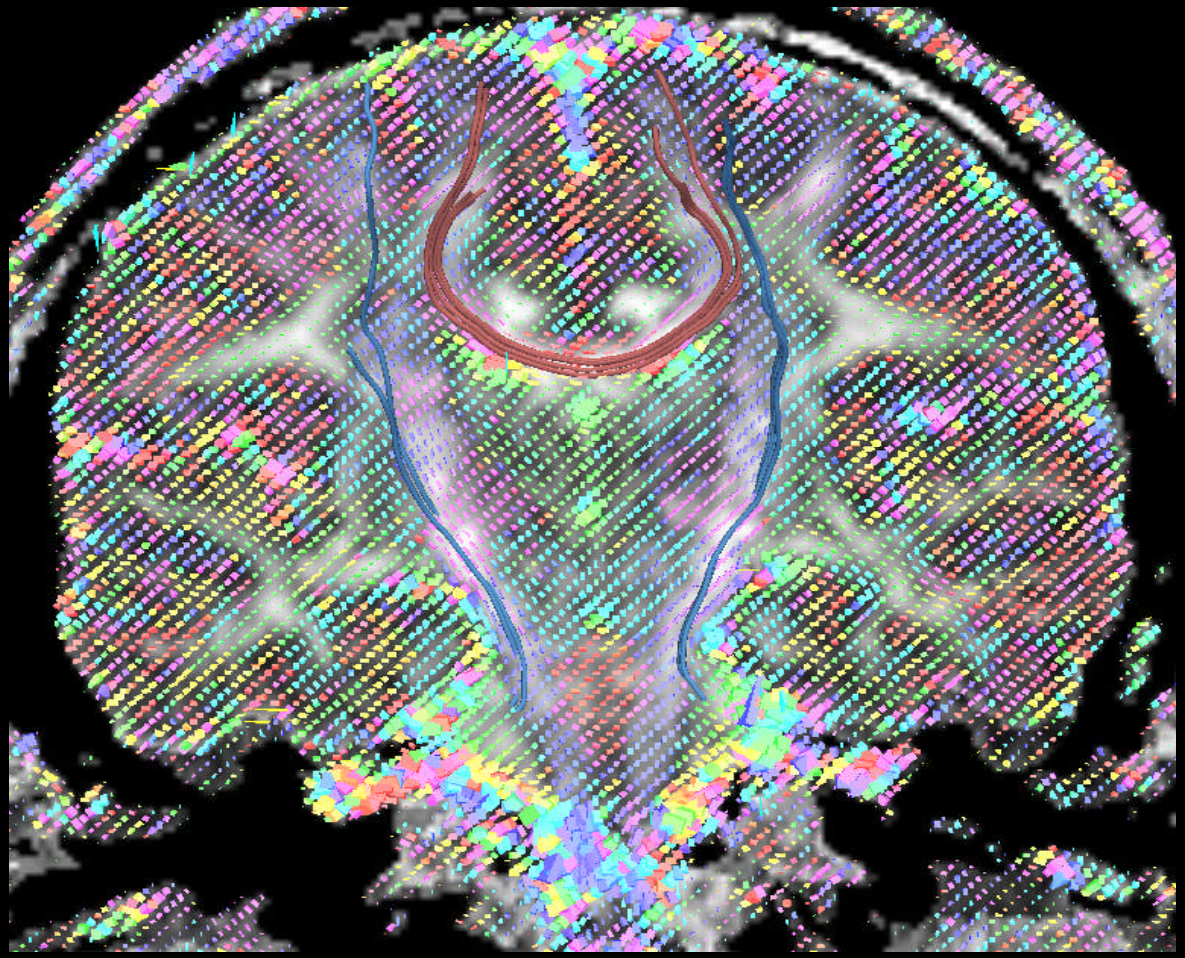

Multimodal Brain Connectivity

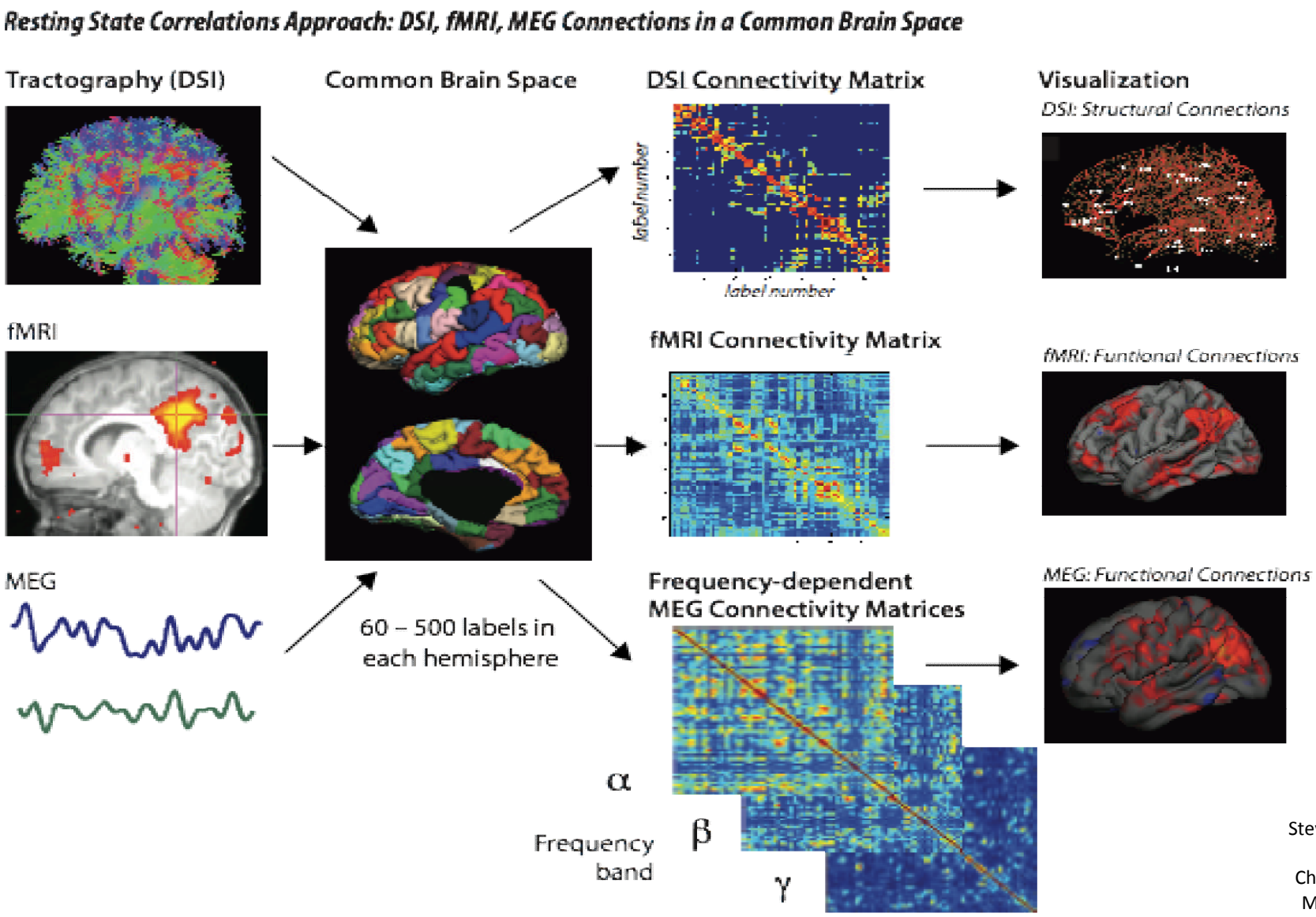

Courtesy of:
Steven Stufflebeam
Patric Hagmann
Christopher Honey
Matti Hämäläinen

How does assessment of large neuronal circuits using functional connectivity MRI work?

While people are simply resting, the brain shows large, spontaneous, activity fluctuations

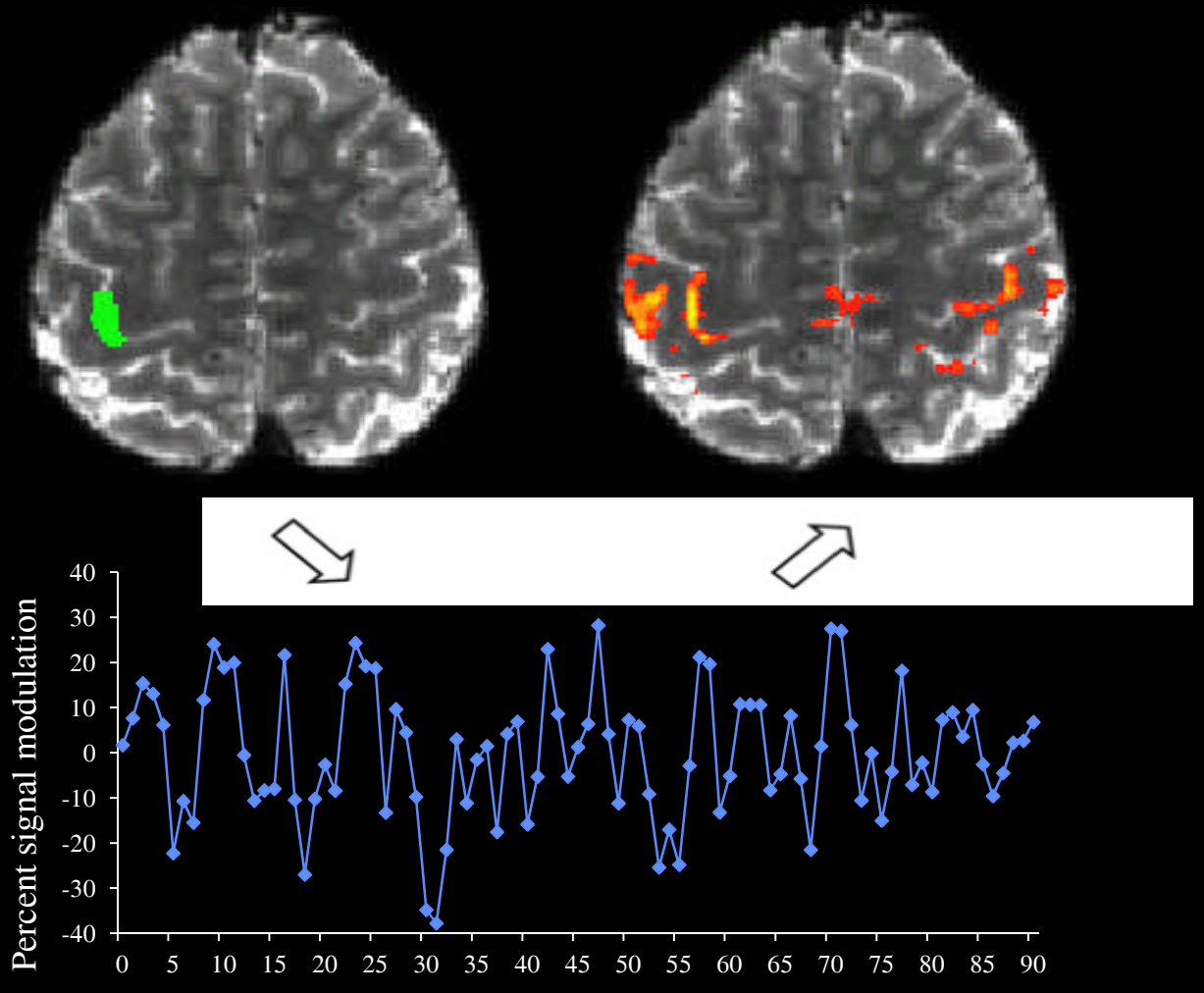

Spontaneous BOLD fluctuations within seed region

Biswal et al., MRM, 1995

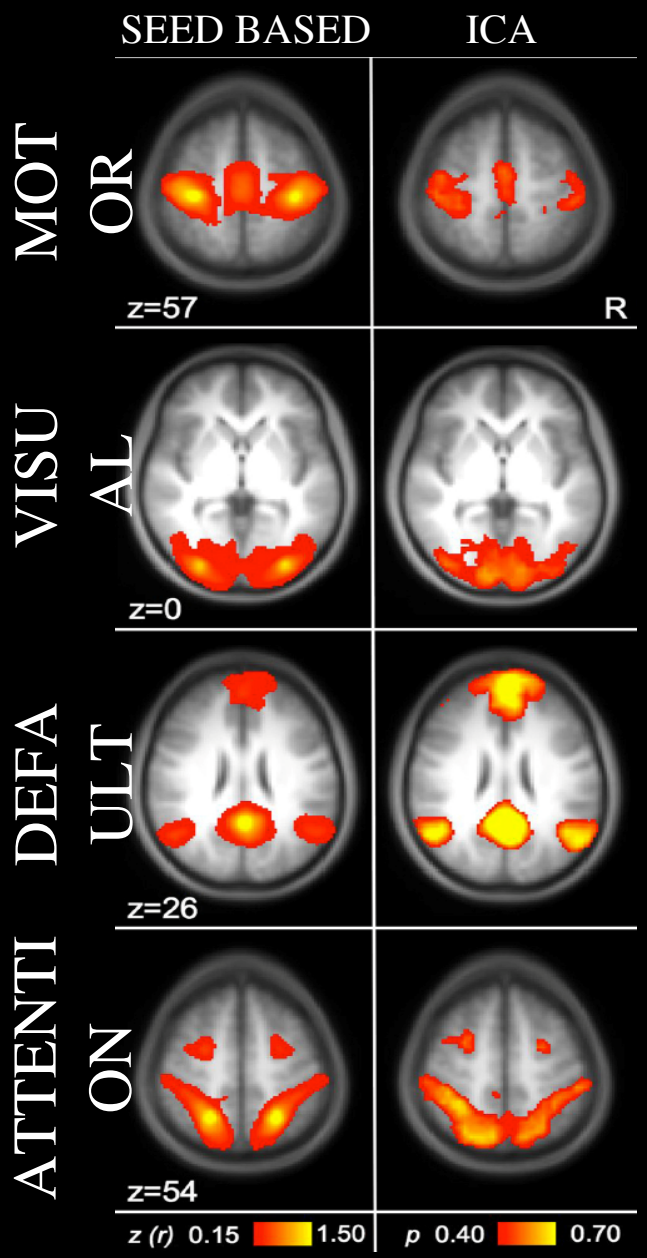
SEED BASED
ICA
MOTOR
VISUAL
DEFAULT
ATTENTION
z=57
R
z=0
z=26
z=54
z (r) 0.15
1.50
p 0.40
0.70

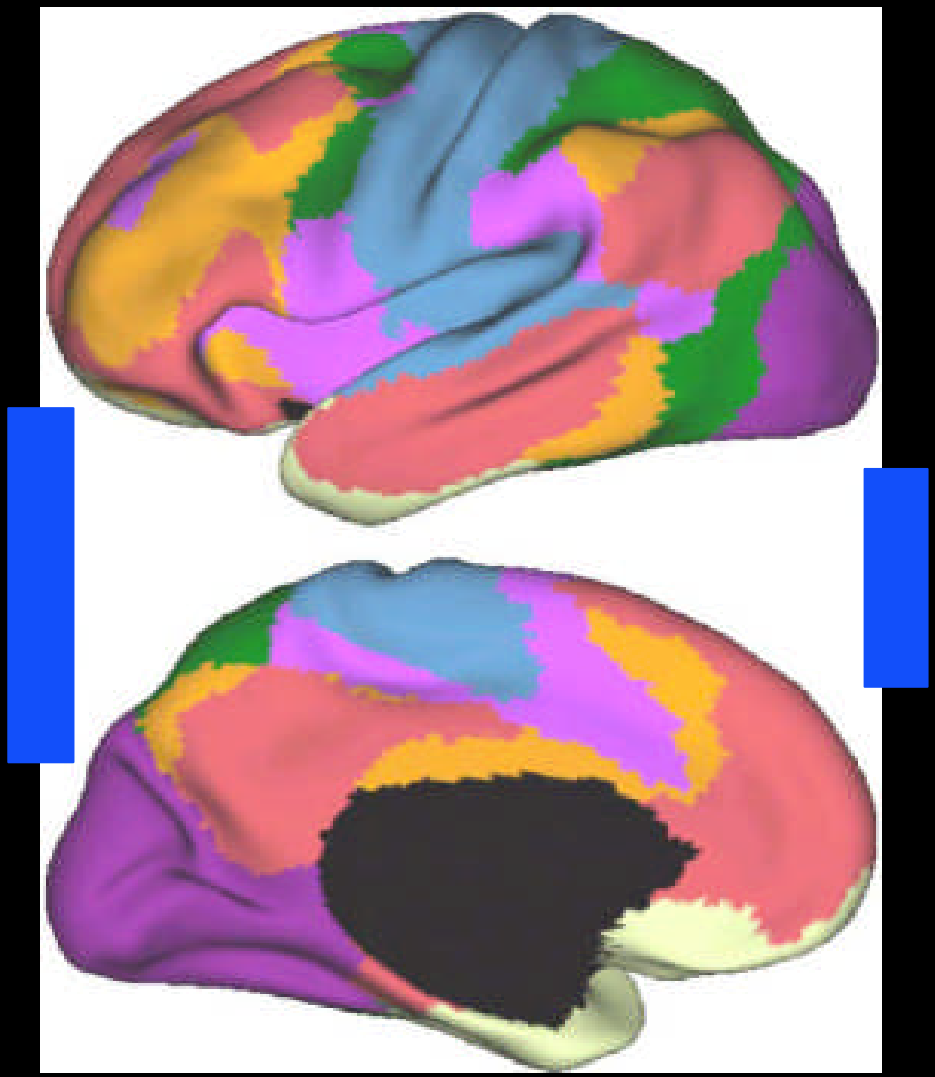

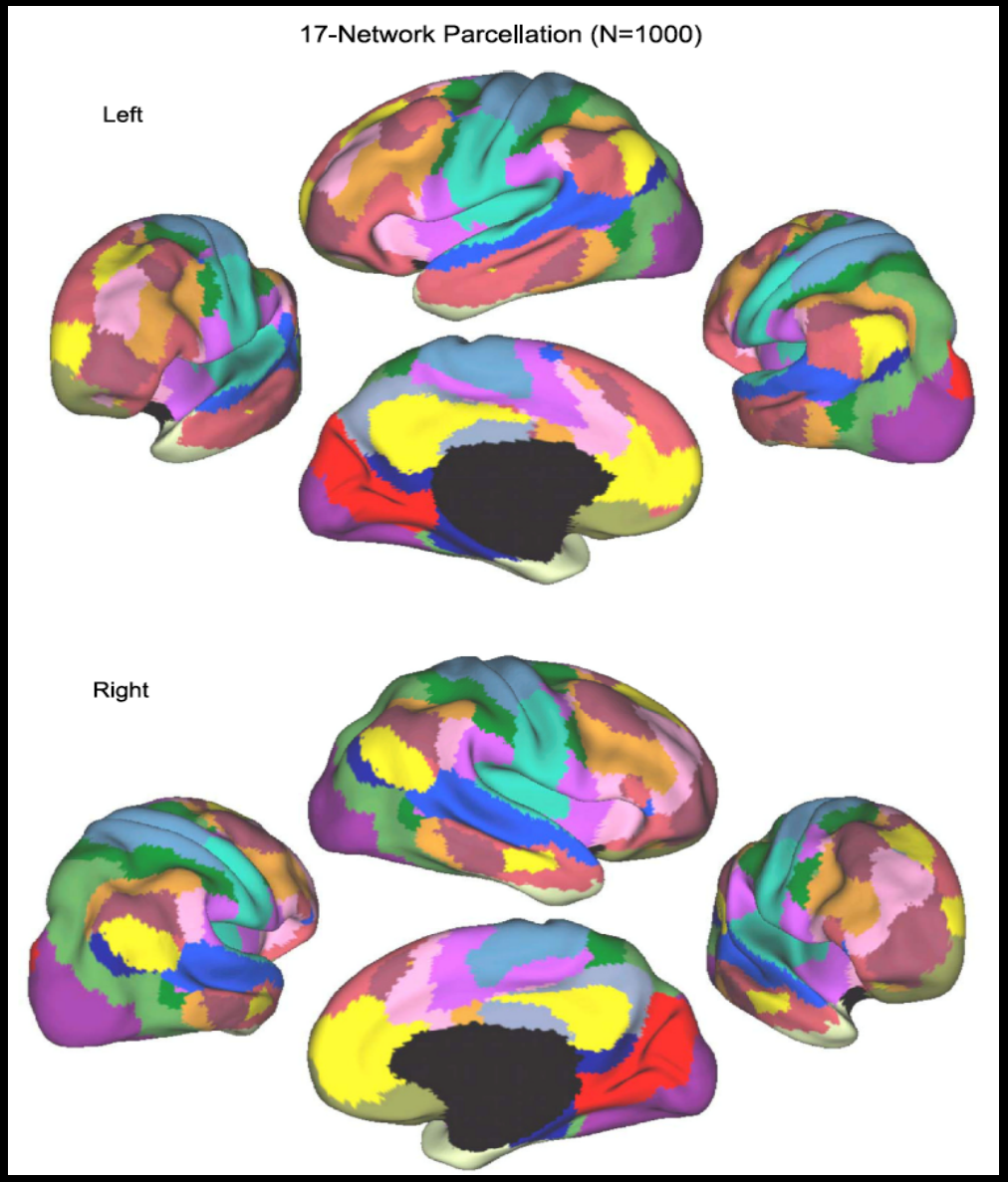

Fig. 13. A fine-resolution (17-network) parcellation of the human cerebral cortex based on 1,000 subjects. To provide the best estimates of the 17 cortical networks, clustering was performed on the fMRI data of the full 1,000 subjects. The 17-network estimate fractionated the 7-network into smaller networks. Some aspects of the fractionations have been previously noted in other studies.

Yeo BT, Krienen FM, Sepulcre J, Sabuncu MR, Lashkari D, Hollinshead M, Roffman JL, Smoller JW, Zollei L, Polimeni JR, Fischl B, Liu H, Buckner RL. The organization of the human cerebral cortex estimated by intrinsic functional connectivity. *Journal of neurophysiology*. 106(3):1125-65. Pubmed PMID: 21653723; PMCID: PMC3174820.

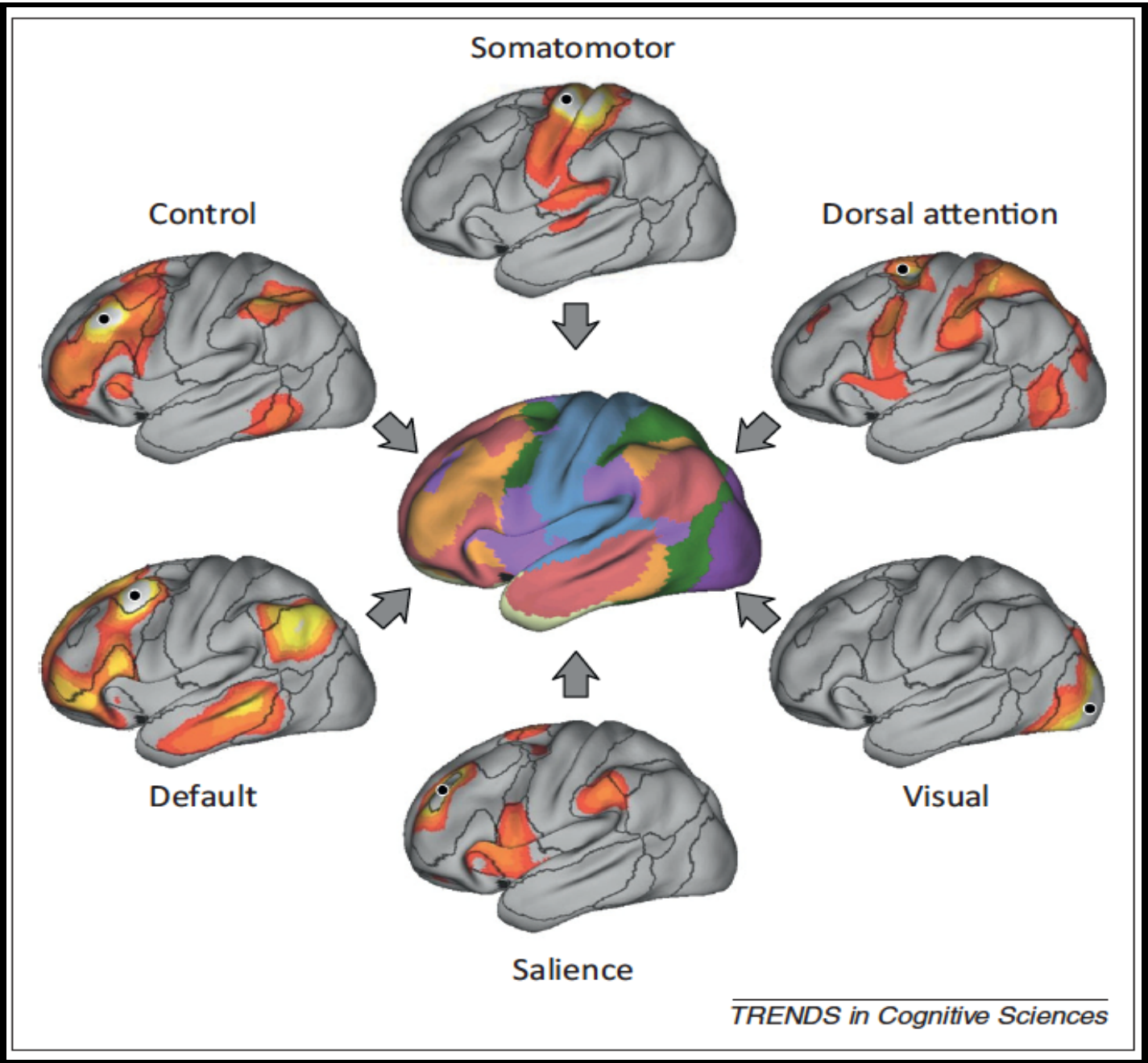

Buckner RL, Krienen FM. (2013) The evolution of distributed association networks in the human brain. *Trends in cognitive sciences*. 17(12):648-65. Pubmed PMID: 24210963.

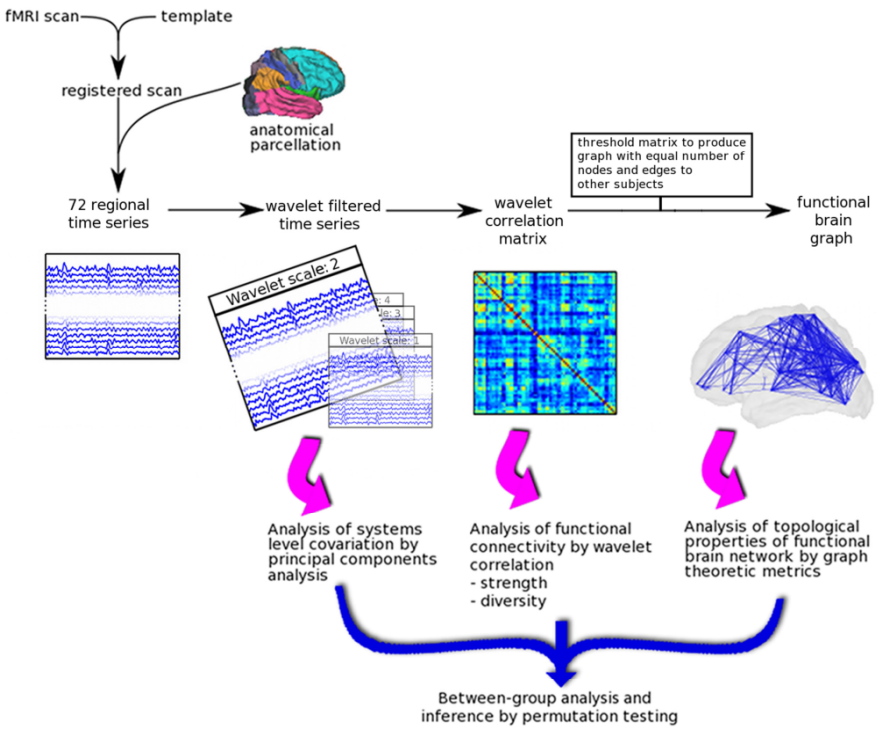

Figure 1. Schematic of fMRI data analysis pipeline. Regional mean fMRI time series were estimated by applying a prior anatomical template image to each individual fMRI dataset after its coregistration with the template in standard space; wavelet analysis was used to bandpass filter the regional time series and to estimate frequency-specific measures of functional connectivity between regions; functional connectivity matrices were thresholded to generate binary undirected graphs or brain functional networks; between-group differences in functional connectivity, principal components, and network topological metrics were assessed by permutation testing.

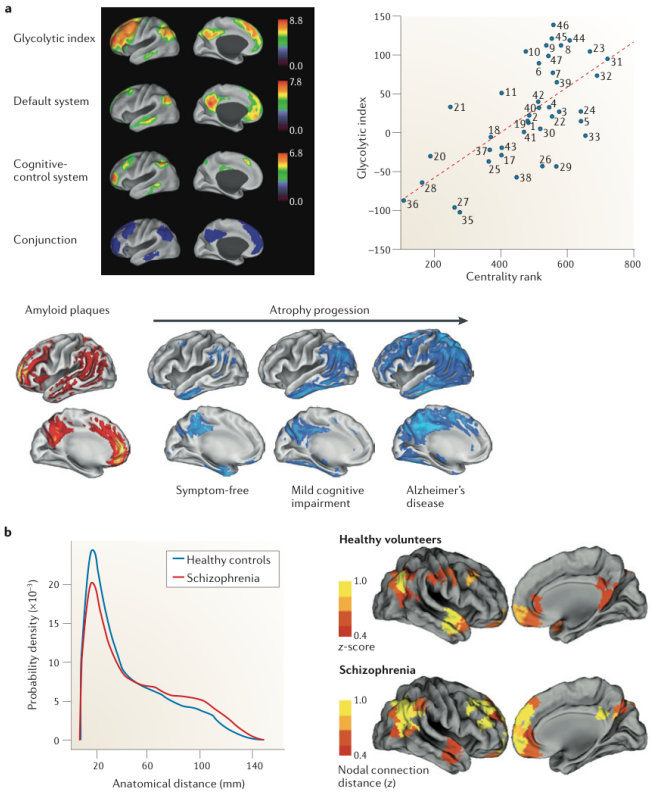

Figure 4 | **Brain disorders affect high-cost components of networks. a** | Brain networks and brain metabolism. The top left panel shows the regional distribution of aerobic glycolysis (as measured using the glycolytic index), the default mode system and the cognitive control system (as mapped by resting-state functional MRI (fMRI)) and the conjunction of these two systems with the glycolytic index, illustrating their overlap[161]. The top right panel shows a scatter plot of the centrality rank (which is estimated from the betweenness centrality of the connectomes of five participants[64]) and the glycolytic index[161] for 41 Brodmann areas of the cerebral cortex. The correlation is highly significant, with $r = 0.66$ ($P < 0.00005$), indicating that areas with high centrality — that is, the structural hubs — have a high glycolytic index[64,161]. Several of these hub nodes are members of the default and cognitive control systems. The bottom panel shows that high-cost hub nodes (including regions comprising the default mode system and the cognitive control system; see top left panel) are typically first affected by amyloid deposition and grey-matter atrophy in Alzheimer's disease, leading to disruption of memory functions that are dependent on large-scale network integrity[162,163]. **b** | fMRI networks in patients with schizophrenia contain proportionally more long-distance connections than fMRI networks in healthy controls (left panel), perhaps owing to excessive developmental pruning of shorter-distance connections. Accordingly, inter-modular connector hubs that have a large number of long-distance connections (indicated by areas with high connection distance in the right panel) are more extensive in functional brain networks of people with schizophrenia than in healthy volunteers[46]. Part **a** is reproduced, with permission, from REF. 161 © (2010) National Academy of Sciences, and from REF. 163 © (2008) New York Academy of Sciences. Part **b** is reproduced, with permission, from REF. 46 © (2012) Oxford Journals.

© 2012 Macmillan Publishers Limited. All rights reserved

For Multimodal Imaging Analysis we need AUTOMATION

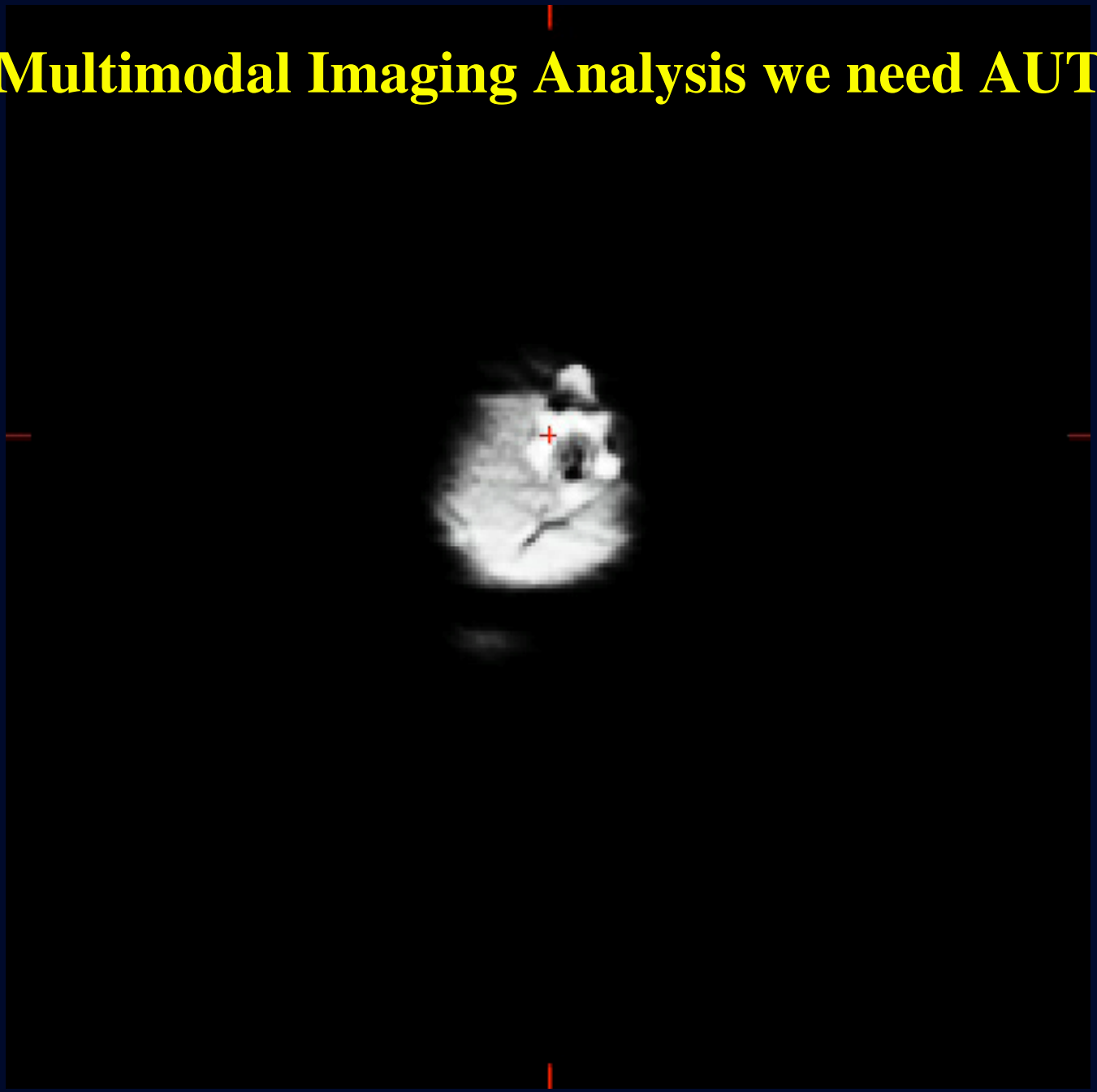

Methodologies

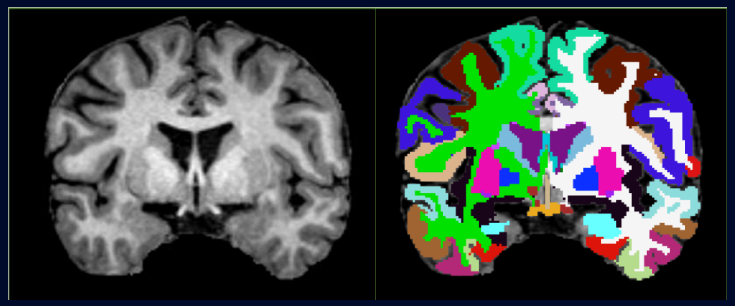

Volume - Morphometry

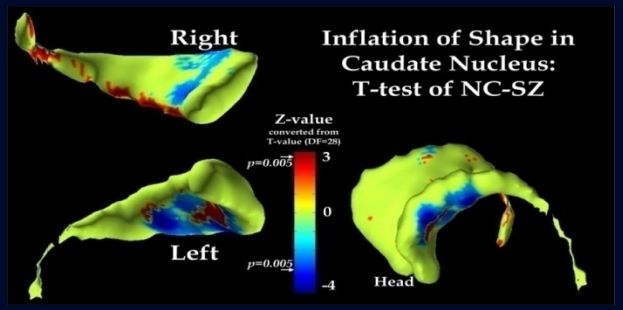

Shape - Morphometry

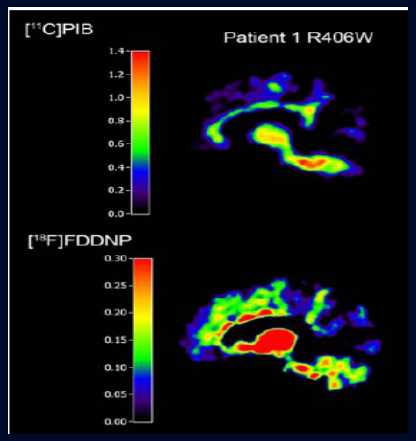

PET

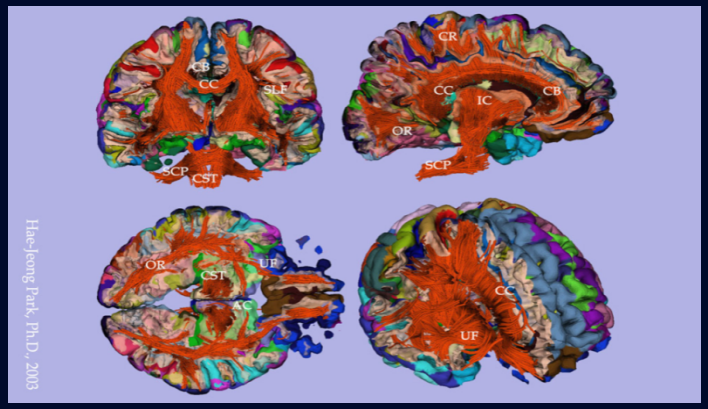

Diffusion Imaging

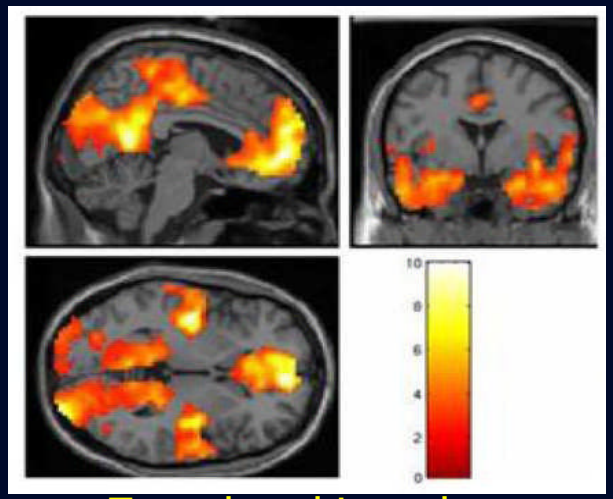

Functional Imaging

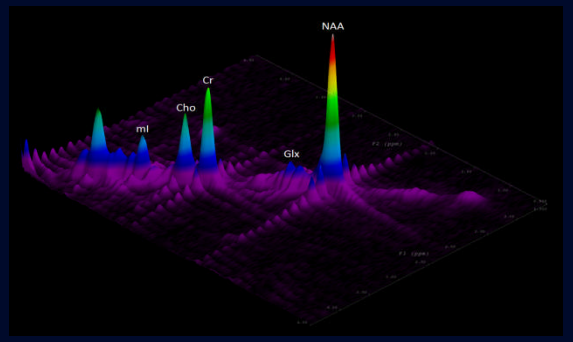

MR Spectroscopy

Data Infrastructure

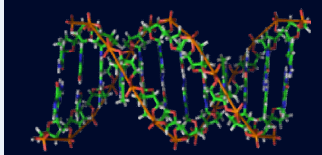

Genetics

PNL Pipeline

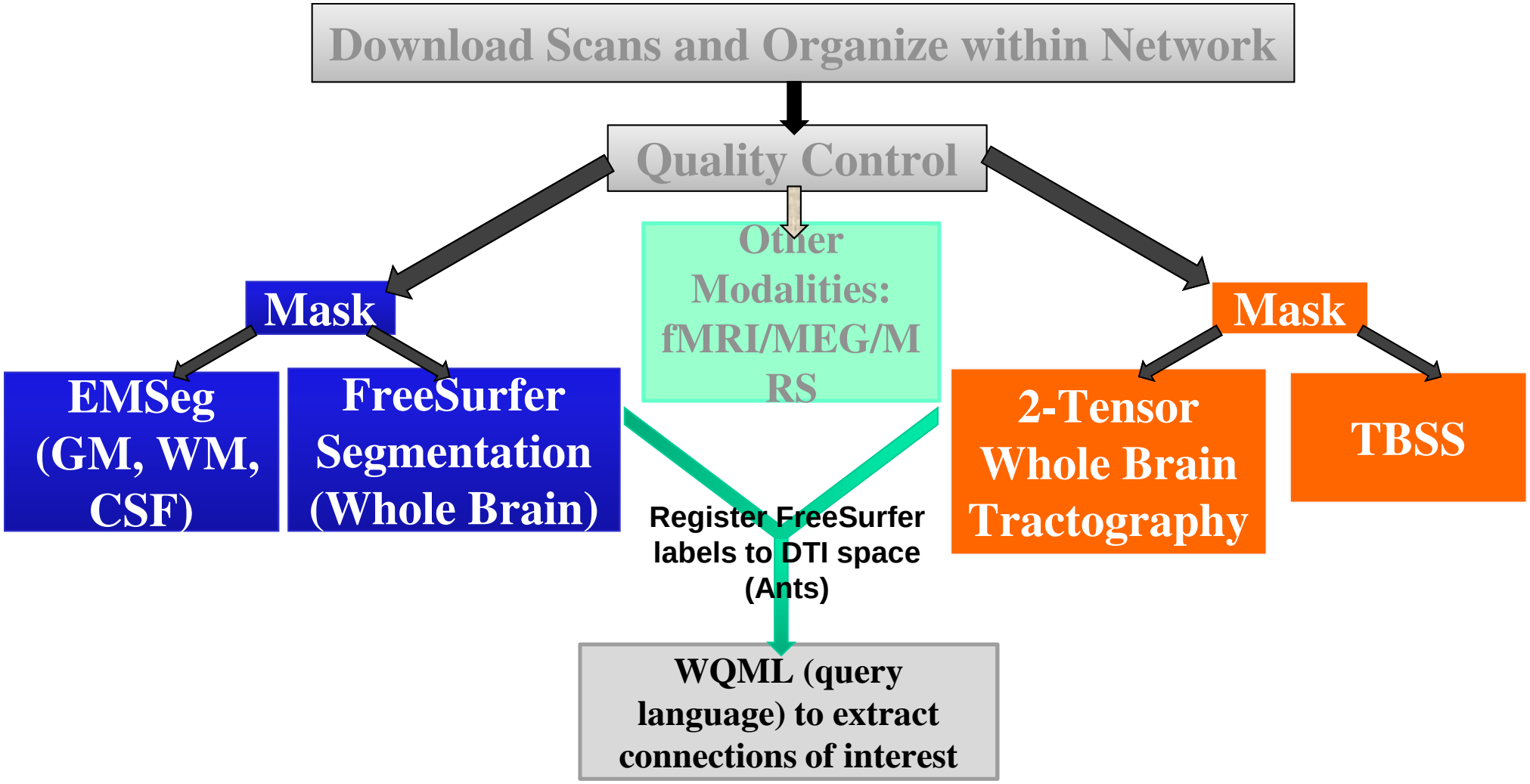

As methodologies seem to have limitations, these should be known thoroughly to be able to use any given technique optimally and efficiently

"A real man knows his limits" Clint Eastwood

Imaging Brain Circuitries in Basic and Clinical Neuroscience

Large-scale cognitive systems
understrood through resting state fMRI

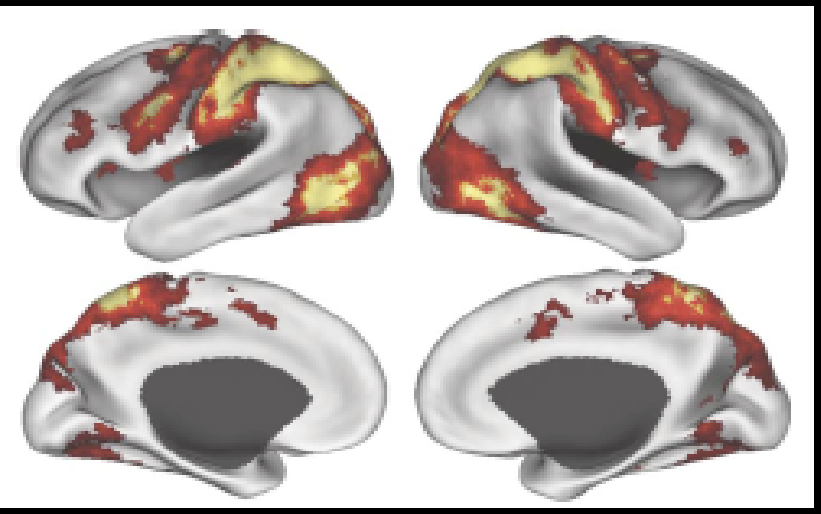

Dorsal visuospatial attention system

Frontoparietal executive control system

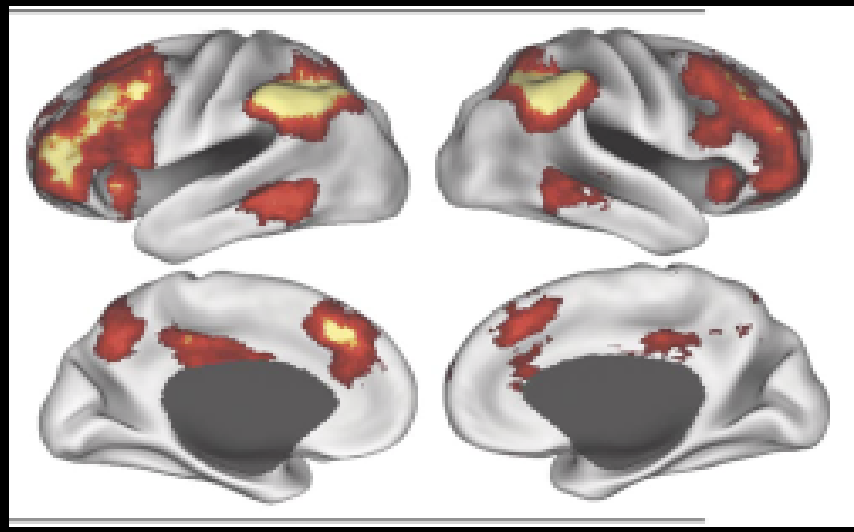

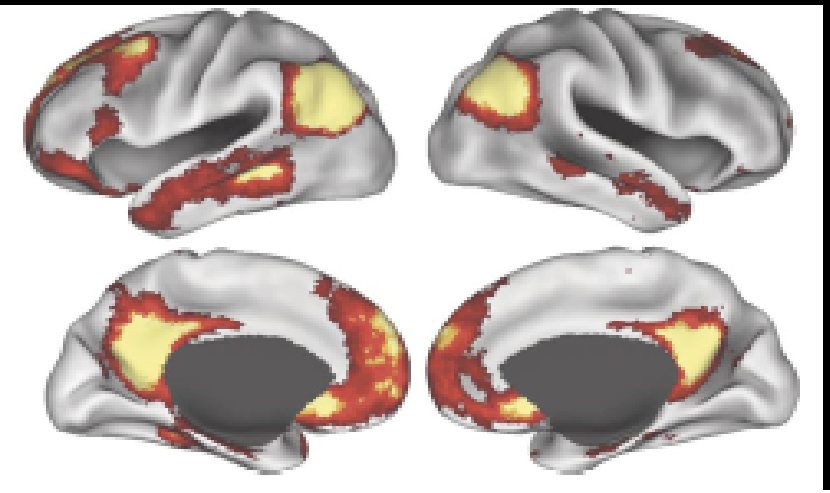

Episodic memory/Default-mode system

Vincent et al., J Neurophys, 2008

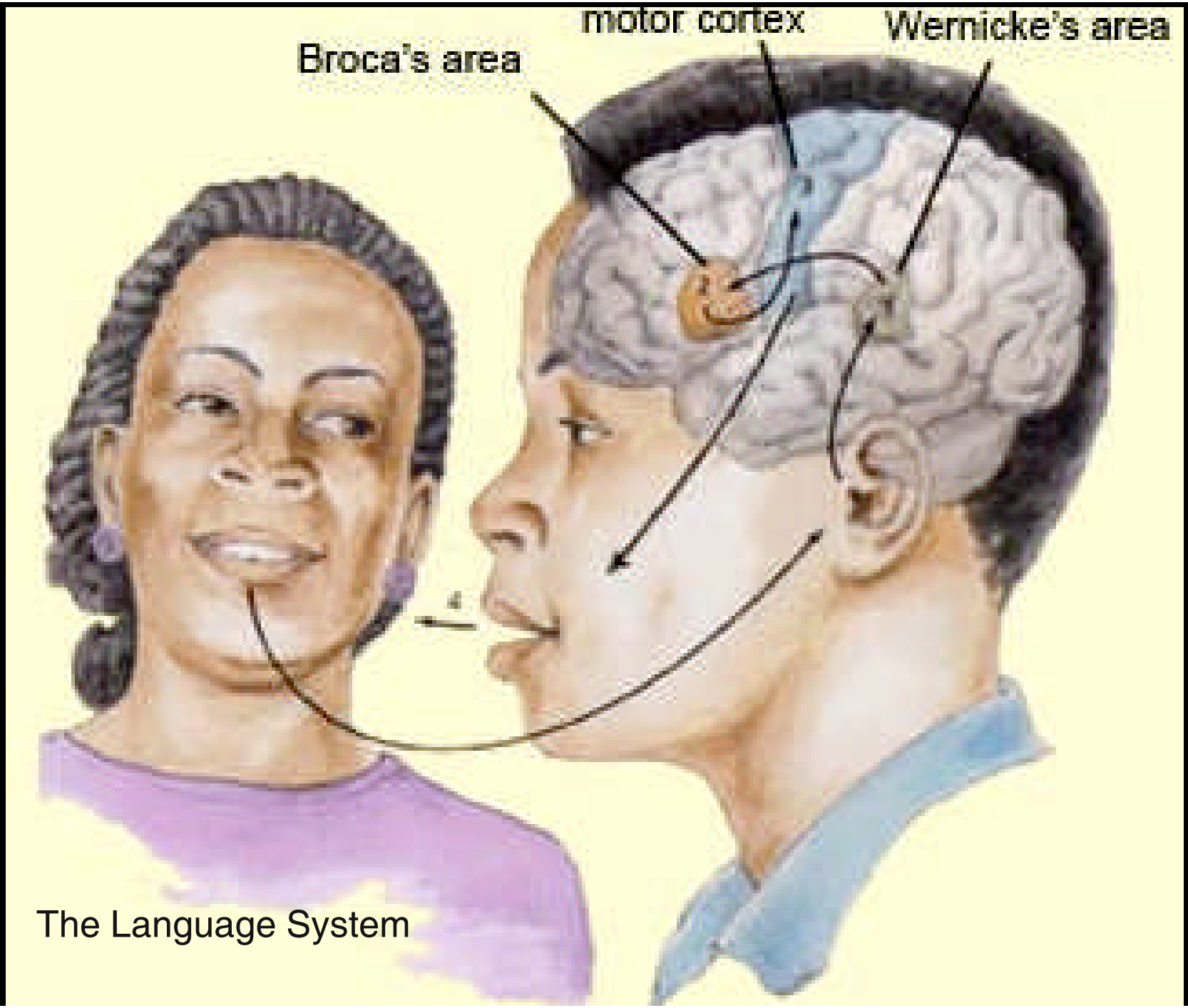

The Language System

Dorsal Streams

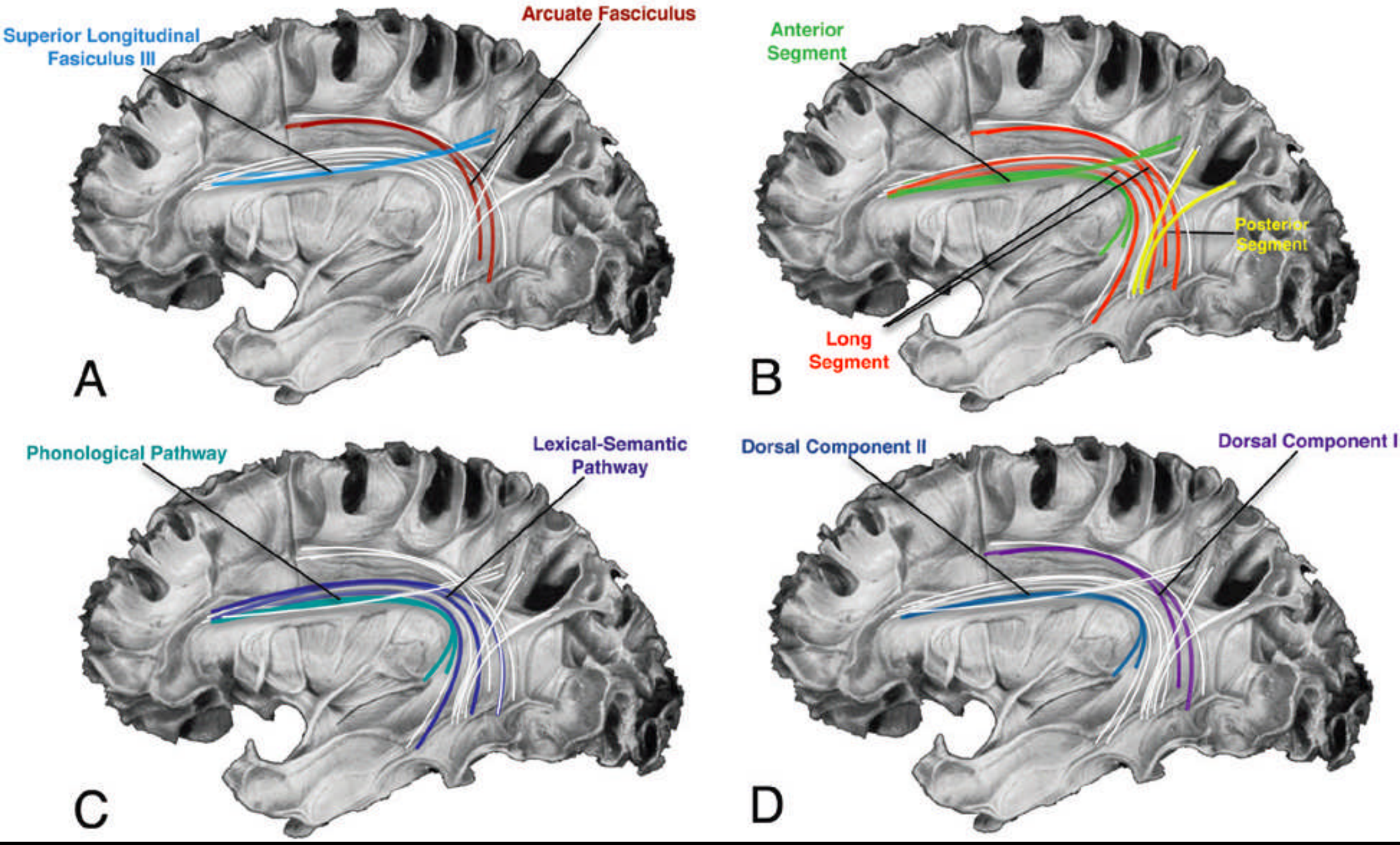

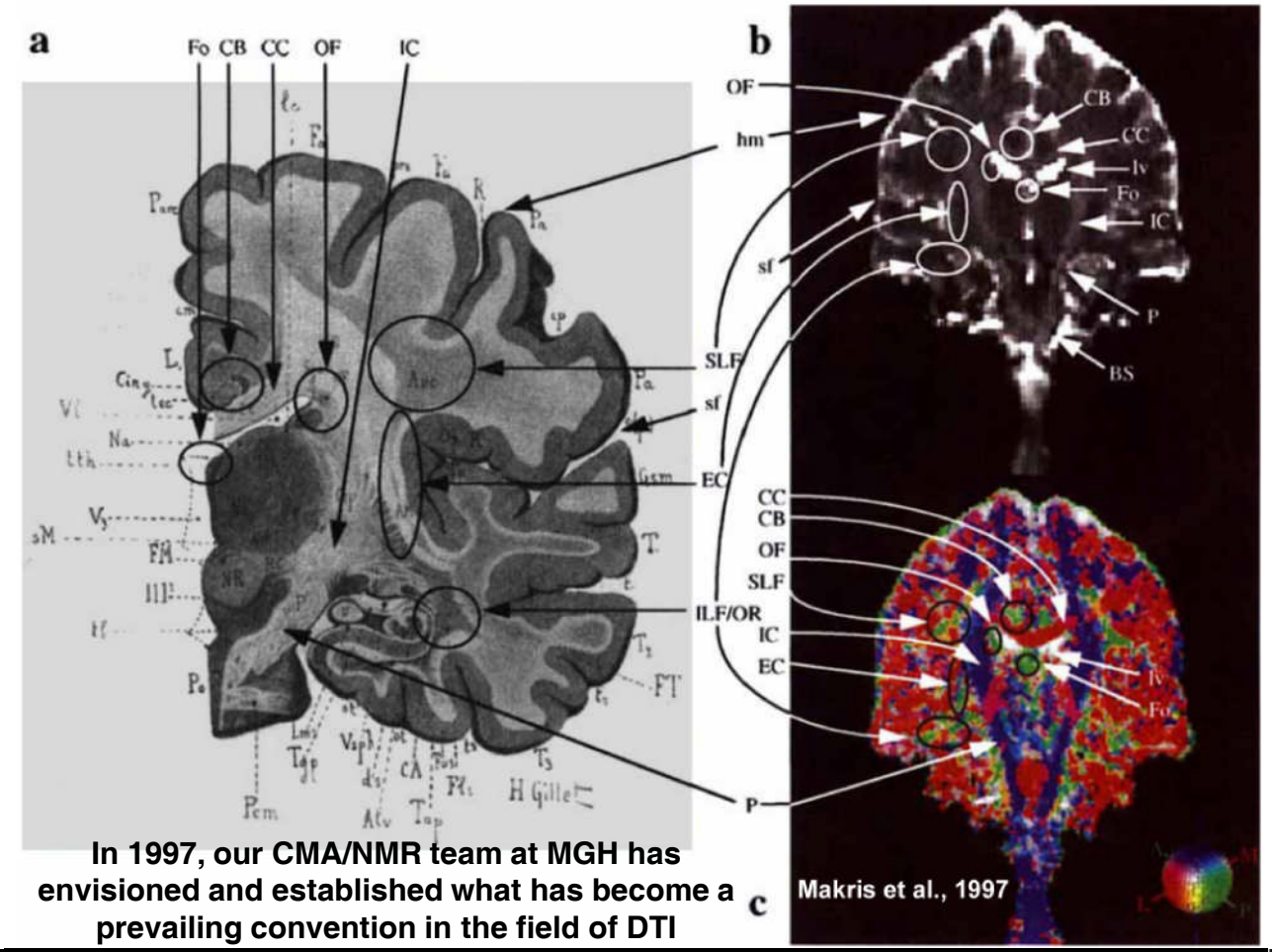

In 1997, our CMA/NMR team at MGH has envisioned and established what has become a prevailing convention in the field of DTI

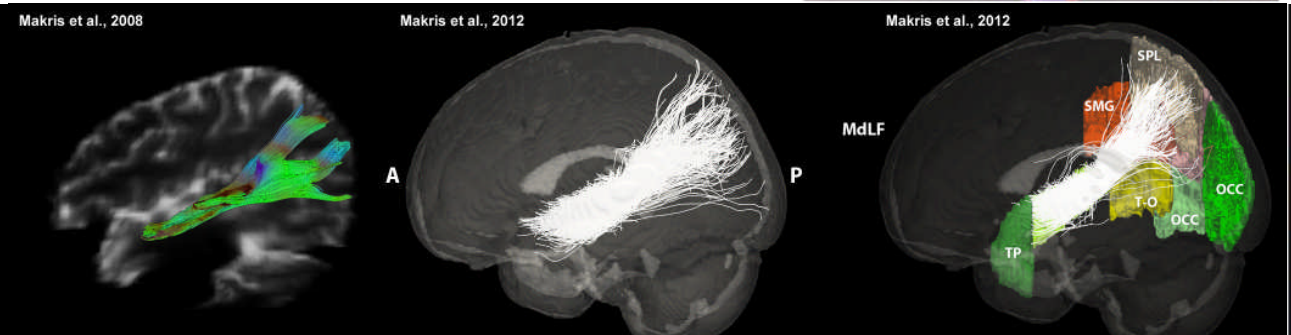

Between 1999 (Makris PhD thesis) and 2012 (Makris et al., 2008, 2012, 2013), Makris and Pandya have provided evidence for a novel fiber tract in humans, named, by them, the "Middle Longitudinal Fascicle" (MdLF) *(Makris, Pandya, et al., Cer Cor, 2008)*

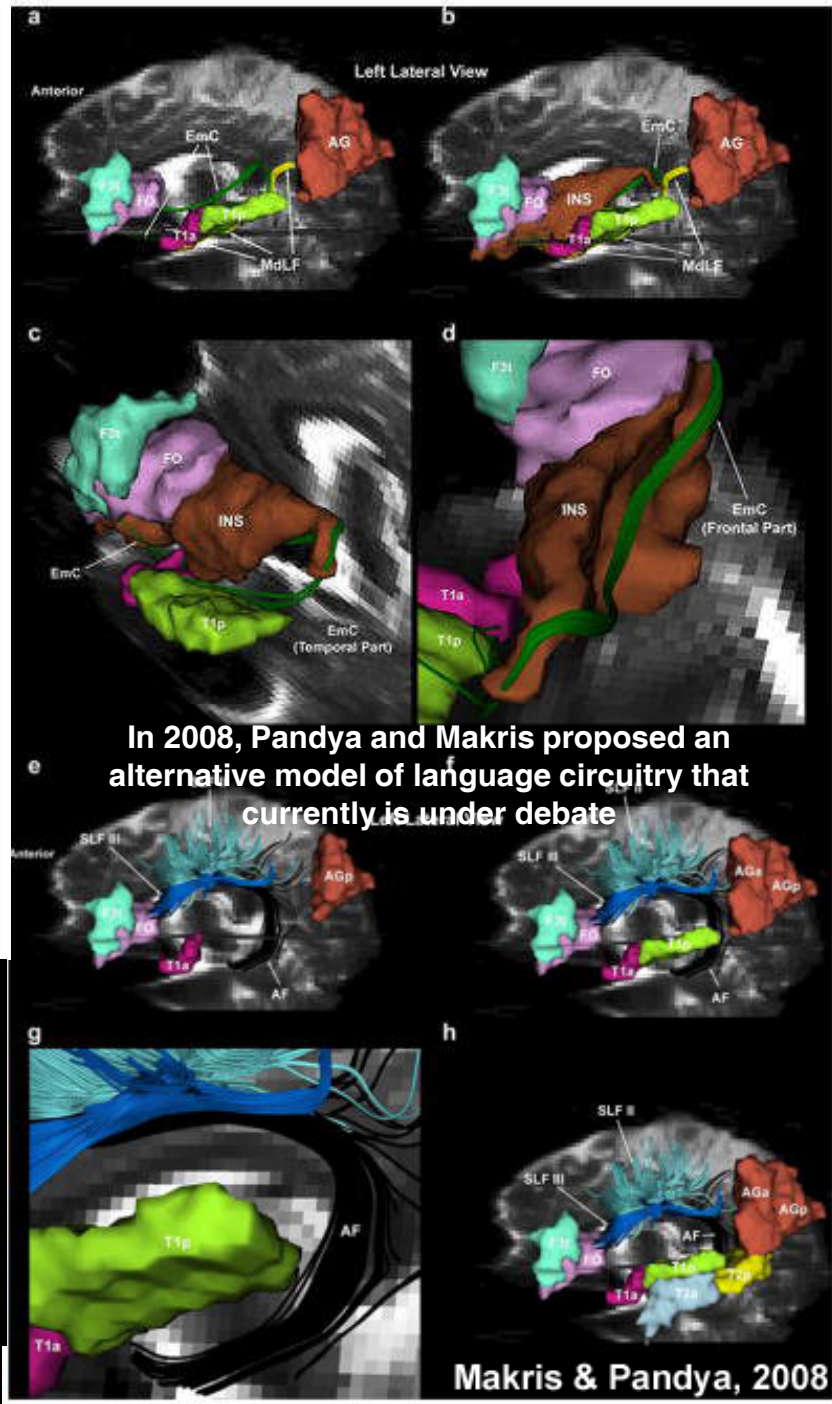

In 2008, Pandya and Makris proposed an alternative model of language circuitry that currently is under debate

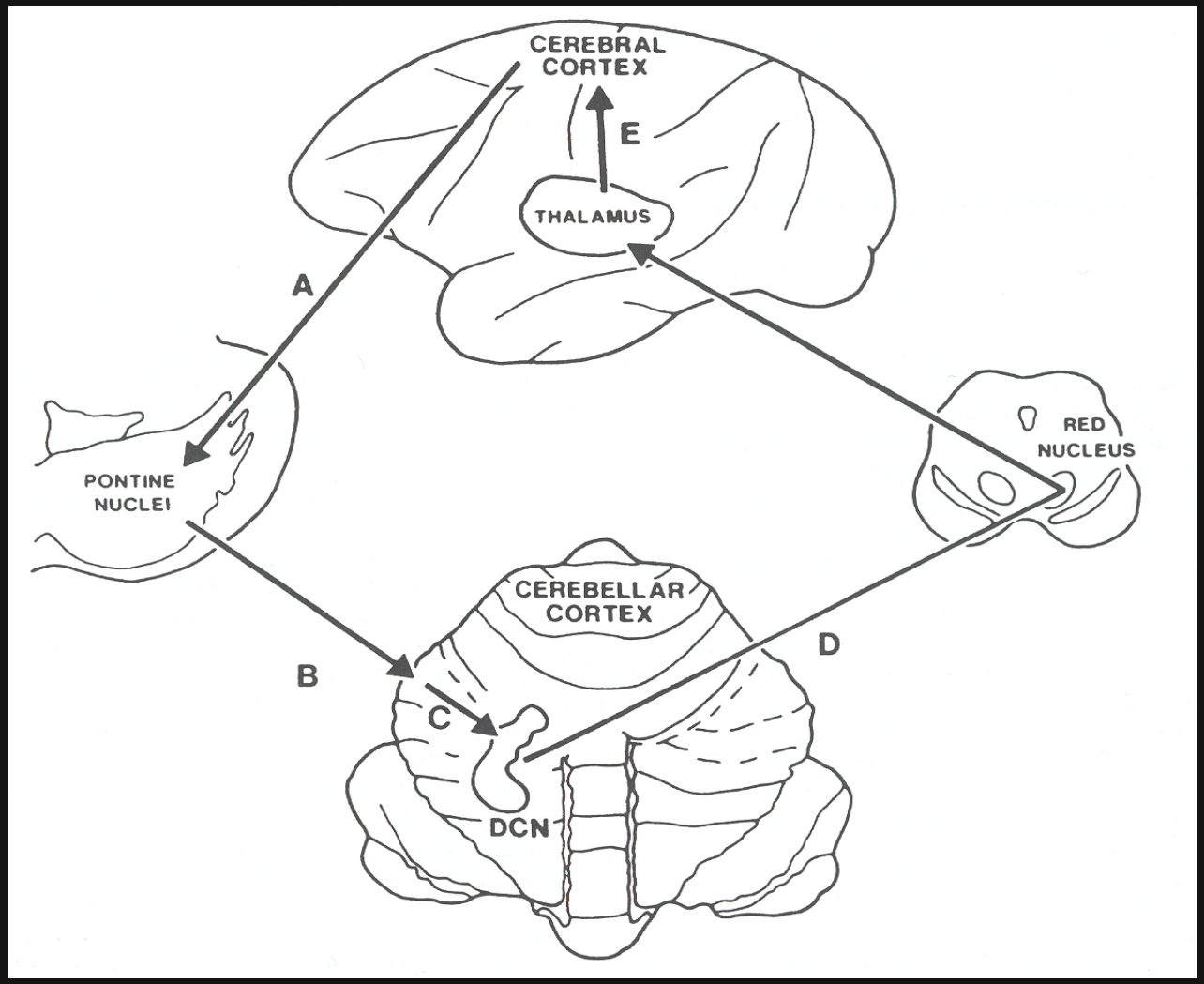

Diagrammatic representation of the cerebrocerebellar circuitry, including corticopontine connections which carry higher-order (*Cognitive*) information as well as sensorimotor inputs to the cerebellar cortex.

From Schmahmann 2000

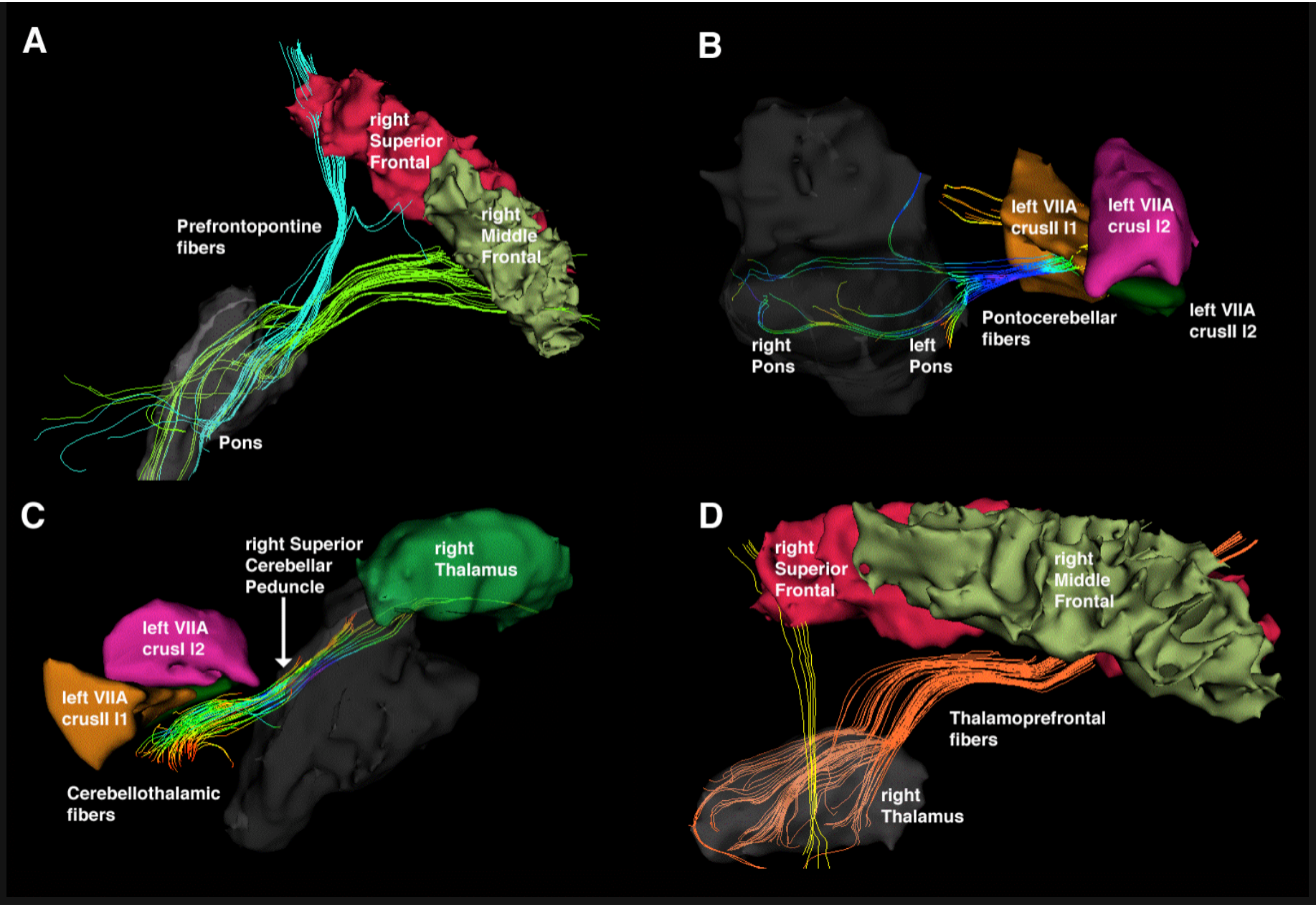

Prefrontocerebellar circuitry: A) Prefrontoponine ipsilateral projection, B) c rossing pontocerebellar projection, C) crossing cerebellothalamic projection, and D) thalamoprefrontal ipsilateral projection

Imaging Circuitries in the Developing Brain

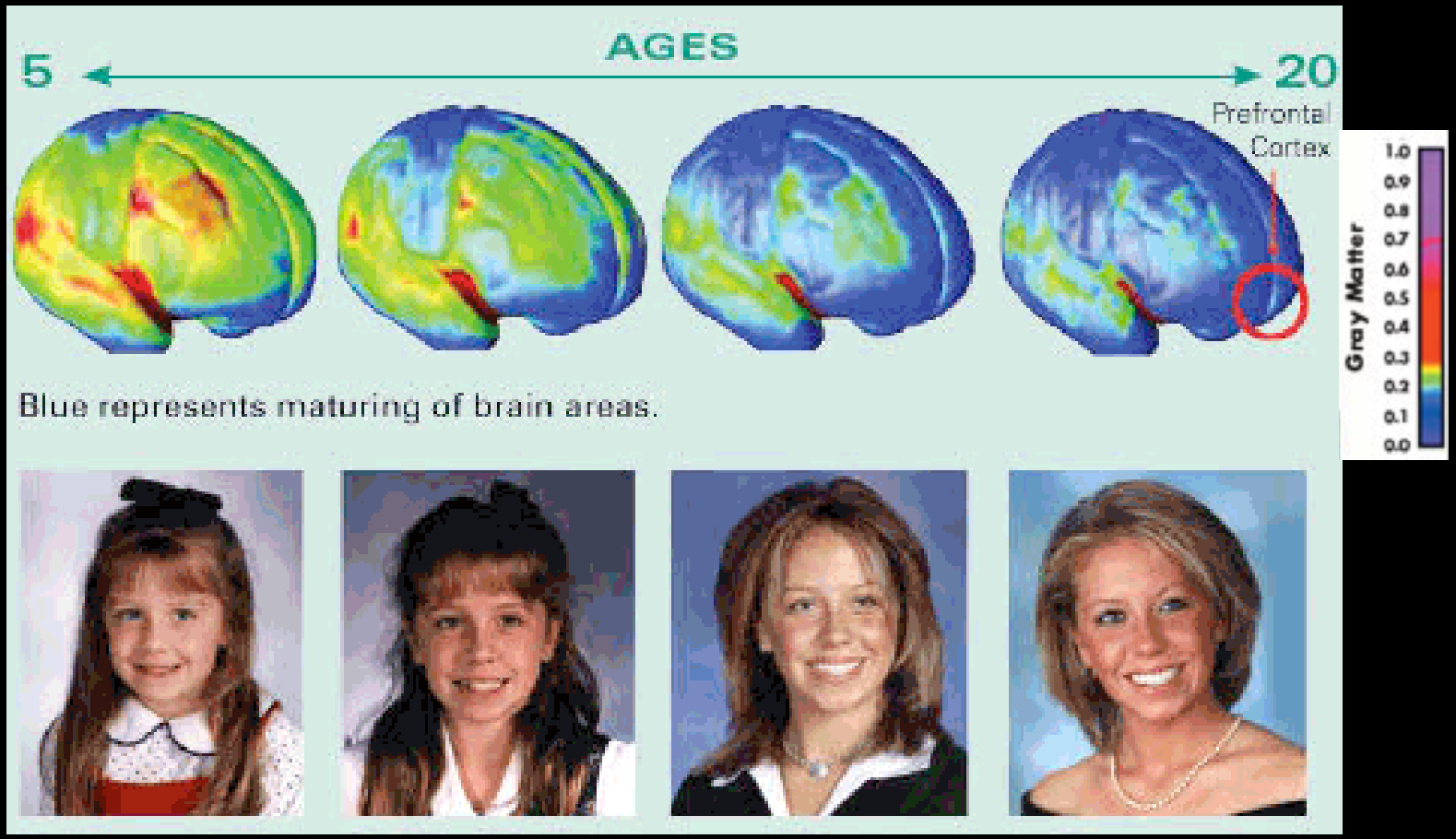

The above composite MRI brain images show top views of the sequence of gray matter maturation over the surface of the brain.

Courtesy of Dr. Scott Lukas

The Developing Brain

Prefrontal Cortex

- Planning behavior
- Use of strategies
- Cognitive flexibility (can you change your mind)
- Fluid methods of solving problems

--The *Executive Office* of the brain is still being built during the teenage years--

Courtesy of Dr. Scott Lukas

The Developing Brain

- The brain matures from the back to the front, so the frontal cortex is the last area to be completed.
- Insight, judgment, decision-making, risk taking, impulse control, are all impaired in adolescents.
- During this most vulnerable period is when teens are more likely to experiment with drugs and other damaging activities.

Courtesy of Dr. Scott Lukas

Executive and Attention cognitive systems are critical during development

Dorsal visuospatial attention system

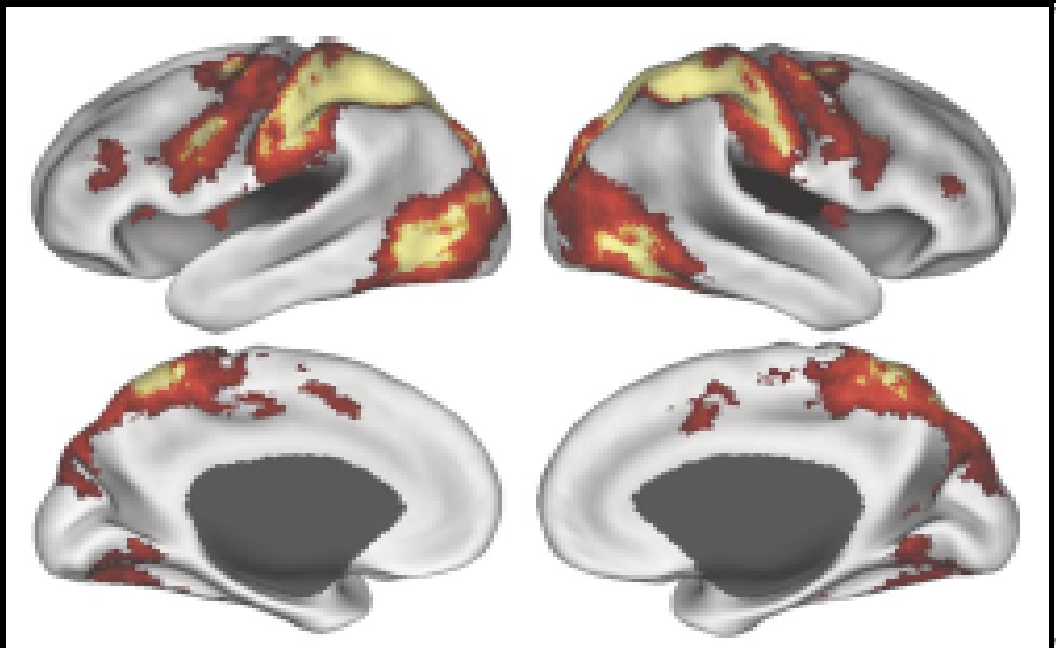

Frontoparietal executive control system

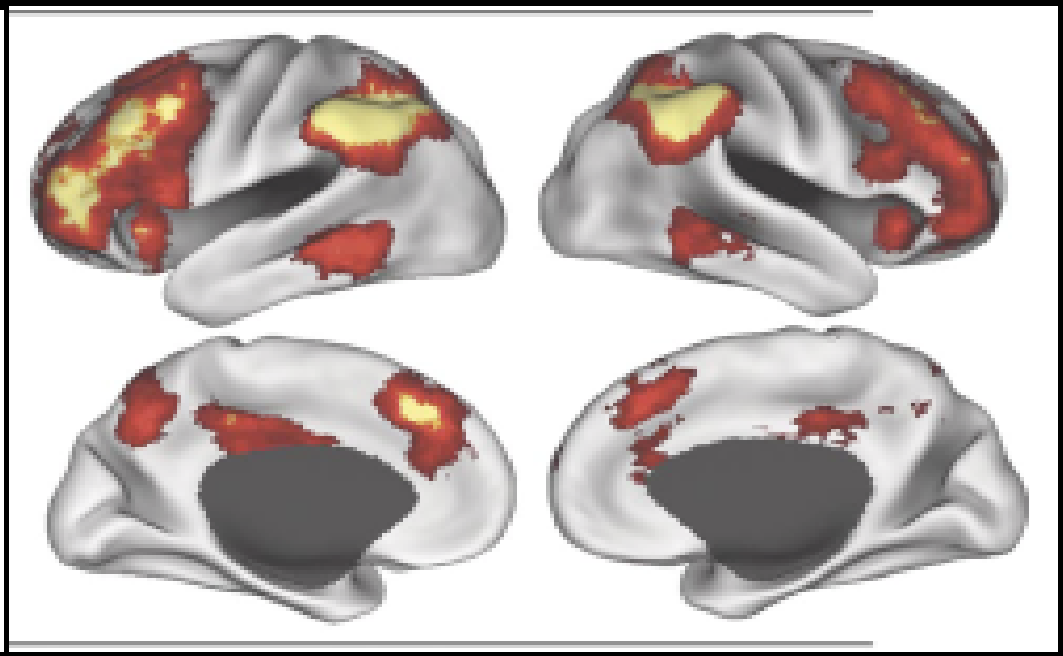

Vincent et al., J Neurophys, 2008

Brain Reward Circuitry (RWC)

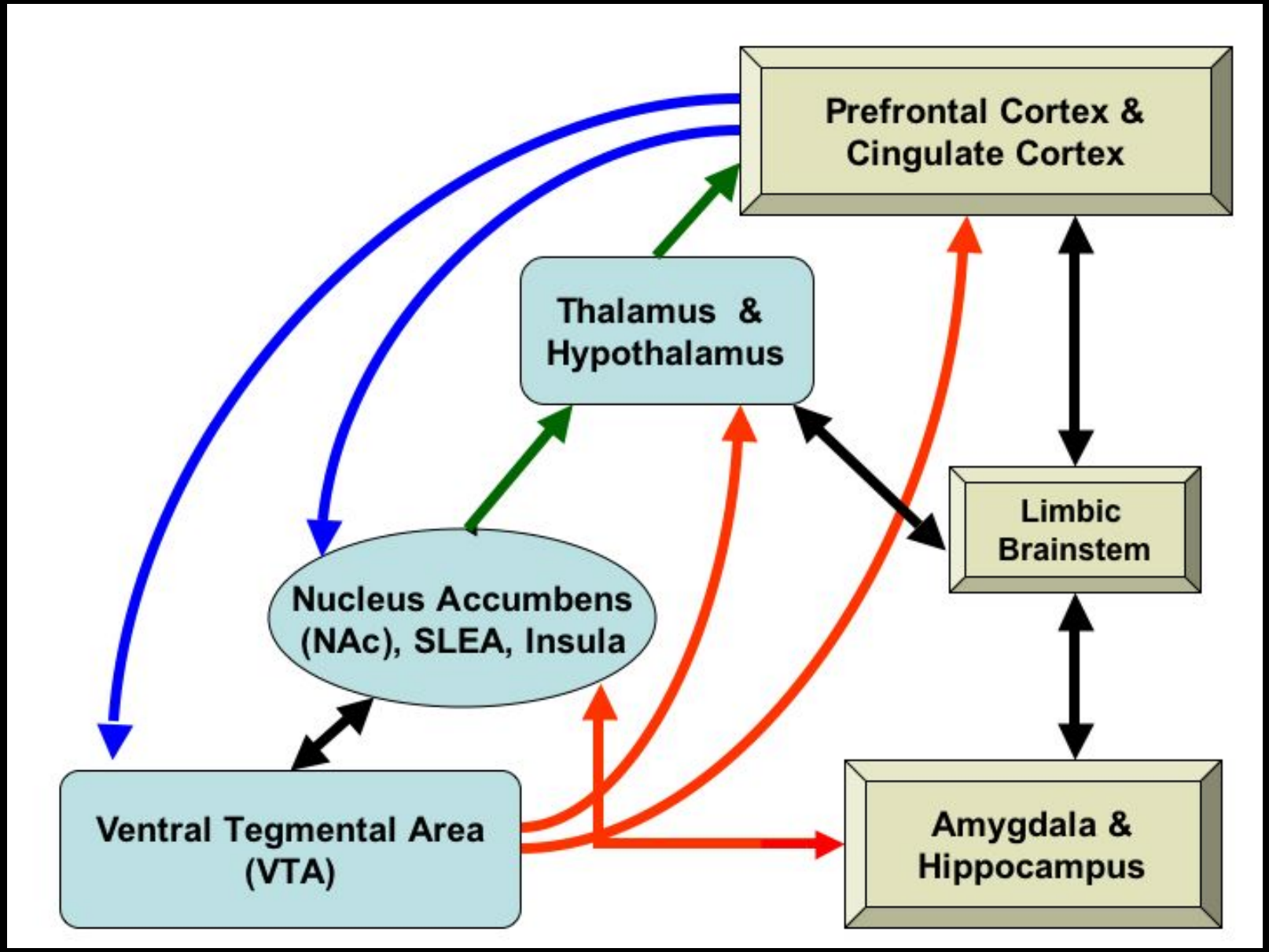

Brain Reward Circuitry:

The Extended Reward and Oversight System consists of cortical and subcortical structures involved in controlling emotion and regulating sensitivity to reinforcements.

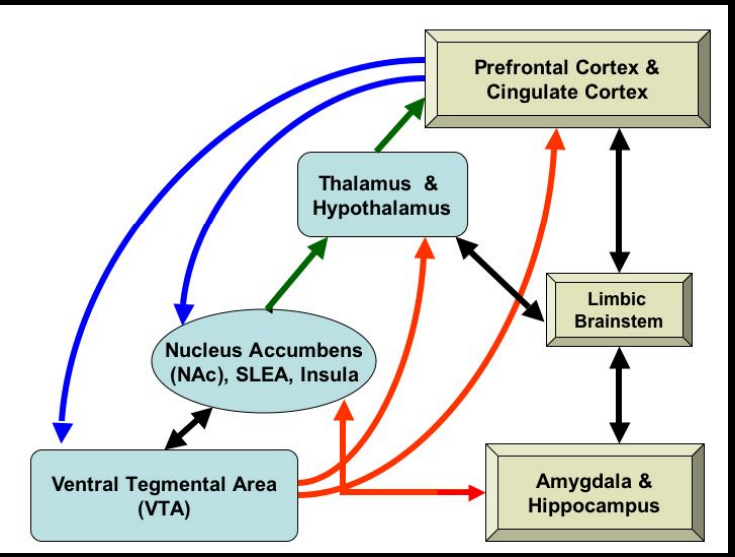

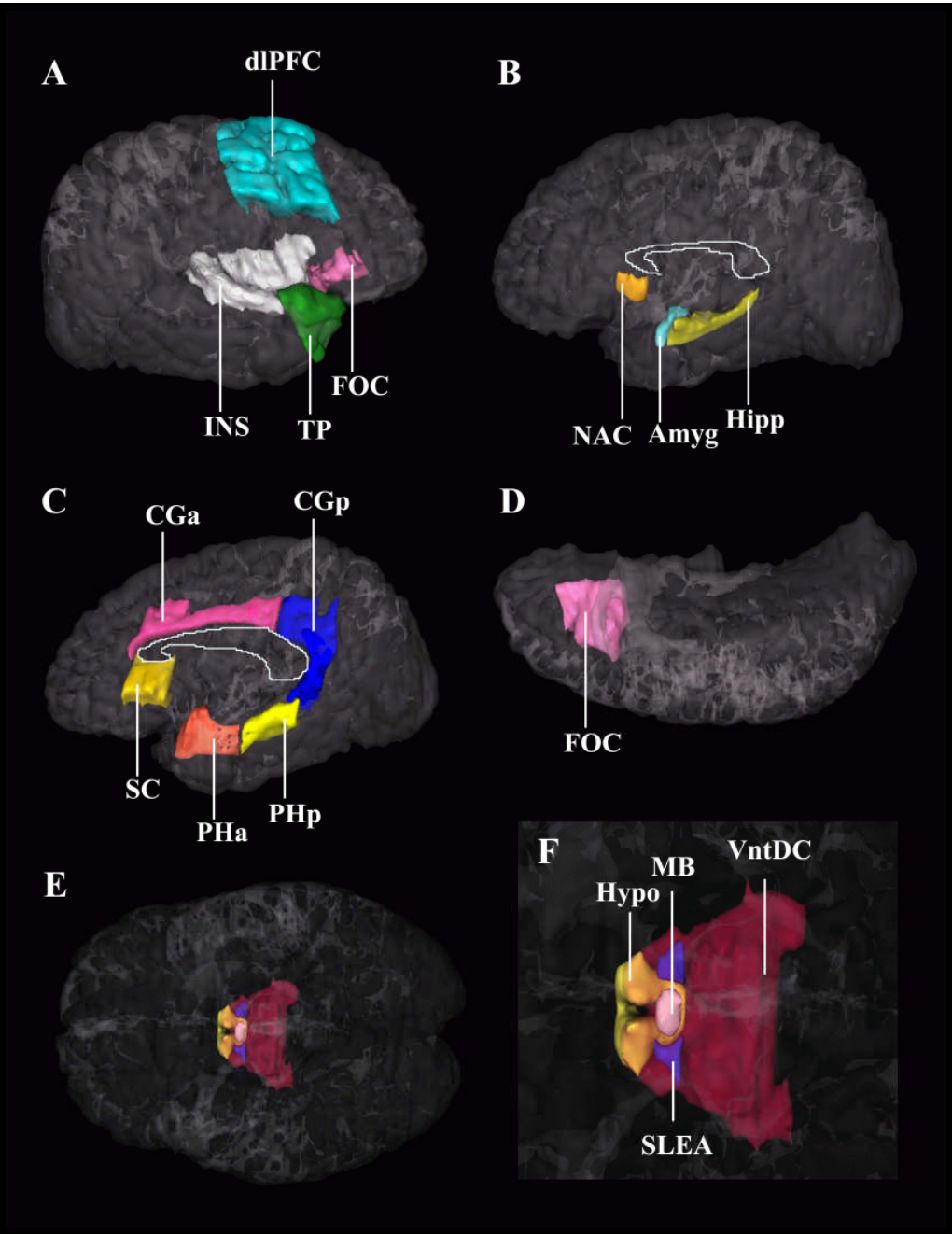

Makris et al., Biological Psychiatry, 2008

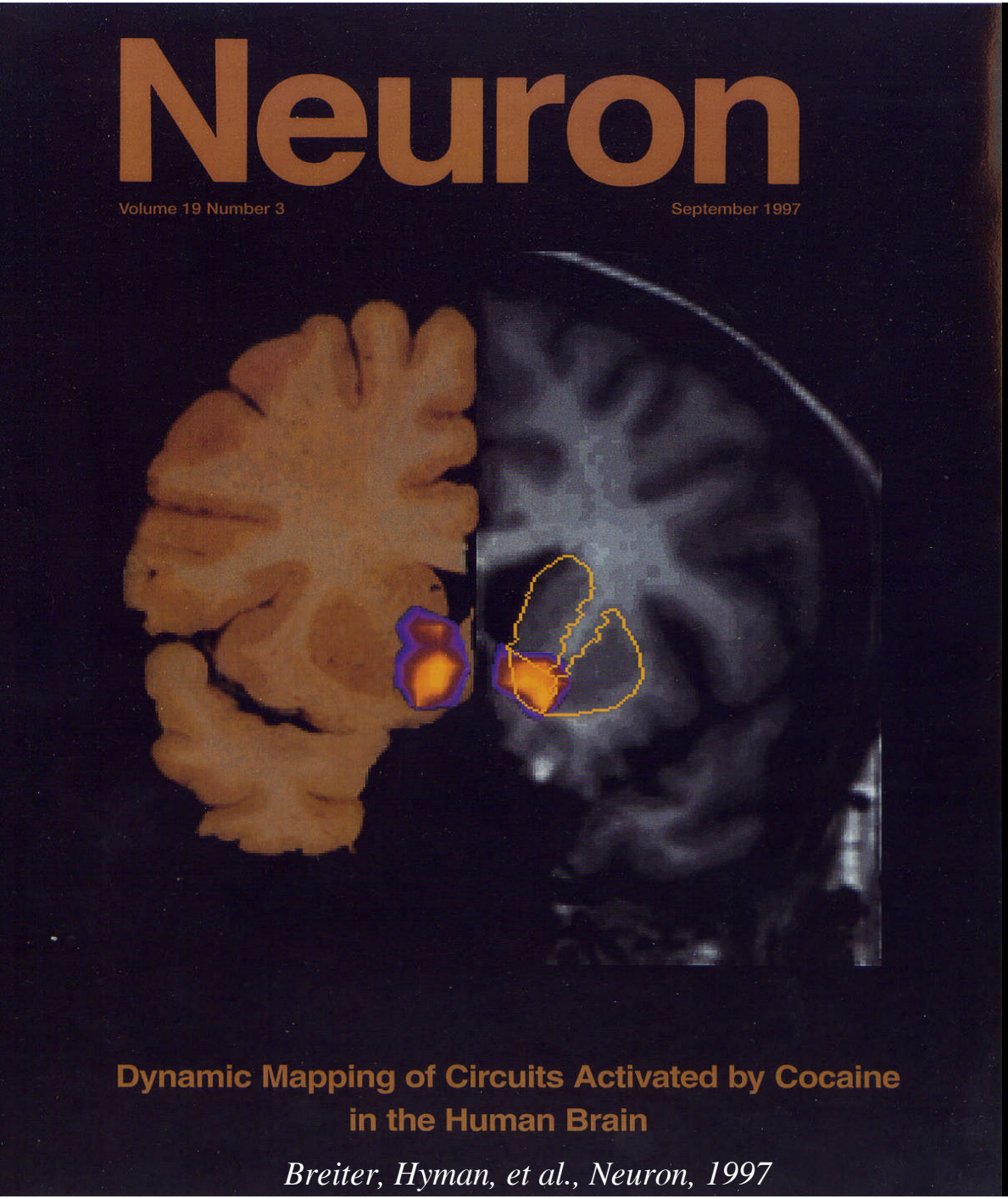

In cocaine abuse there are also observed alterations in the brain network for reward

Amygdala in Cocaine Addiction

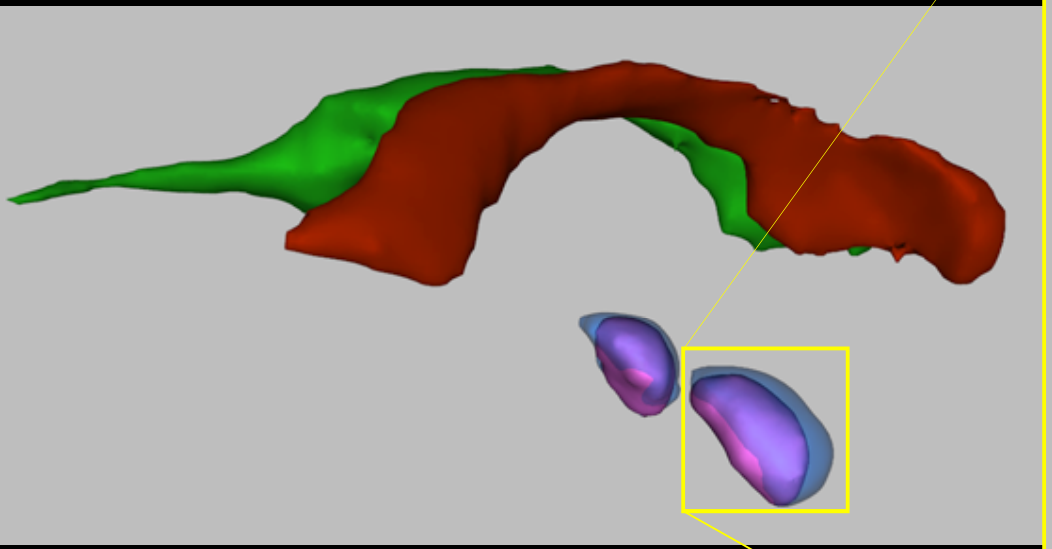

Right Amygdala

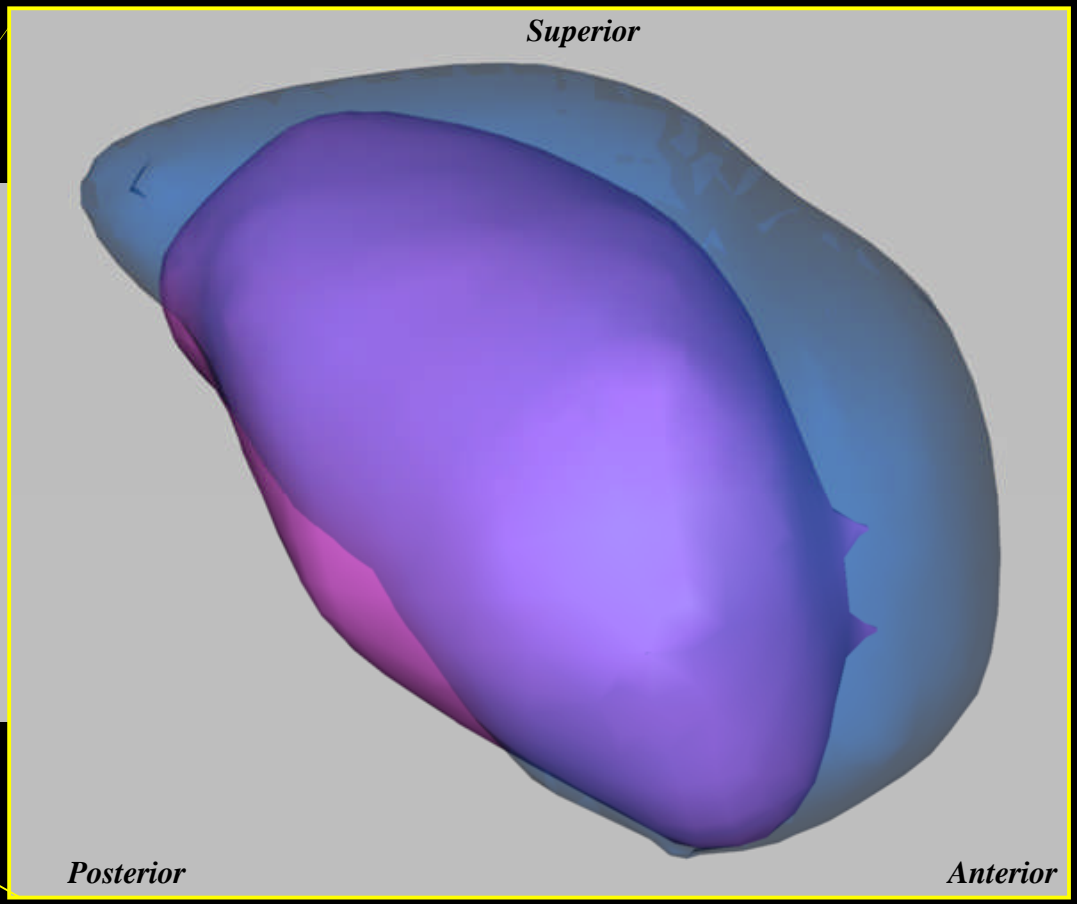

Patients
Normal Controls
Common

Right Lateral Ventricle = red
Left Lateral Ventricle = green

23% Volume Reduction

Makris et al., Neuron, 2004

Cortical Thinning in Reward System in Cocaine Addiction

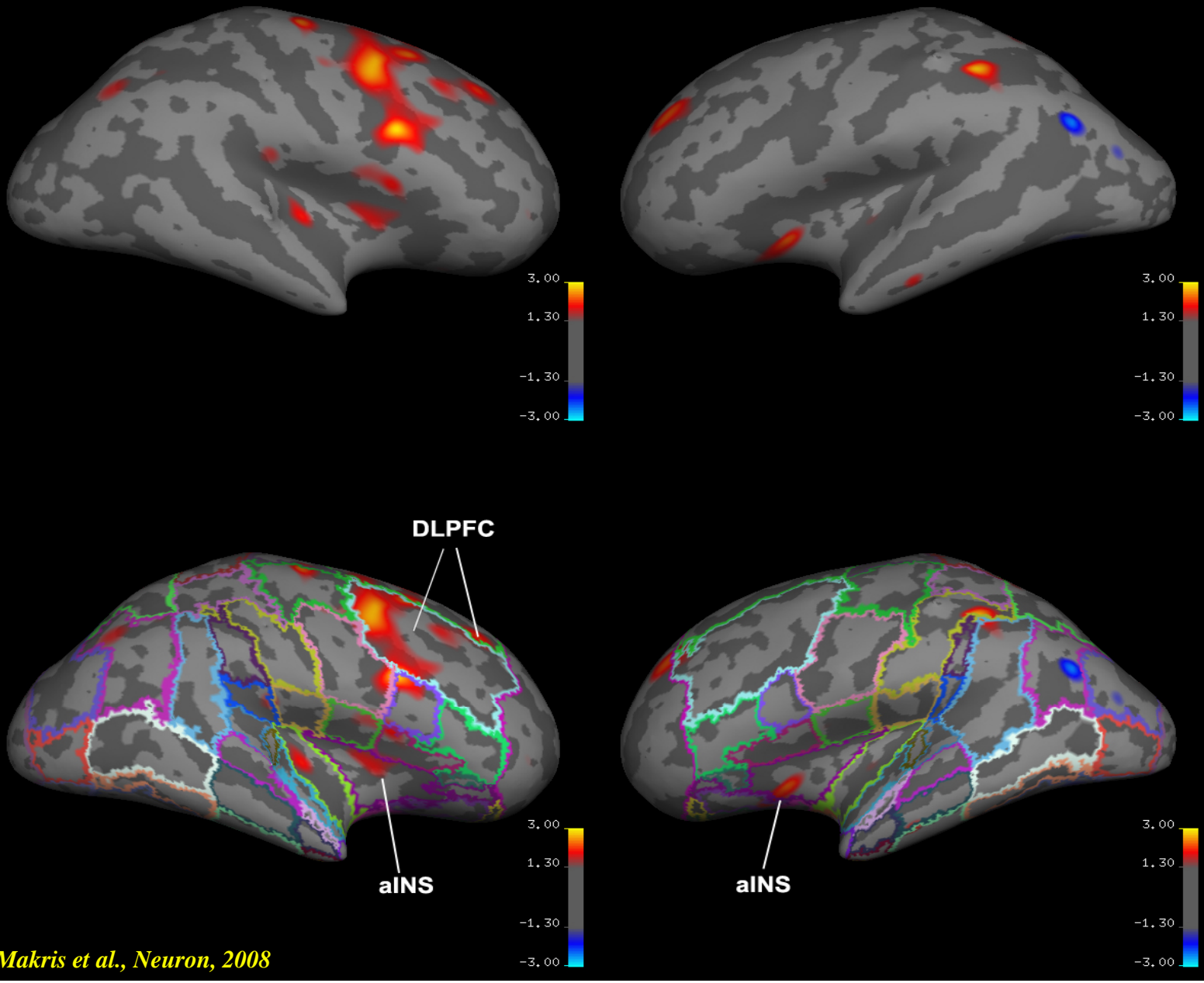

Makris et al., Neuron, 2008

Tobacco: Role in Drug of Abuse

Reduced brain metabolism in smokers

- Lower test scores
- Poor athletic ability
- Lower cognitive function
- Poor decision making

Courtesy of Dr. Scott Lukas

Smoked Marihuana and fMRI

GLM analyses reveals extensive orbitofrontal and ventromedial prefrontal cortical regions with significant group differences (marihuana > placebo smoking ($p<0.05$ corrected, shown in red-yellow). The single-group analysis shows that marihuana activated these regions and bilateral caudate and nucleus accumbens, while placebo smoking did not.

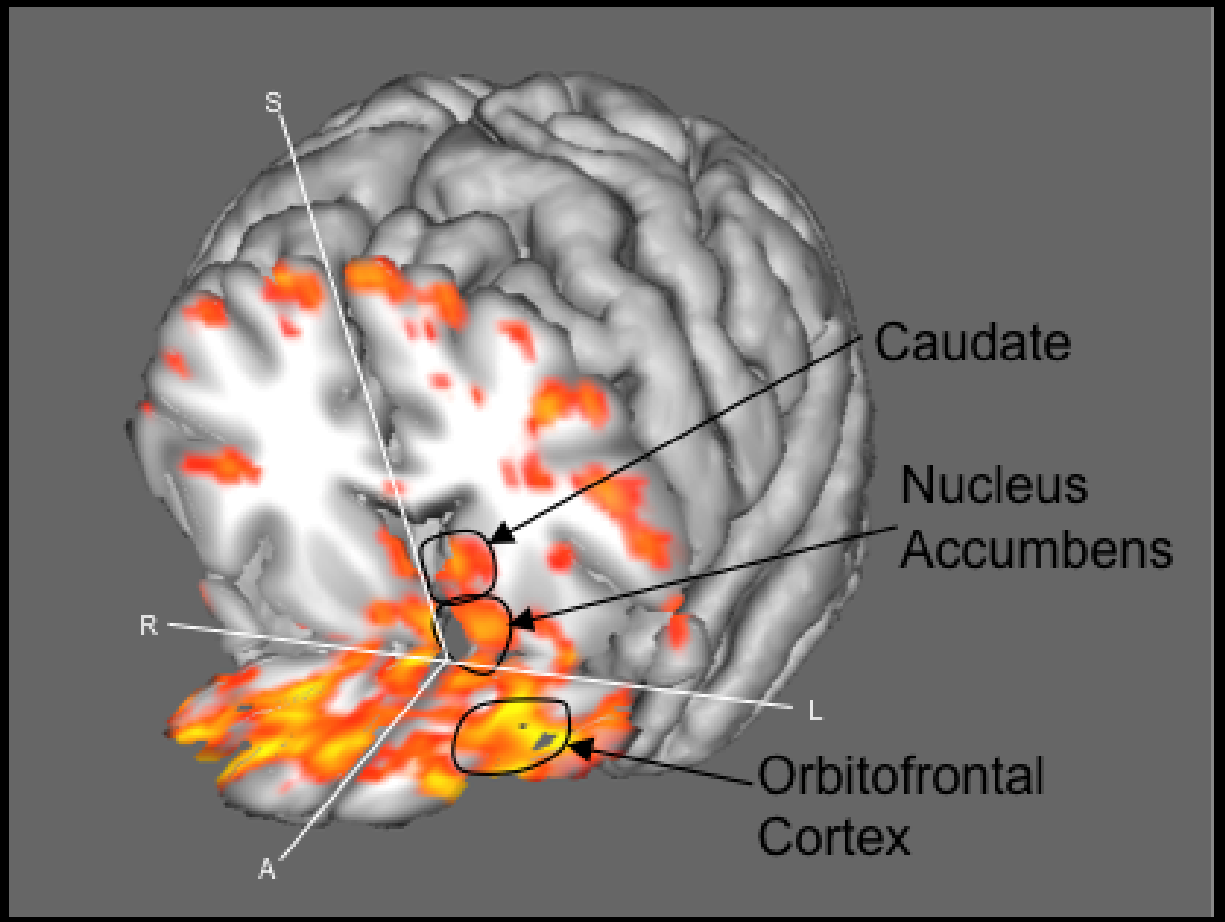

Courtesy of Dr. Scott Lukas

Imaging Neural Systems in Attention Deficit-Hyperactivity Disorder (ADHD)

Neural Systems approach addresses at least three questions

1) Are the structures shown to be altered in ADHD indeed component parts of well-understood neural systems?

2) Do these structural neural systems correlate with specific behaviors?

3) Are these neural systems associated with specific genotypes?

Makris N., et al.,
Dev Neurosci 2009

Figure 1: Conceptual mod el of the pathophysiology and etiology of ADHD

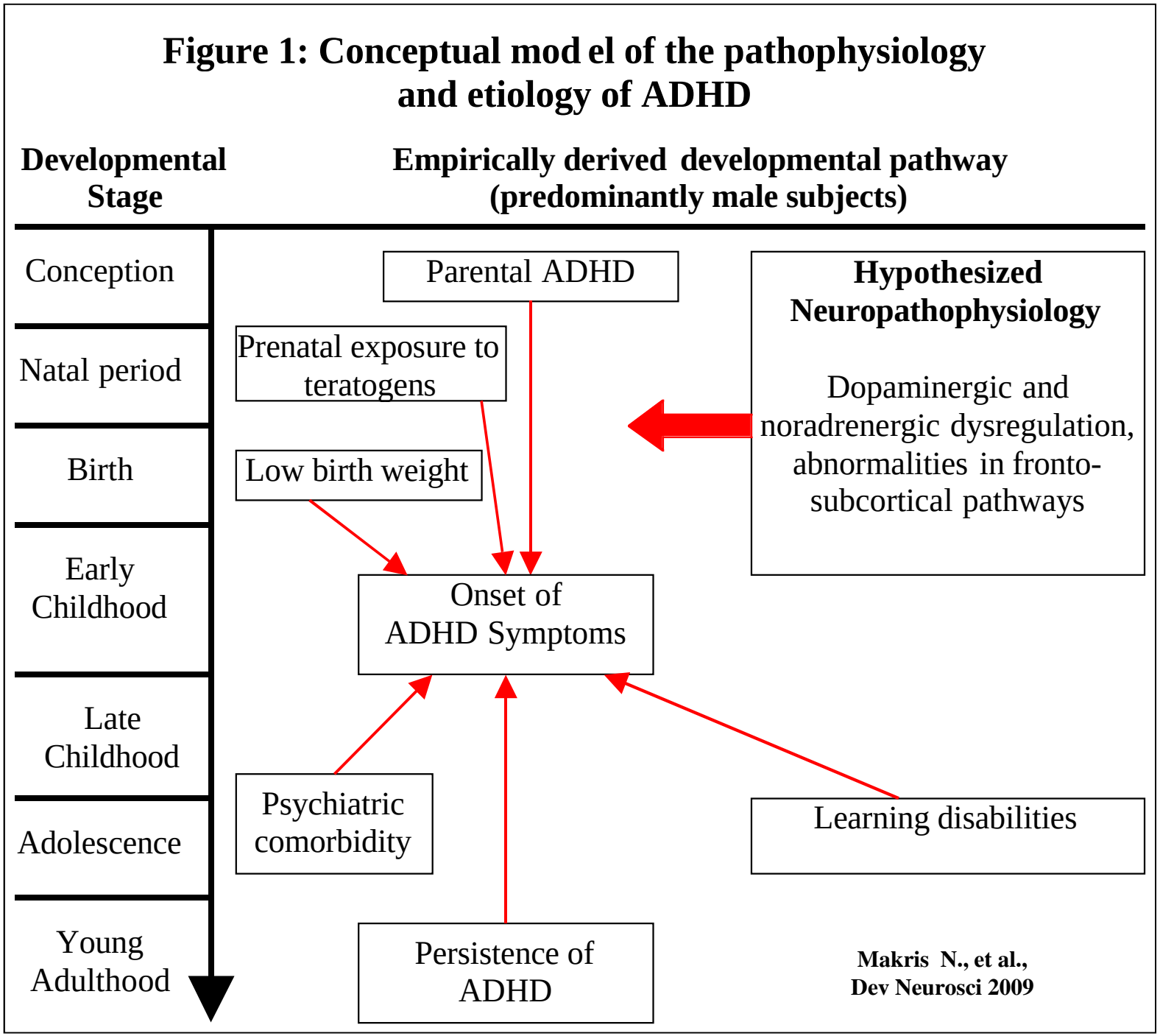

Functional neuroanatomy of neural systems involved in psychiatric disorders

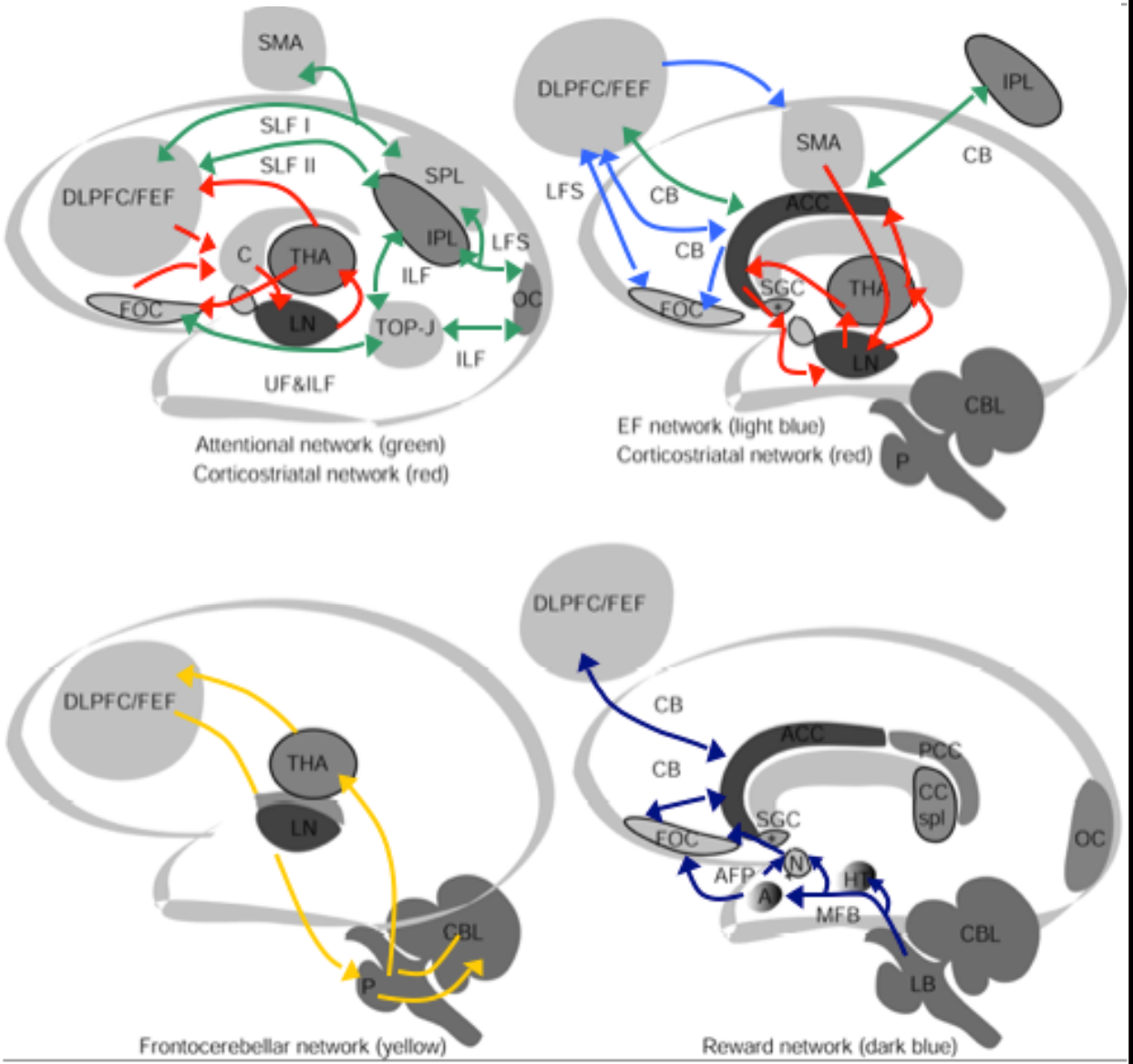

A=amygdala; ACC=anterior cingulate cortex; AFP=amygdalofugal pathway; C=caudate nucleus; CB=cingulum bundle; CBL=cerebellum; CCspl=splenium of corpus callosum (incl. isthmus); DLPFC=dorsolateral prefrontal cortex; FEF=frontal eye field; FOC=fronto-orbital cortex; HT=hypothalamus; ILF=inferior longitudinal fascicle; IPL= inferior parietal lobule; LB=limbic brainstem; LFS=local fiber system; LN=lenticular nucleus; MFB=medial forebrain bundle; N=nucleus accumbens; OC=occipital cortex; P=pons; PCC=posterior cingulate cortex; SGC=subgenual cingulate cortex; SLF=superior longitudinal fascicle; SMA=supplementary motor area; SPL=superior parietal lobule; THA=thalamus; TOP-J=tempro-occipito-parietal junction; UF=uncinate fascicle

Makris N., et al., Dev Neurosci 2009

A major goal of MRI brain research is the study of endophenotypes

Once we quantify **imaging-based markers (or endo-phenotypes)**, for example, size of brain structures (such as cingulate cortex or prefrontal cortex) or **neural systems** (such as the reward, the attention or executive function systems), we may be able to **diagnose** psychiatric illnesses, **assess** treatment and **identify genes** that will lead to **new medications**.

Figure 4: Neural systems biology acts as an interface between behavior and the genome

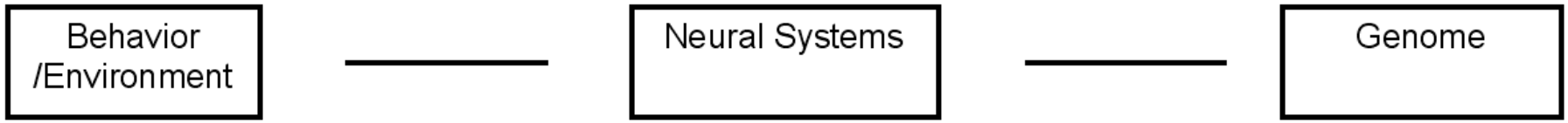

Systems biology *acts as an interface between the* **behavior***/environment and* **genome***/epigenome.*

Makris N., et al.,
Dev Neurosci 2009

Biological Psychiatry

Volume 60, Number 10
November 15, 2006

ISSN 0006-3223
www.sobp.org/journal

Official Journal of the Society of Biological Psychiatry

ADHD: Neurobiological Basis – Neural Systems

Attention Networks

EXECUTIVE CONTROL

ORIENTING (SELECTIVE ATTENTION)

ALERTING

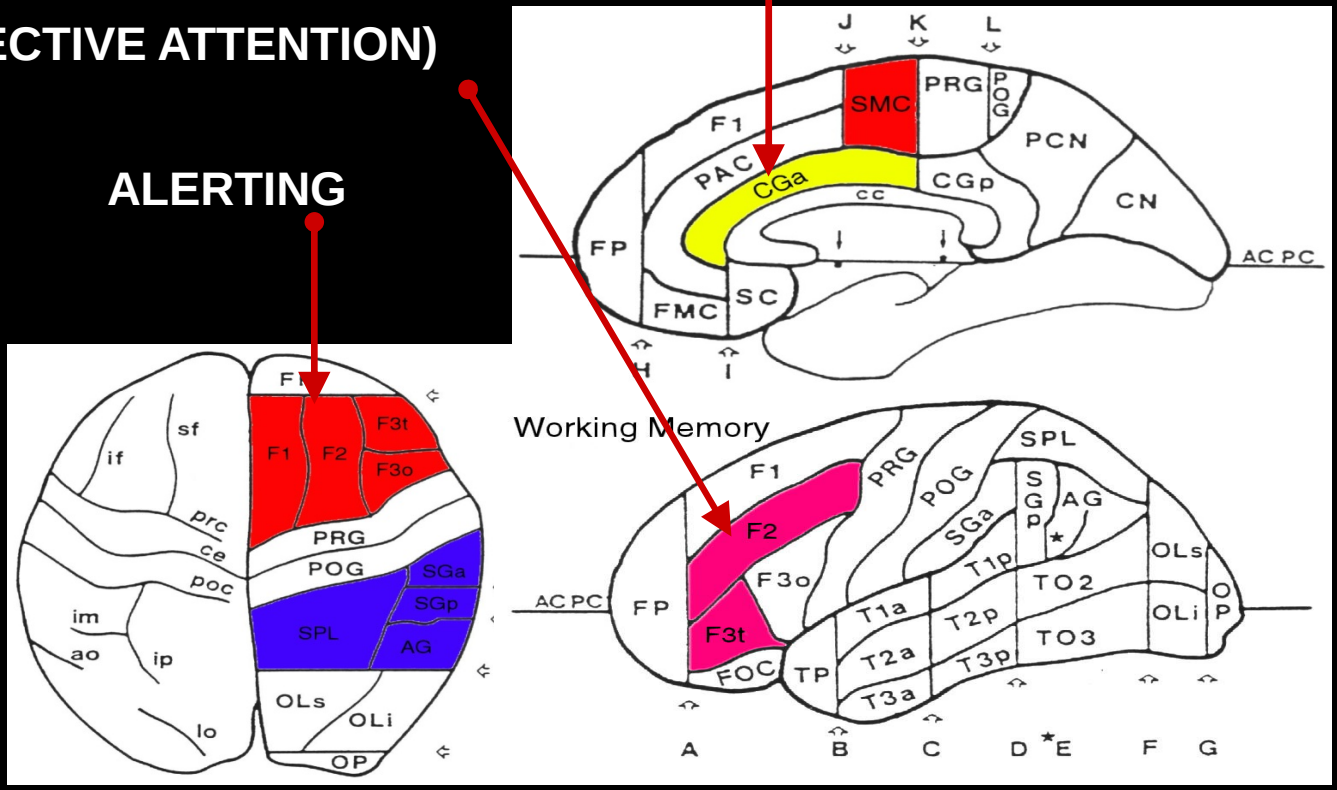

Posner MI, Raichle ME. *Images of Mind*. New York, Scientific American Books; 1996.

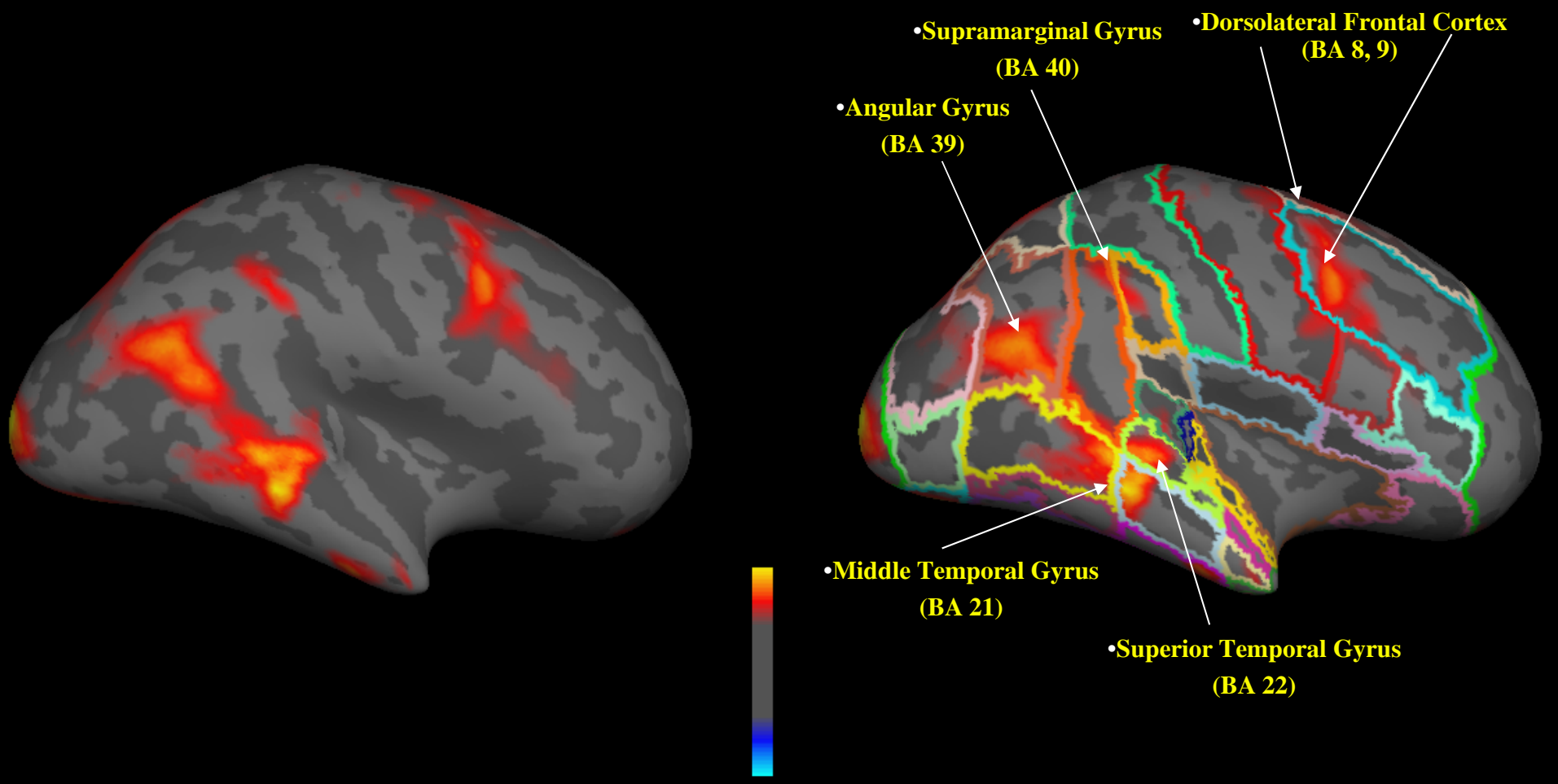

Makris, Seidman et al., *Cerebral Cortex*, 2007

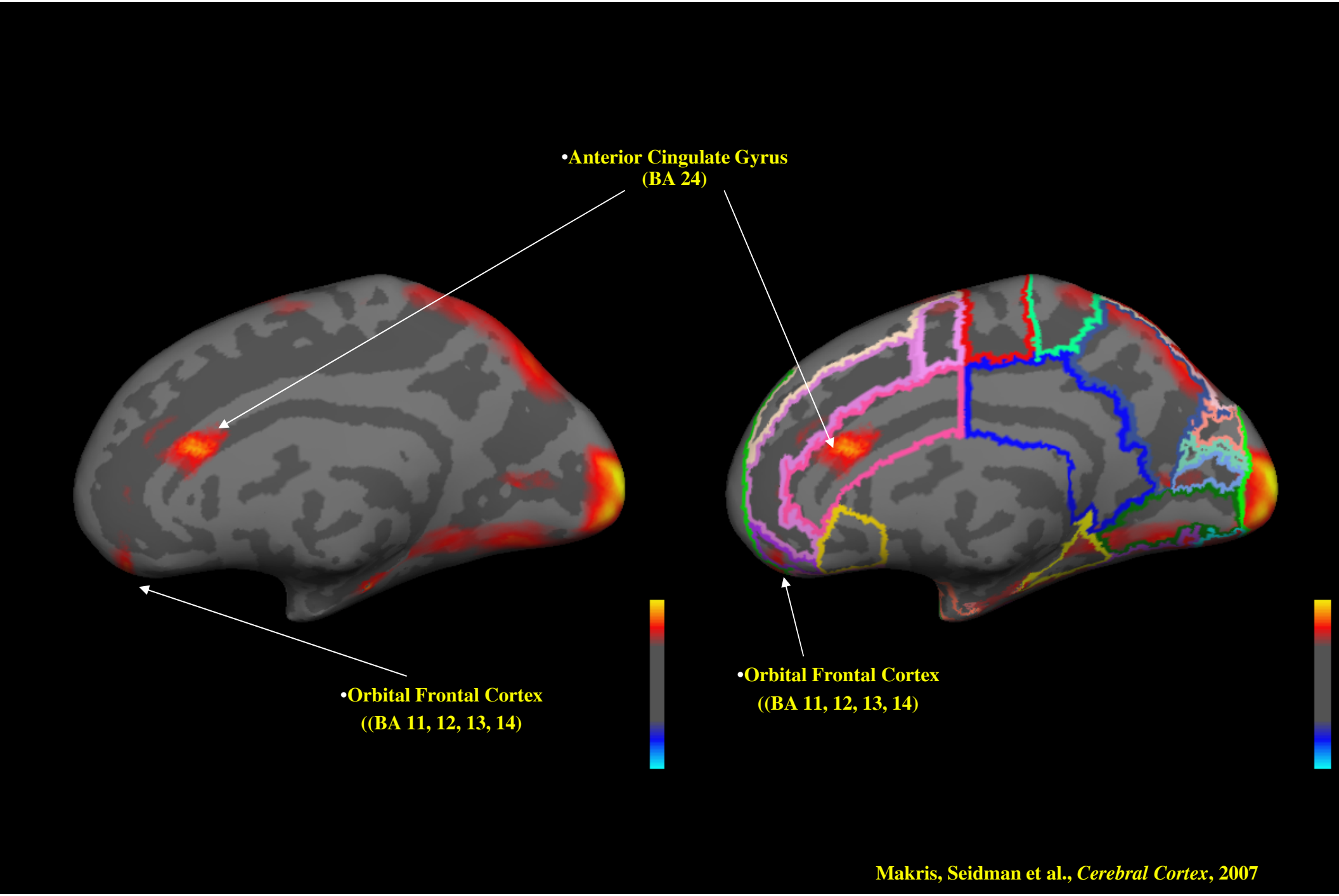

Makris, Seidman et al., *Cerebral Cortex*, 2007

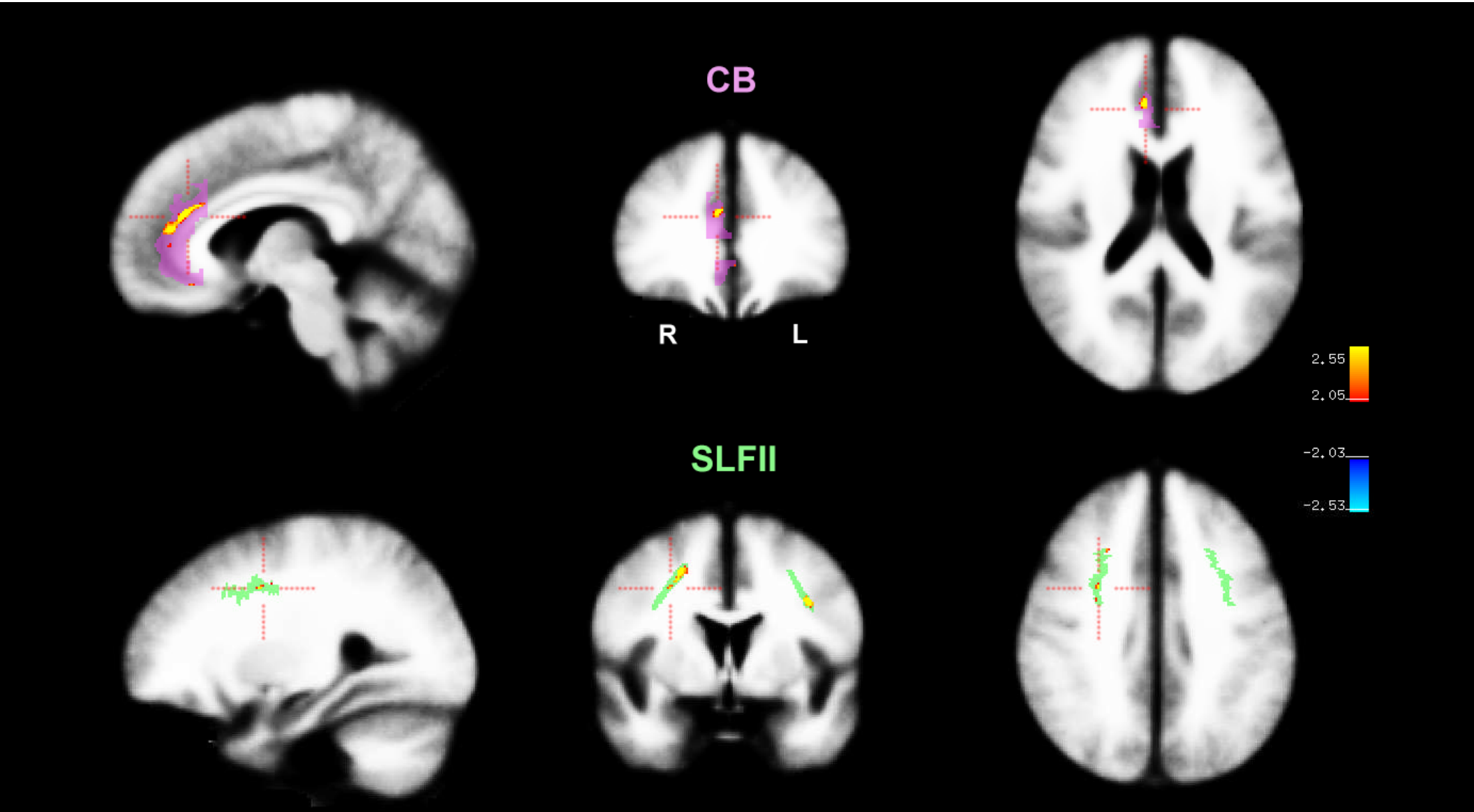

Fractional anisotropy decrease in ROIs for the cingulum bundle and the superior longitudinal fascicle II (SLF II) in adults with ADHD

Makris, Seidman et al., *Cerebral Cortex*, 2008

Some challenges in psychiatric imaging

Diagnosis at a brain circuitry level

Clear localization of abnormalities

Instantaneous results with treatment

Use of advanced mathematical modeling

Subgenual Cingulate Cortex (BA 25)

Increased activity with sadness and depression (a, b) (using PET)

Decreased activity with chronic fluoxetine treatment for depression (c) or natural placebo recovery (d)

Decreased activity in responders vs non-responders to CBT and citalopram for social phobia (e, f)

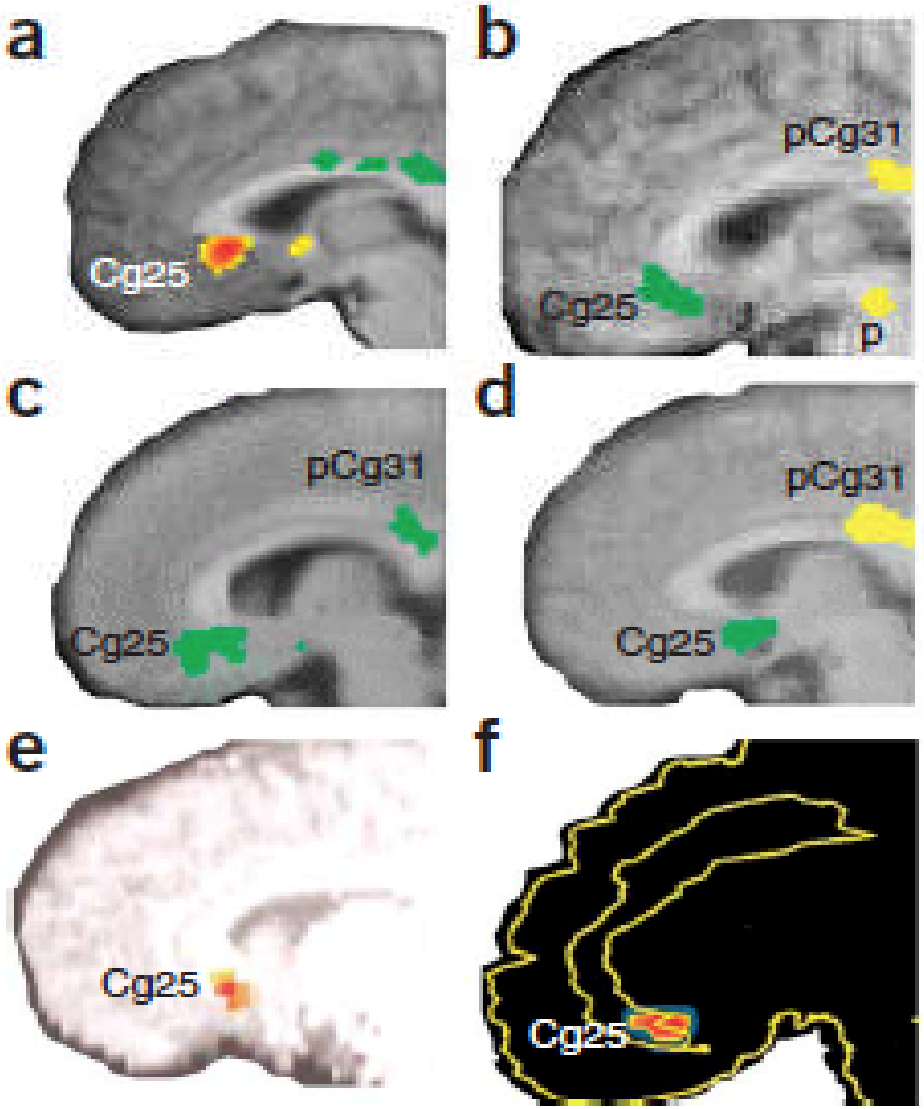

Figure 1 Subgenual cingulate cortex activation across studies. (**a**) Transient sadness in healthy volunteers increases activity (red) in Cg25 (arrow) measured with positron emission tomography (PET) (from ref. 12. Reprinted with permission from the *American Journal of Psychiatry*, copyright 1999, American Psychiatric Association.). (**b**) Decreased Cg25 activity (green) with chronic fluoxetine treatment for depression. (**c**) Cg25 decrease (green) in recovery with chronic fluoxetine from Parkinson's disease–related depression. (**d**) Natural recovery with decreased Cg25 activity (green) in patients treated with placebo. Panels **b**–**d** reprinted from ref. 11 by permission of Oxford University Press. (**e**) Predictors of response in subjects responding to CBT for depression included low pretreatment Cg25 activity (red) (from ref. 15. Reprinted with permission from the *American Journal of Psychiatry*, copyright 1999, American Psychiatric Association.). (**f**) Subgenual cortical decreased activity (red) was common in responders compared with nonresponders for those responding both to citalopram and to CBT for social phobia (from ref. 16. Reprinted from *Archives of General Psychiatry*, copyright 2002, American Medical Association. All rights reserved.).

Ressler and Mayberg, Nature Neuroscience, 2007

Deep Brain Stimulation (DBS)

One possible mechanism: DBS-induced inhibition [e.g., DBS in PD at GPi: discharges from high-frequency discharge neurons showing inhibitory periods after each stimulus pulse (a, b)]

DBS at Cg25 for depression (c-f)
Preoperative (d)
At 3 months in treatment responders (f)

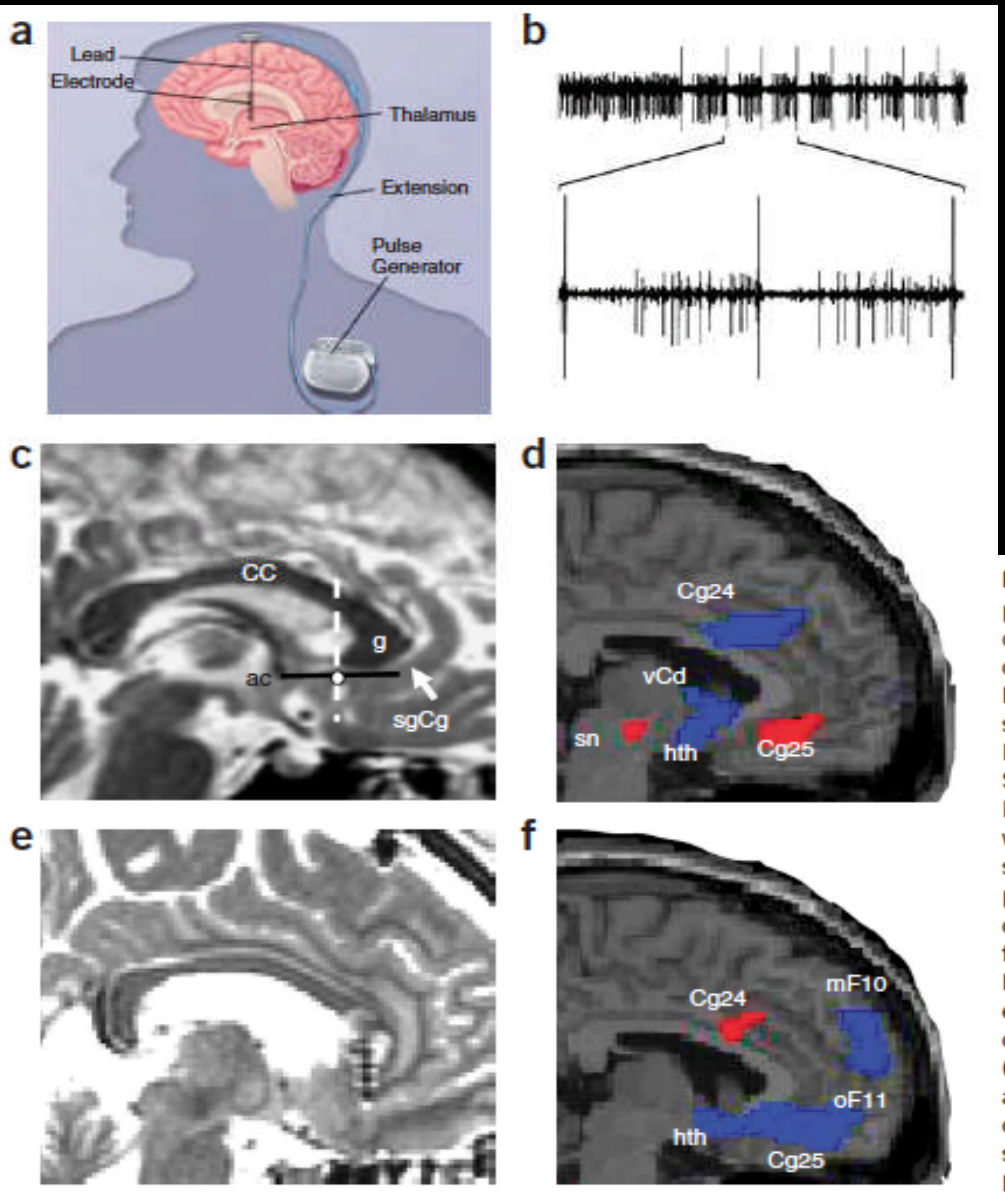

Figure 4 Deep brain stimulation. (**a**) Schematic of DBS used for Parkinson's patients (modified from WebMD, http://www.medicinenet.com/deep_brain_stimulation/article.htm). (**b**) One possible mechanism of action of DBS-induced inhibition: recordings from a globus pallidus internus (GPi) high-frequency-discharge neuron showing inhibitory periods after each stimulus pulse (50 μA) (from ref. 100. Copyright 2000 by American Physiological Society. Reproduced with permission of American Physiological Society via Copyright Clearance Center.). (**c**) Preoperative MRI target localization for DBS for refractory depression. White dot, location of the sgCg white matter targeted for electrode placement in the DBS depression study, shown in a single subject; white arrow, sgCg gyrus; dotted line, anterior-posterior location of the electrode along the line (black) between anterior commissure and genu of the corpus callosum. (**d**) Baseline PET-derived blood flow: depressed patients show increased activity (red) in Cg25 compared with healthy controls. (**e**) Postoperative MRI in a single DBS patient showing the electrode tip in the sgCg white matter. (**f**) At 3 months, regions of blood flow change measured with PET in treatment responders show decreased activity (blue) compared with pretreatment. Panels **c**–**f** reprinted by permission from an article published in *Neuron*, ref. 58, copyright Elsevier 2005. CC, corpus callosum; ac, anterior commissure; g, genu of the corpus callosum; sgCg, subgenual cingulate; Cg24, cingulate area 24; sn, substantia nigra; hth, hypothalamus; mF10, medial frontal area 10; oF11, orbito-frontal area 11.

Ressler and Mayberg, Nature Neuroscience, 2007

Brain Stimulation-Neuromodulation

Invasive

Deep Brain Stimulation (DBS)

Vagal Nerve Stimulation (VNS)

Noninvasive

Transcranial Magnetic Stimulation (TMS)

Transcranial Direct Current Stimulation (tDCS)

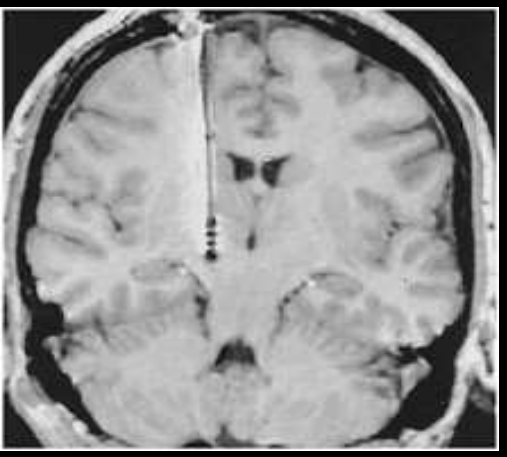

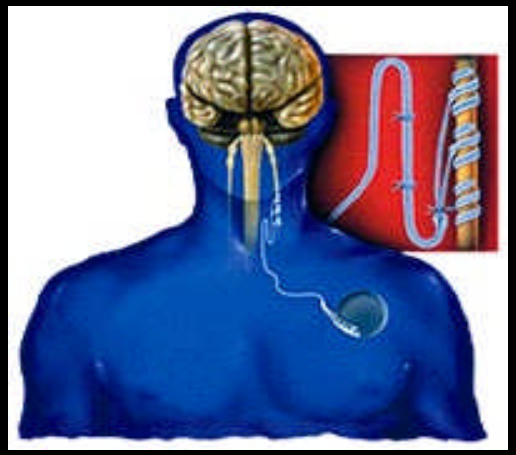

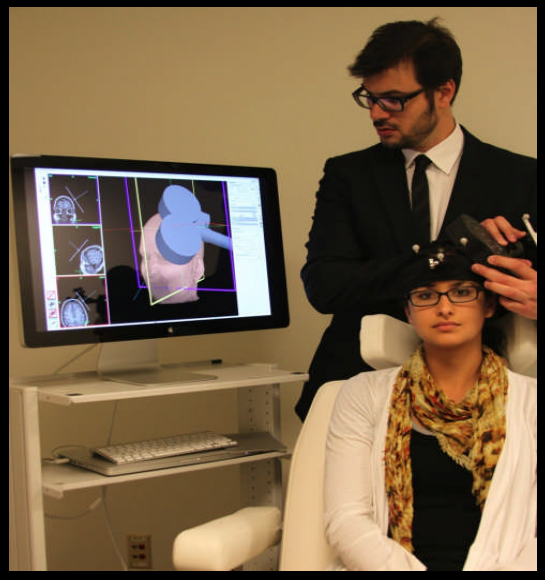

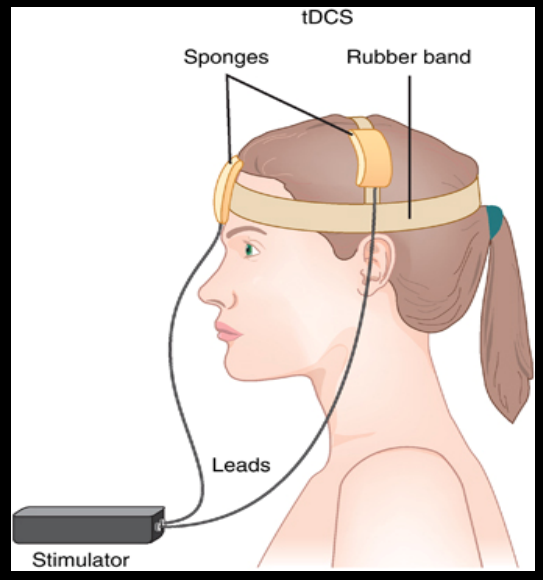

Neuromodulation

- **Neural Pacemaker:** Forces a population of neurons to fire at a specific frequency, changing excitability and functional connectivity both locally and within a given network

- Chronic vs. Discrete Stimulation
- Invasive vs Noninvasive
- All aim to induce adaptive neuroplasticity

Transcranial Magnetic Stimulation

Anthony Barker 1984

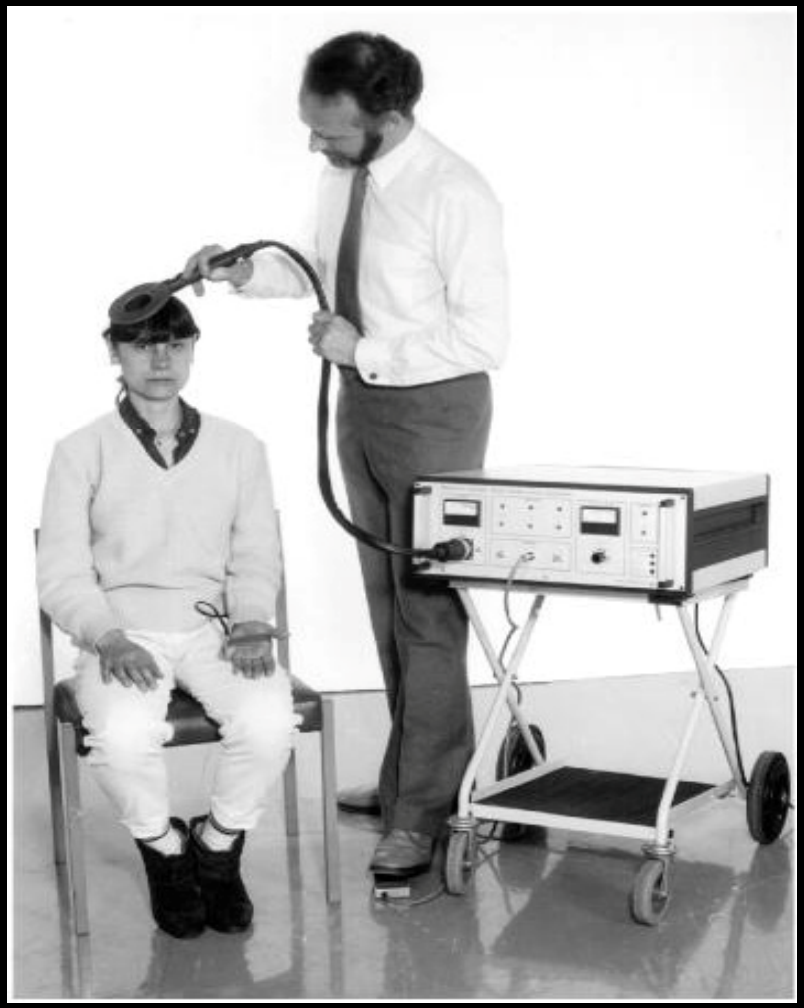

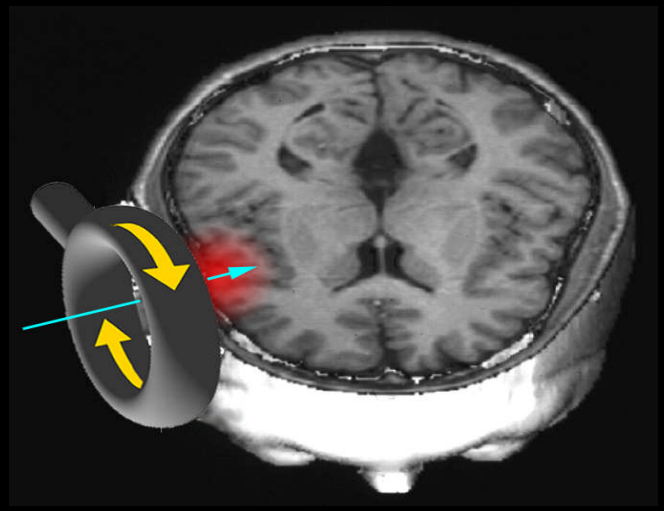

Transcranial Magnetic Stimulation

Anthony Barker 1984

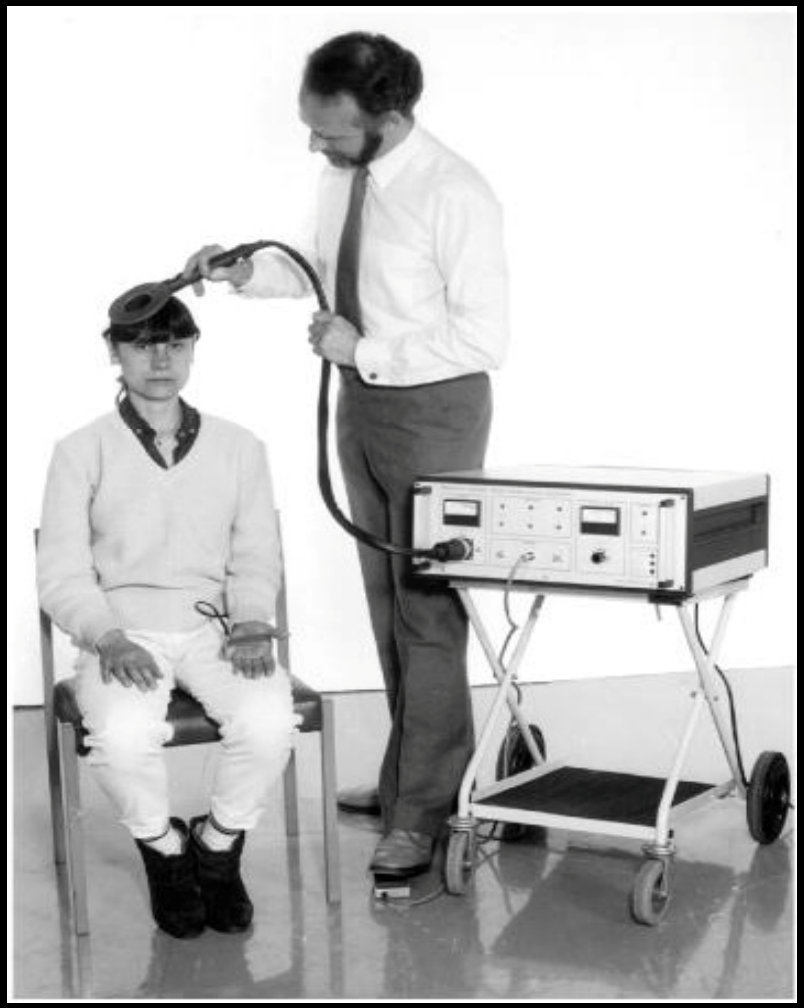

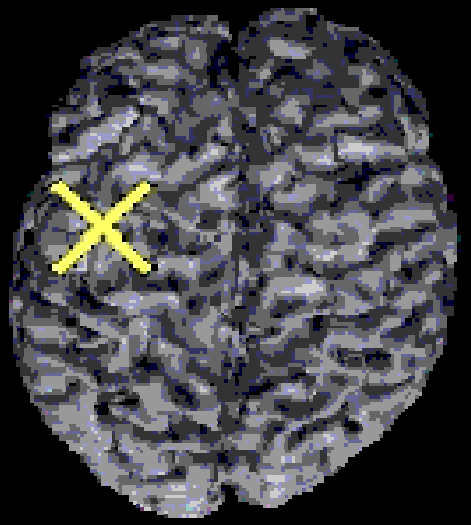

Imaging in Deep Brain Stimulation

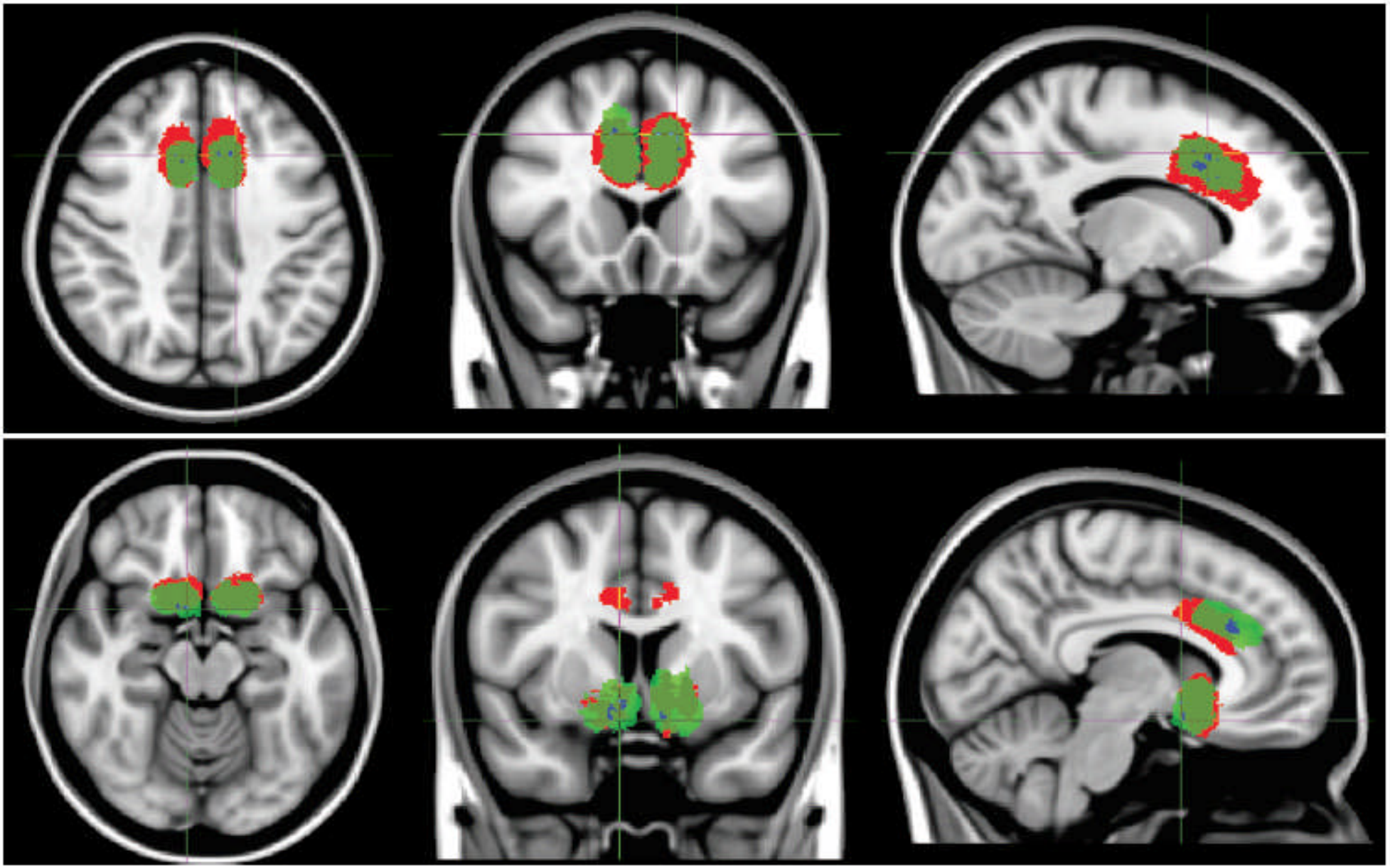

Fig. 8. Voxel-based lesion-outcome mapping for anterior cingulotomy and limbic leucotomy. Voxels found to be significant by VLSM are shown in *blue* (subareas within *green* areas). Nonresponder *(red)* and responder *(green)* lesion masks were collectively summed and are projected on the T1-weighted MNI152 template. **Upper:** Anterior cingulotomy. Axial, coronal, and sagittal images (*left* to *right*). **Lower:** Limbic leucotomy. Axial, coronal, and sagittal images (*left* to *right*). ***Yang et al., Journal of Neurosurgery, 2013***

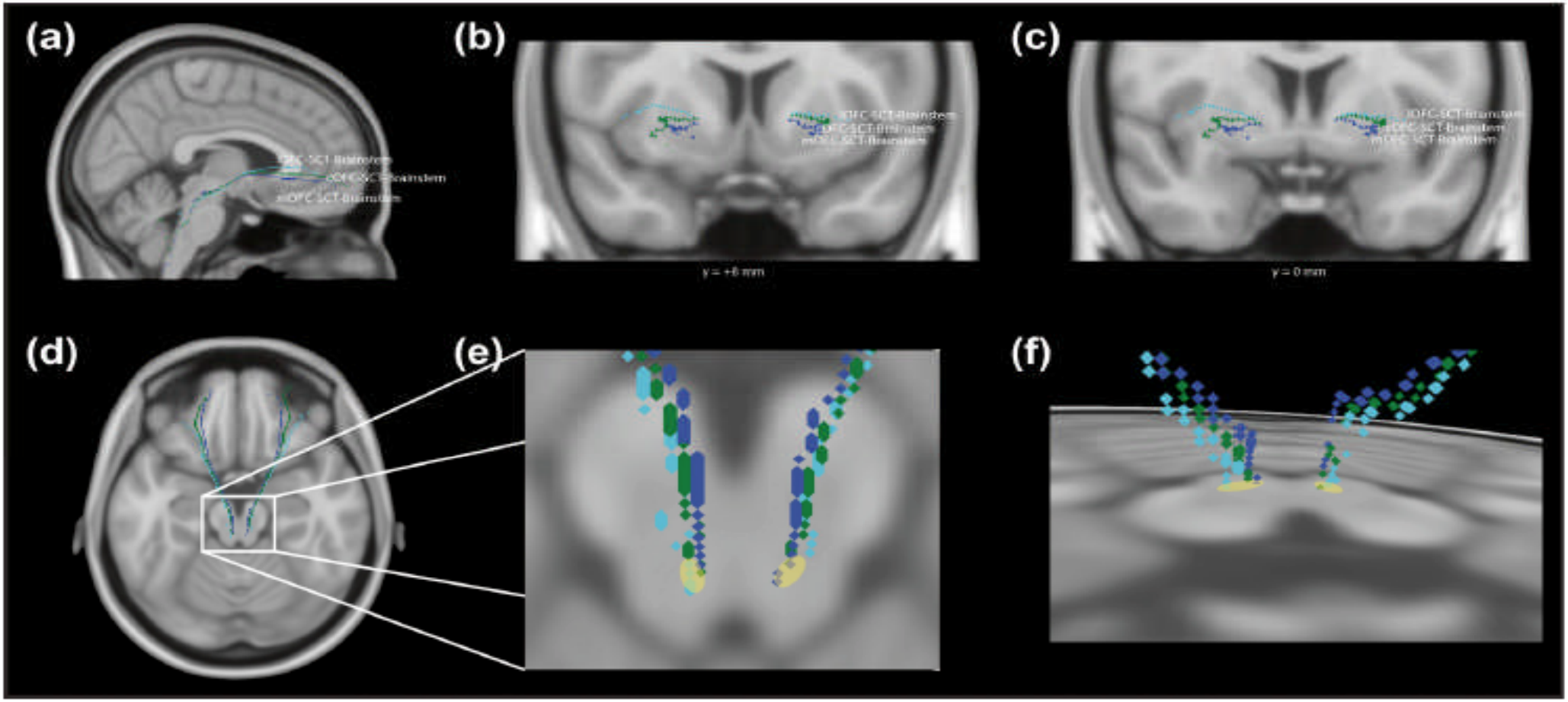

Fig. 6 3D Projections of Talairach Coordinates for Orbitofrontal Cortex-Brainstem Tract (**a**) 3D sagittal, (**b**) coronal (level of the nucleus accumbens, Talairach y-coordinate=+8 mm), (**c**) coronal (level of the anterior commissure, Talairach y-coordinate=0 mm), and (**d**) axial projections of tracts in Talairach space, using center-of-mass coordinates. These tracts run through the medial orbitofrontal cortex (mOFC), central orbitofrontal cortex (cOFC), or lateral orbitofrontal cortex (lOFC); subcaudate tractotomy lesion (SCT); and brainstem. Tracts: mOFC-SCT-brainstem (*blue*), cOFC-SCT-brainstem (*green*), and lOFC-SCT-brainstem (*cyan*). (**e**) Expanded region of brainstem of (**d**). The yellow region indicates the approximate area of intersection between the tracts and the axial slice. (**f**) 3D oblique projection of tracts in Talairach space, with a view from the dorsal aspect

Yang et al., brain Imaging and Behavior, 2014

Connectome data acquisition and analysis

Scanner: Siemens 3 Tesla "Skyra Connectom" at the MGH A. Martinos Center for Biomedical Imaging

Acquisition: multi-shell Q-ball imaging (QBI) data with a spin-echo echo planar imaging (EPI) pulse sequence (TR= 8,800 ms, TE= 57 ms, 96 slices, 21 cm^2 field of view, 1.5 mm isotropic voxels, at multiple b-values of 1,000 s/mm^2, 3,000 s/mm^2,5000 s/mm^2 and 10,000 s/mm^2).

Analysis: Fiber tracts were sampled using deterministic streamline tractographic analysis with TrackVis

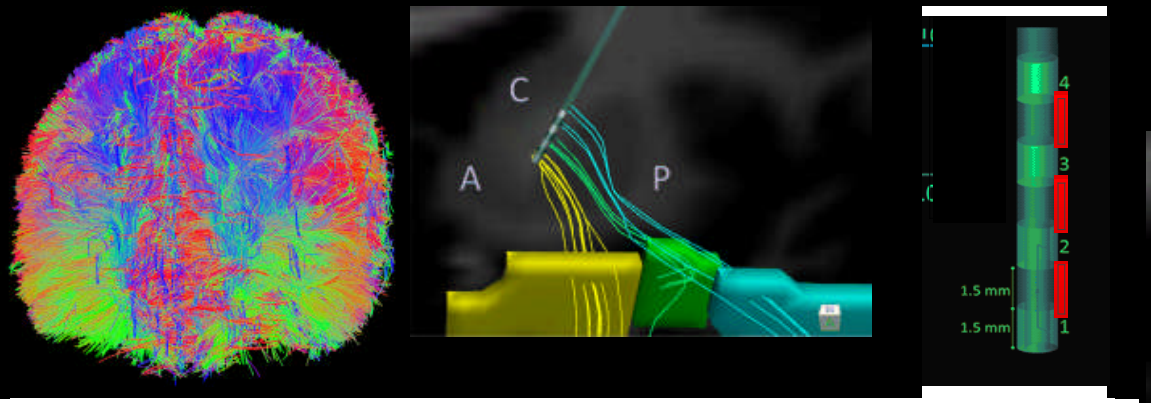

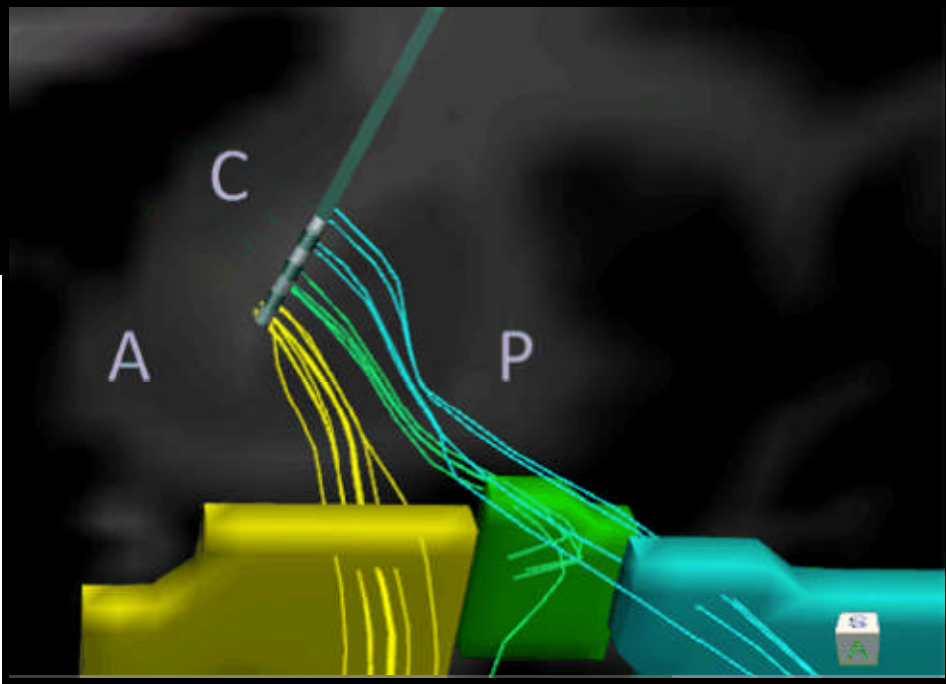

Fig. 3: *(left) DSI connectome data set, (middle) electrode placement in the VC/VS target area traversed by fibers (yellow fibers) of the ventromedial prefrontal-basal ganglia tract at the C.A.P. coronal slice. The latter fibers stem from the ventromedial prefrontal area (yellow block). (A=nucleus accumbens, C=caudate nucleus, P=putamen), and (right) electrode geometry with the proposed embedded thin solid state temperature sensor film (red).*

DBS in OCD using Connectome Technology

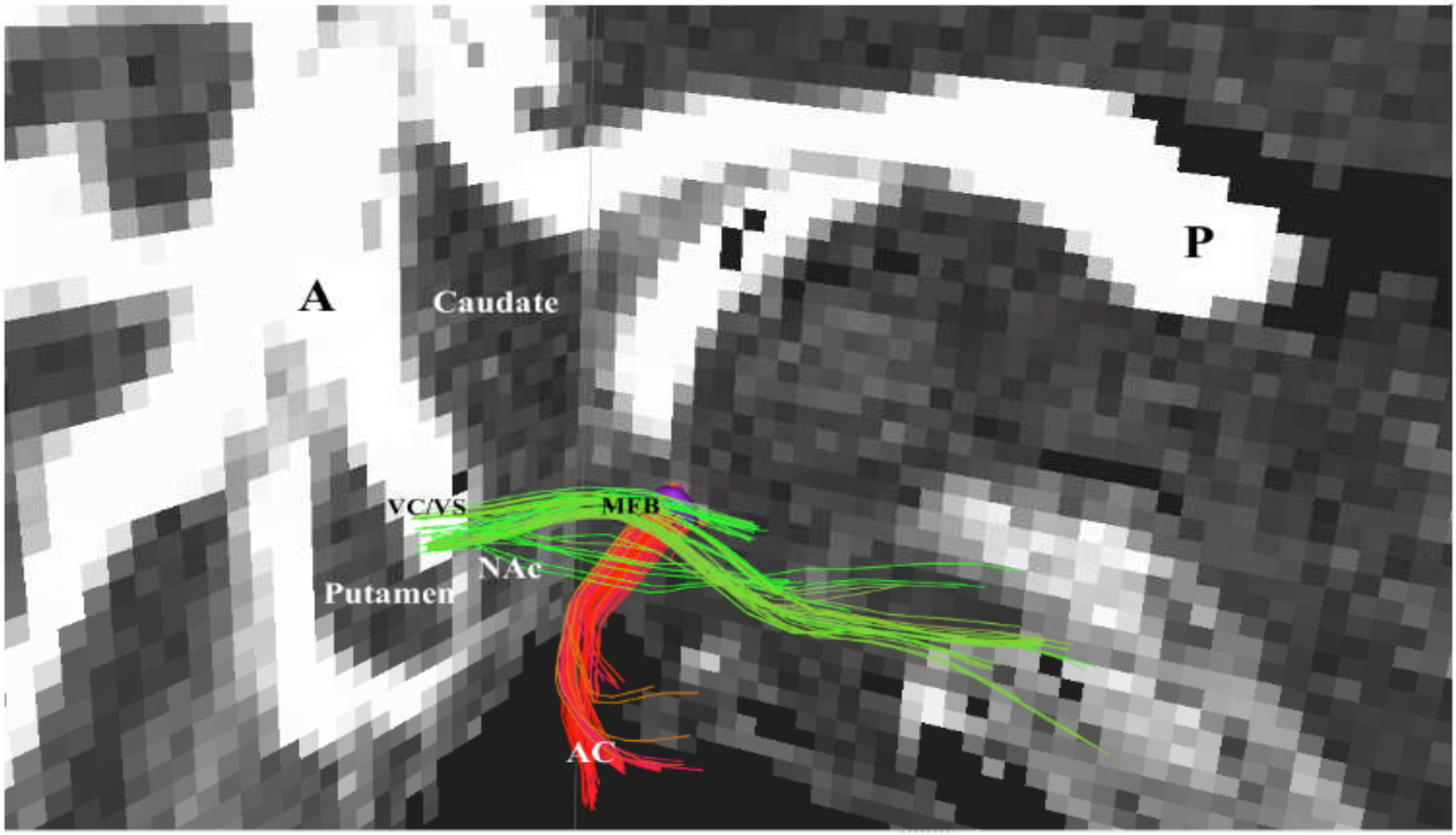

Fig.2. Topographic relationship between the Anterior Commissure (AC) and Medial Forebrain Bundle (MFB) in an individual subject. These data were acquired using the 3 Tesla Siemens Connectome at the A. A. Martinos Center for Biomedical Imaging at MGH. The fiber tracts were sampled and visualized using TrackVis streamline tractography. The MFB (in green) is shown in a position superior to the AC (in red). As is courses from a posterior (P) to an anterior (A) position MFB goes from the midbrain, then passes above the AC and then through the ventral capsule/ventral striatum (VC/VS) area en route to the prefrontal regions. The background of the figure consists of a midsagittal and a coronal section derived from the fractional anisotropy (FA) map of this dataset. The coronal section is at the C.A.P. (Caudate-Accumbens-Putamen) anatomical level to portray the topography of MFB within the VC/VS area above the nucleus accumbens septi (NAc).

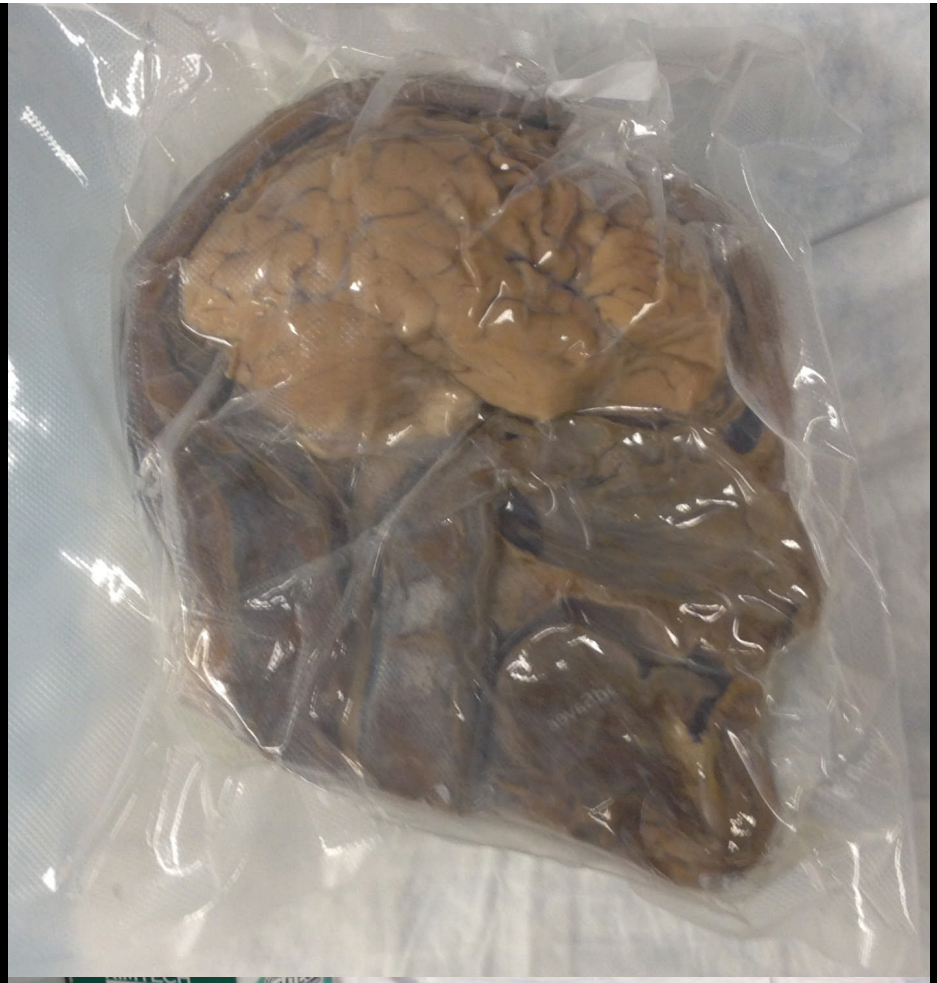

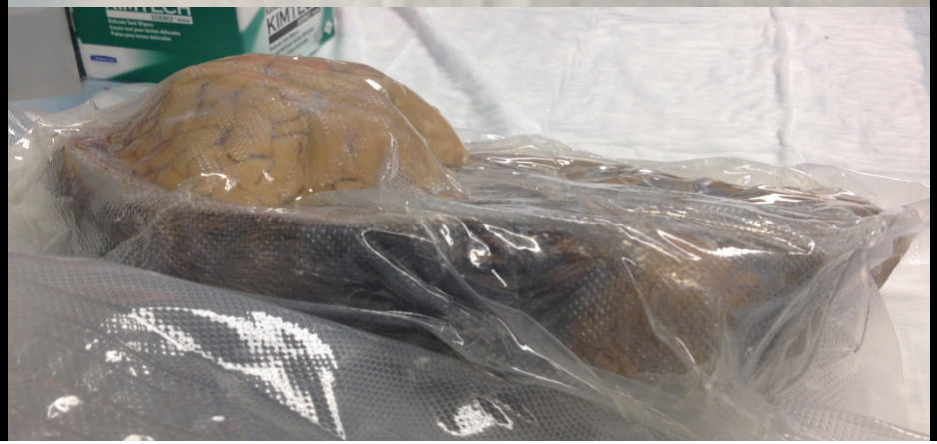

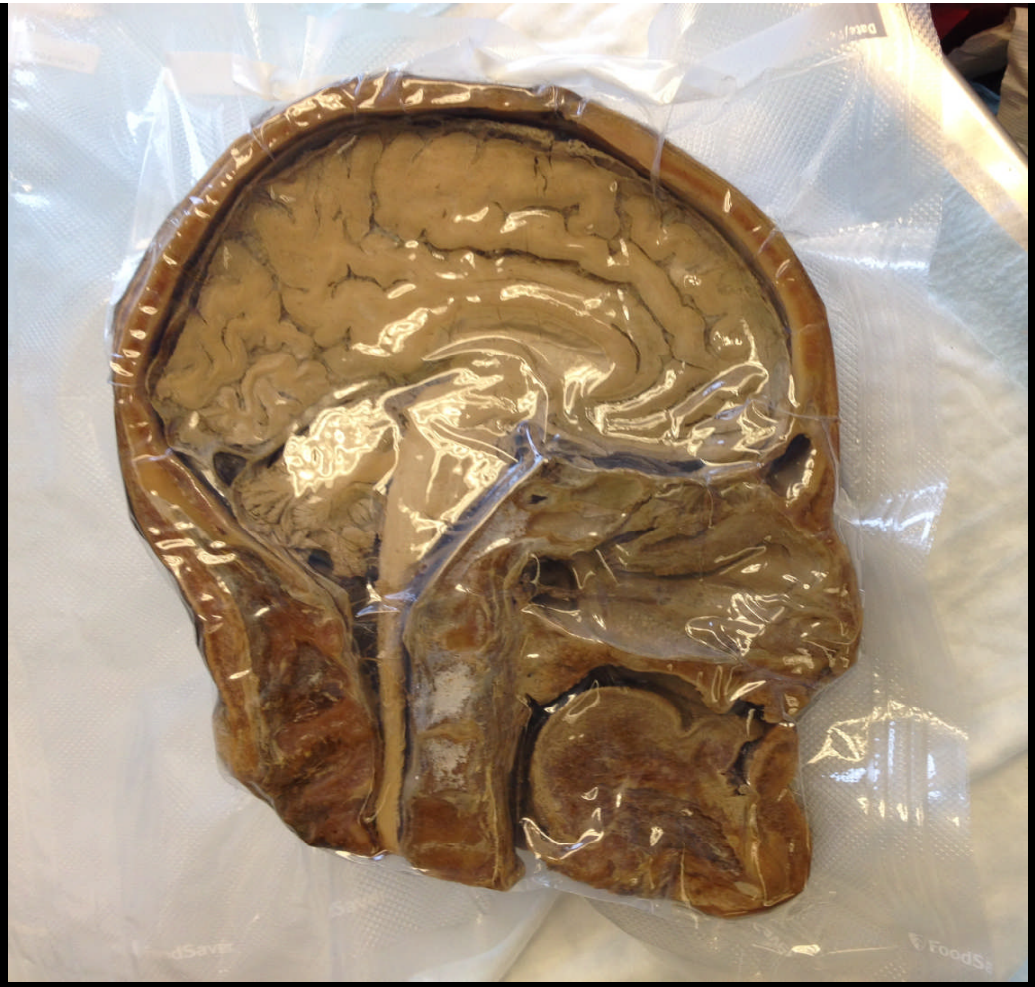

The half-head sample sealed in a vacuumed plastic (top-right) and assembly of a right brain hemisphere opposite to the half-head sample to fill-in the head coil and prohibit image distortion (left images). The assembled half-head-half-brain sample was used for imaging

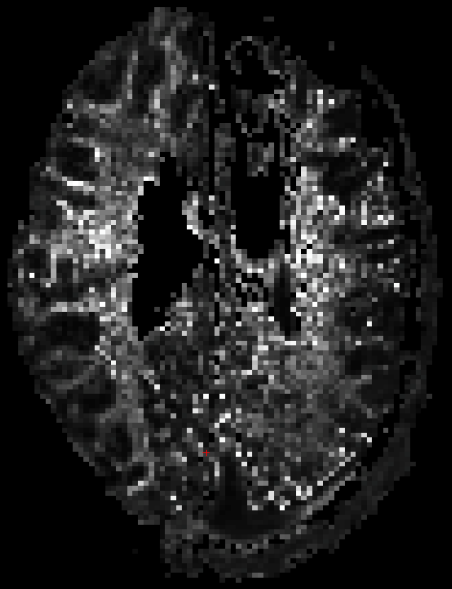

Upper-left image: Axial section of fractional anisotropy map (FA map) of the head sample obtained by Q-ball diffusion imaging

Connectome Scanner @ Martinos Center for Biomedical Imaging; Sequence: 64 dir Q-ball imaging

Voxel size: 1.5 mm isotropic
Total time: 11mins 44s
TR: 8800 ms; TE: 57.0 ms
Echo spacing: 0.63 ms
Number of directions: 64
b-value: 1400
PAT: 3; Fat suppression: strong

Upper-right and bottom images: Coronal sections of high-resolution structural MRI of right (upper-right image) and left (bottom image) subthalamic nucleus (STN); lower-right images: outlined zoomed versions of STN.

7 Tesla Scanner @ Martinos Center for Biomedical Imaging; Sequence: FLASH;
Voxel size: 400um isotropic; Total time: 1:09:08
TR: 23 ms; TE: 10.2 ms; Echo spacing: 10 ms
Flip Angle: 30.0 degrees; PAT: off, Fat supp: off

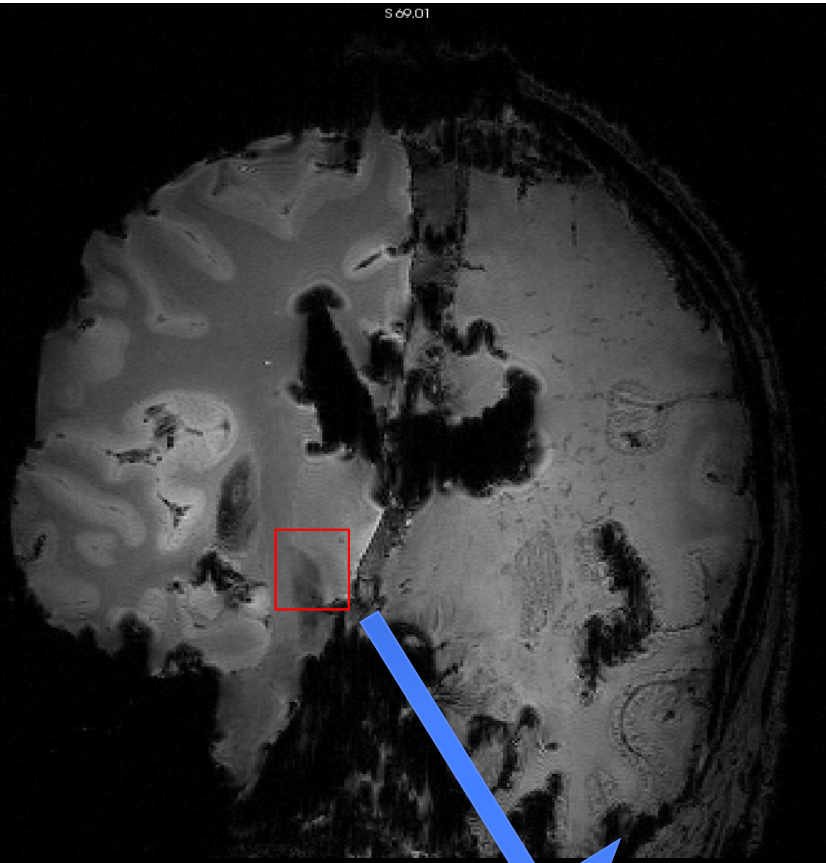

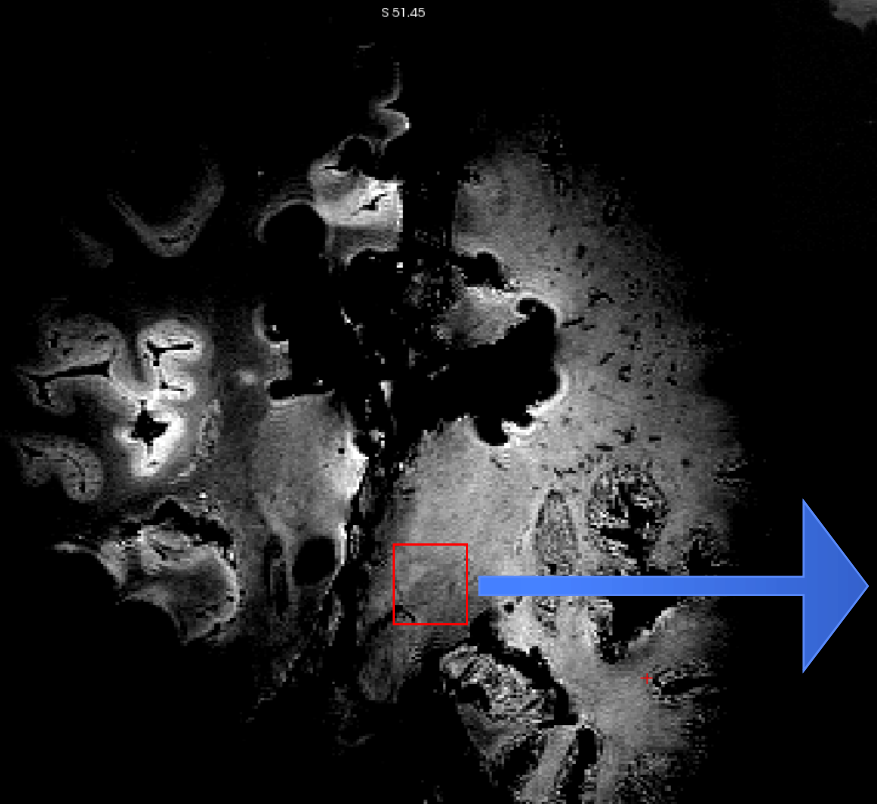

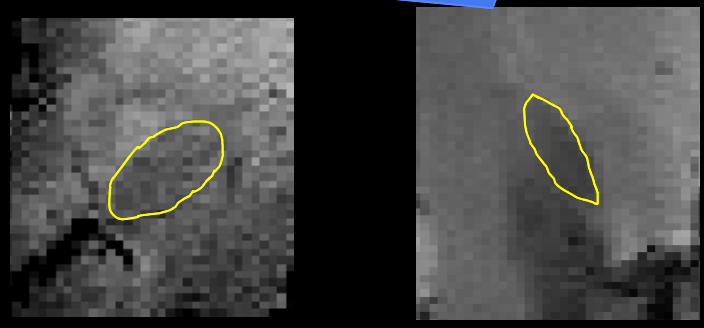

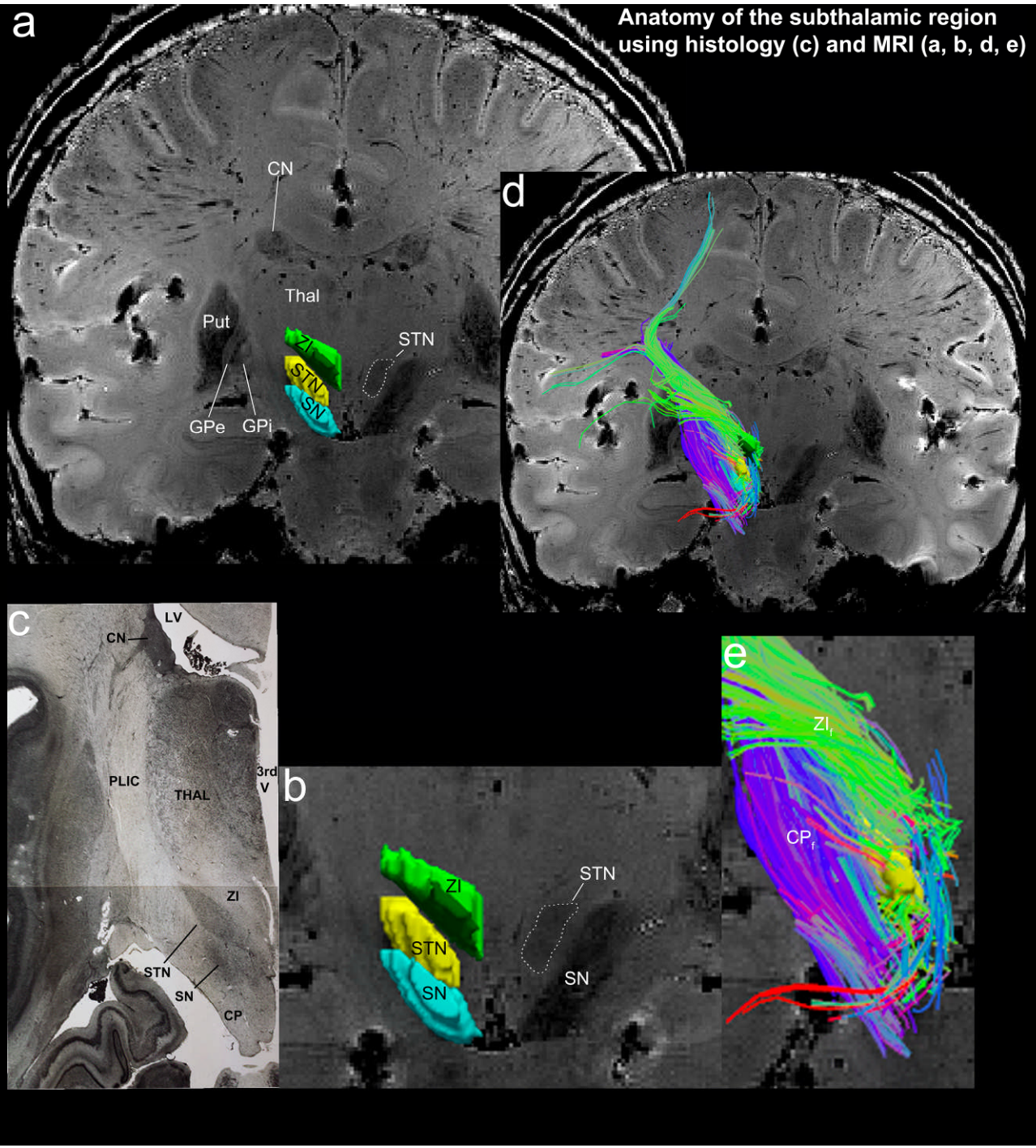
Anatomy of the subthalamic region
using histology (c) and MRI (a, b, d, e)
a
CN
Thal
Put
STN
ZI
STN
SN
GPe
GPi
d
c
LV
CN
PLIC
THAL
3rd
V
ZI
STN
SN
CP
b
ZI
STN
SN
STN
SN
e
ZI
CP

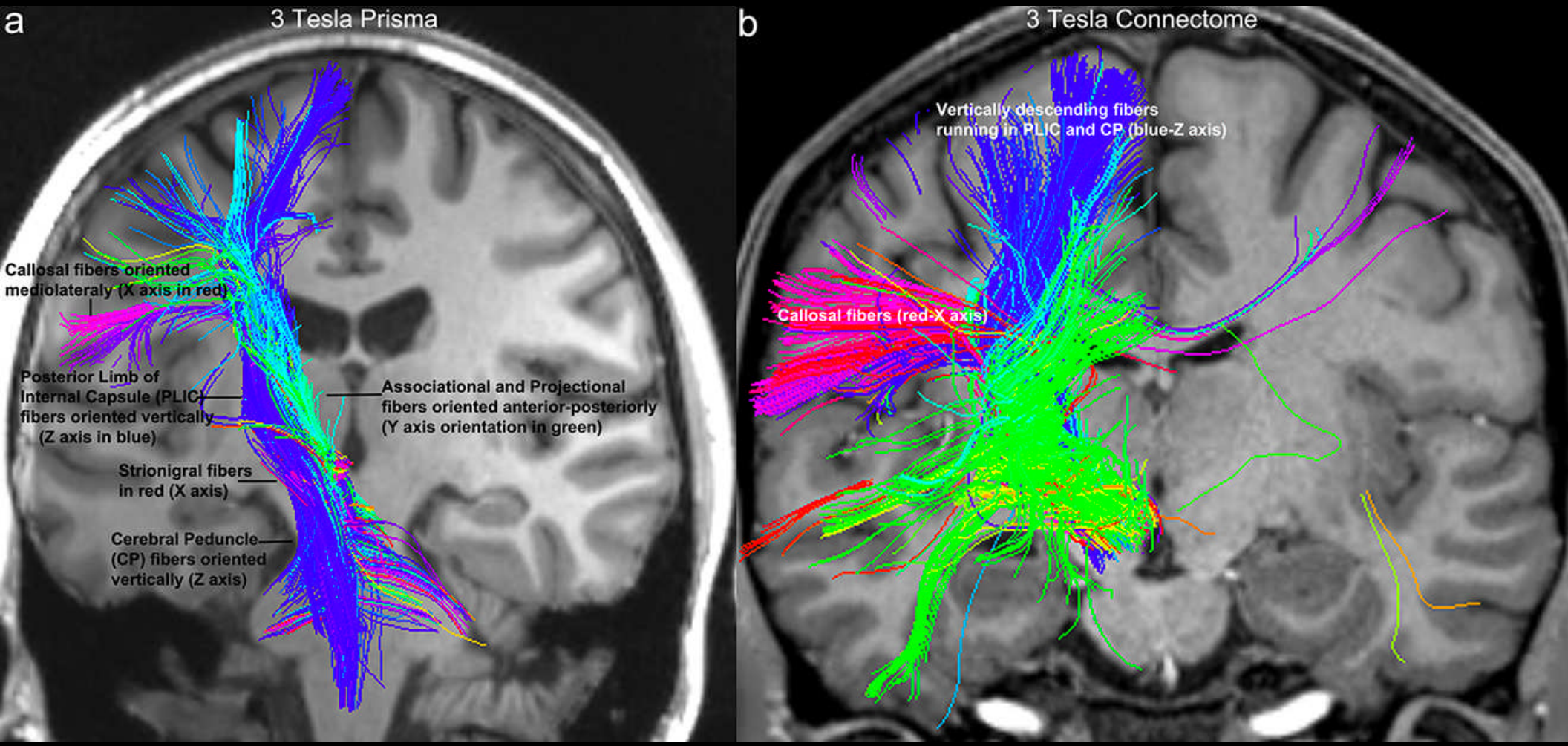
a
3 Tesla Prisma
Callosal fibers oriented mediolateraly (X axis in red)
Posterior Limb of Internal Capsule (PLIC) fibers oriented vertically (Z axis in blue)
Associational and Projectional fibers oriented anterior-posteriorly (Y axis orientation in green)
Strionigral fibers in red (X axis)
Cerebral Peduncle (CP) fibers oriented vertically (Z axis)
b
3 Tesla Connectome
Vertically descending fibers running in PLIC and CP (blue-Z axis)
Callosal fibers (red-X axis)

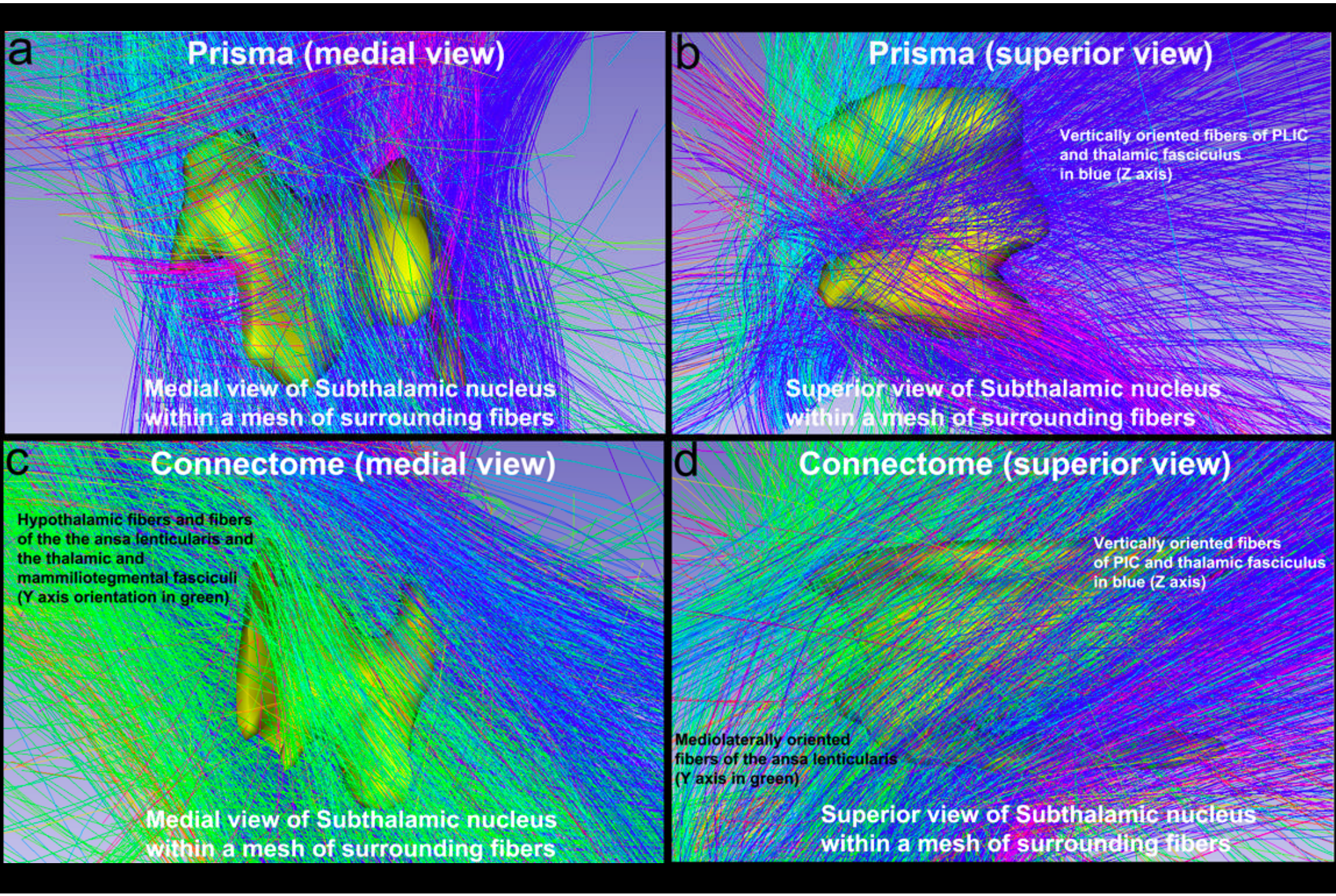
a
Prisma (medial view)
Medial view of Subthalamic nucleus
within a mesh of surrounding fibers
b
Prisma (superior view)
Vertically oriented fibers of PLIC
and thalamic fasciculus
in blue (Z axis)
Superior view of Subthalamic nucleus
within a mesh of surrounding fibers
c
Connectome (medial view)
Hypothalamic fibers and fibers
of the the ansa lenticularis and
the thalamic and
mammiliotegmental fasciculi
(Y axis orientation in green)
Medial view of Subthalamic nucleus
within a mesh of surrounding fibers
d
Connectome (superior view)
Vertically oriented fibers
of PIC and thalamic fasciculus
in blue (Z axis)
Mediolaterally oriented
fibers of the ansa lenticularis
(Y axis in green)
Superior view of Subthalamic nucleus
within a mesh of surrounding fibers

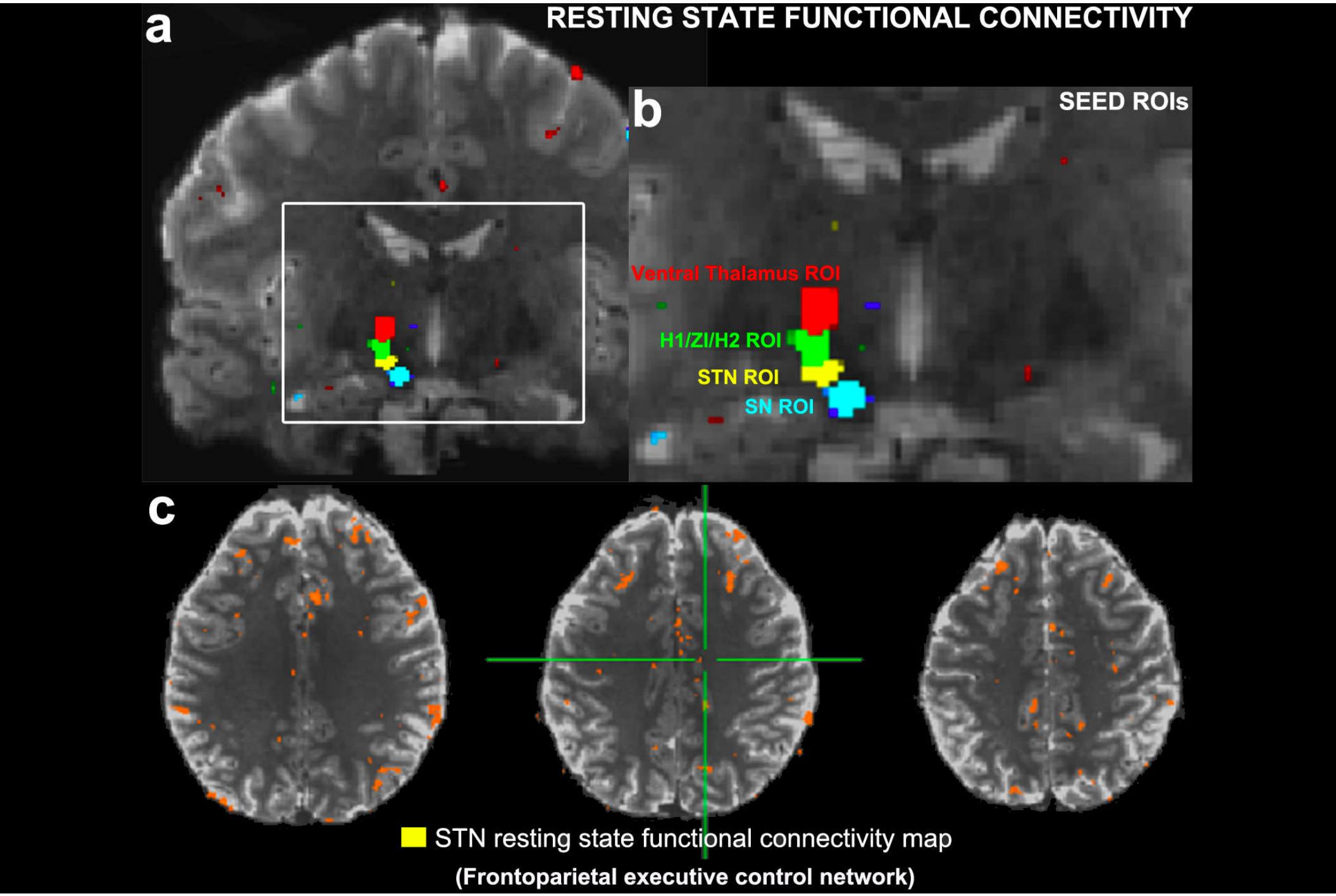
a
RESTING STATE FUNCTIONAL CONNECTIVITY
b
SEED ROIs
Ventral Thalamus ROI
H1/ZI/H2 ROI
STN ROI
SN ROI
c
STN resting state functional connectivity map
(Frontoparietal executive control network)

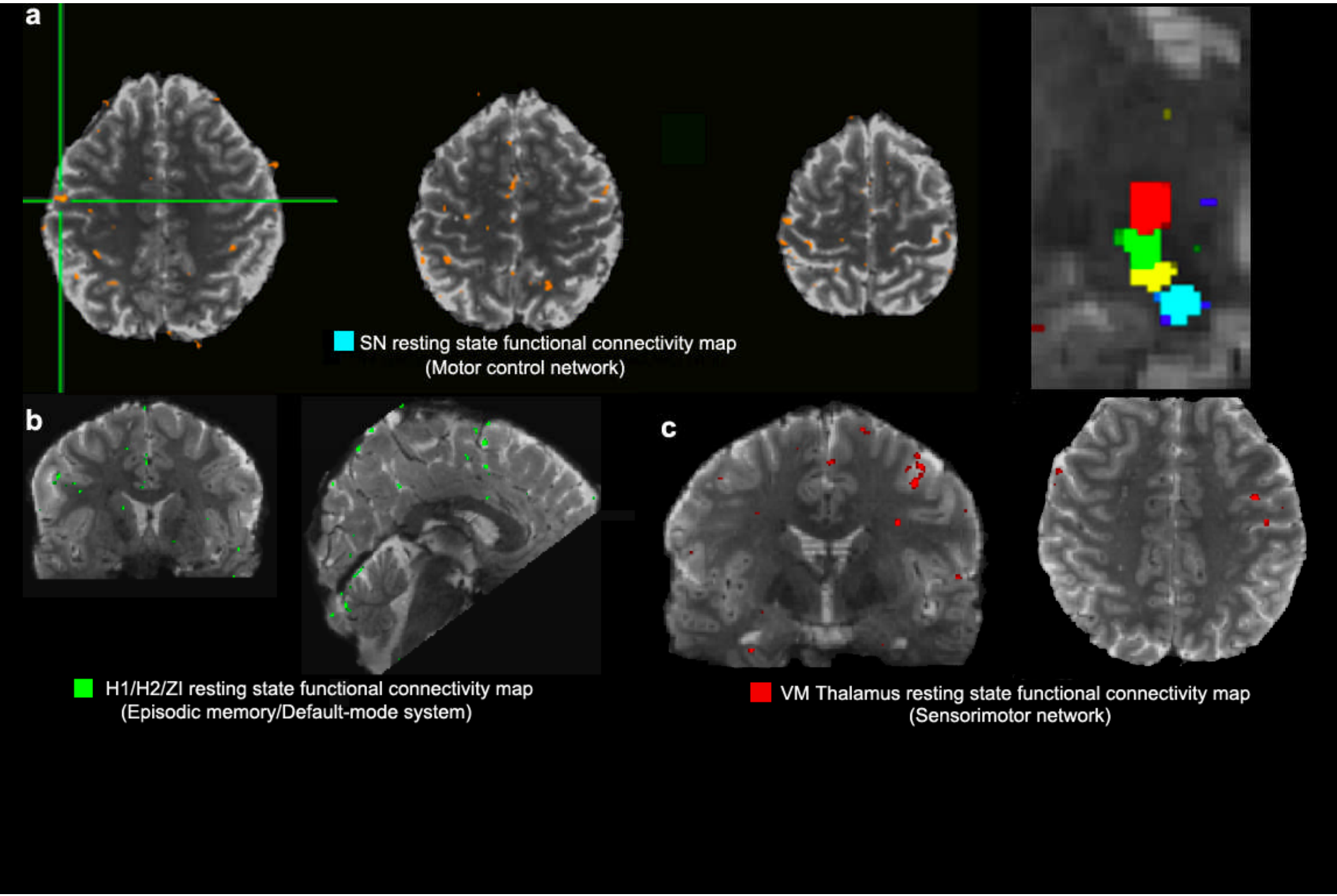
a
SN resting state functional connectivity map
(Motor control network)
b
H1/H2/ZI resting state functional connectivity map
(Episodic memory/Default-mode system)
c
VM Thalamus resting state functional connectivity map
(Sensorimotor network)

Neurodegeneration

Progression of Alzheimer's Disease:
similar model for many other diseases

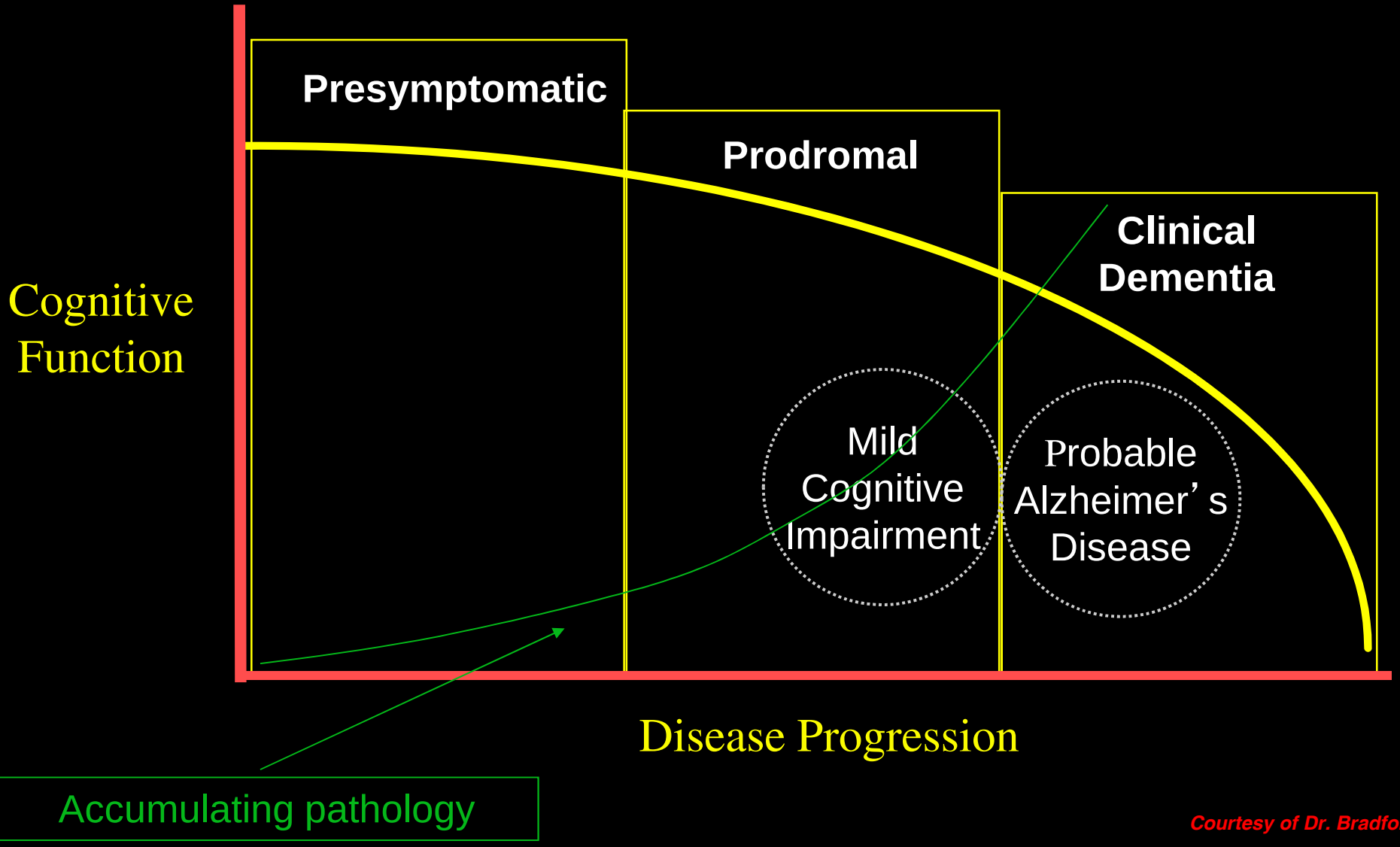

Courtesy of Dr. Bradford Dickerson

Large-scale cognitive systems
understrood through resting state fMRI

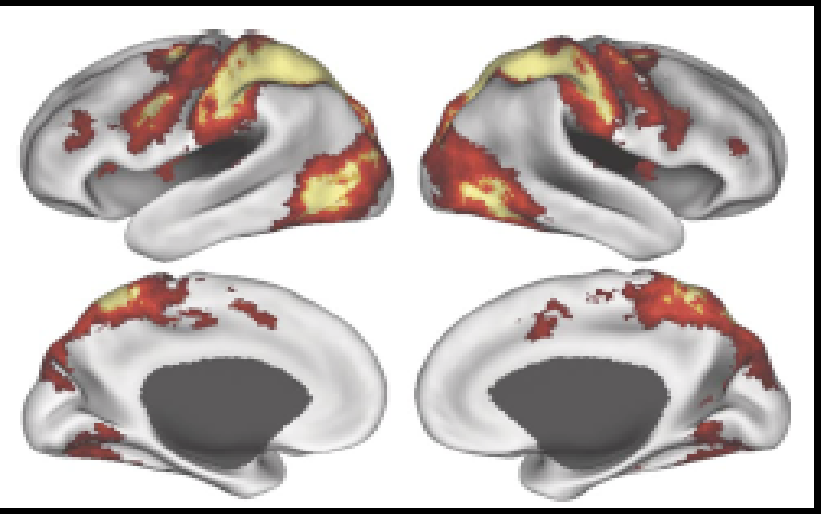

Dorsal visuospatial attention system

Frontoparietal executive control system

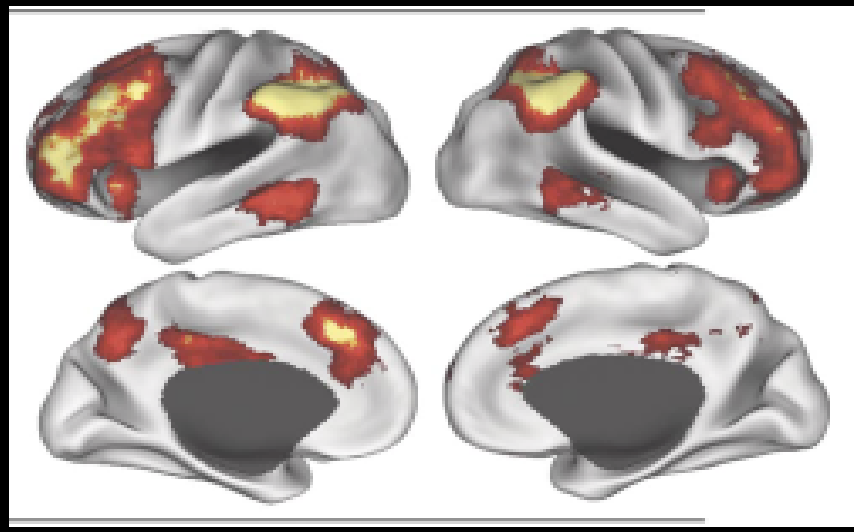

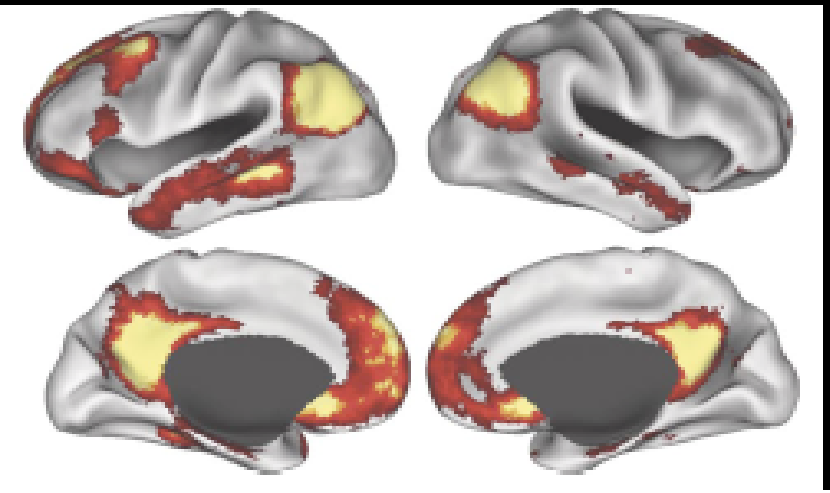

Episodic memory/Default-mode system

Vincent et al., J Neurophys, 2008

AD cortical signature:
Cortical atrophy compared to normals

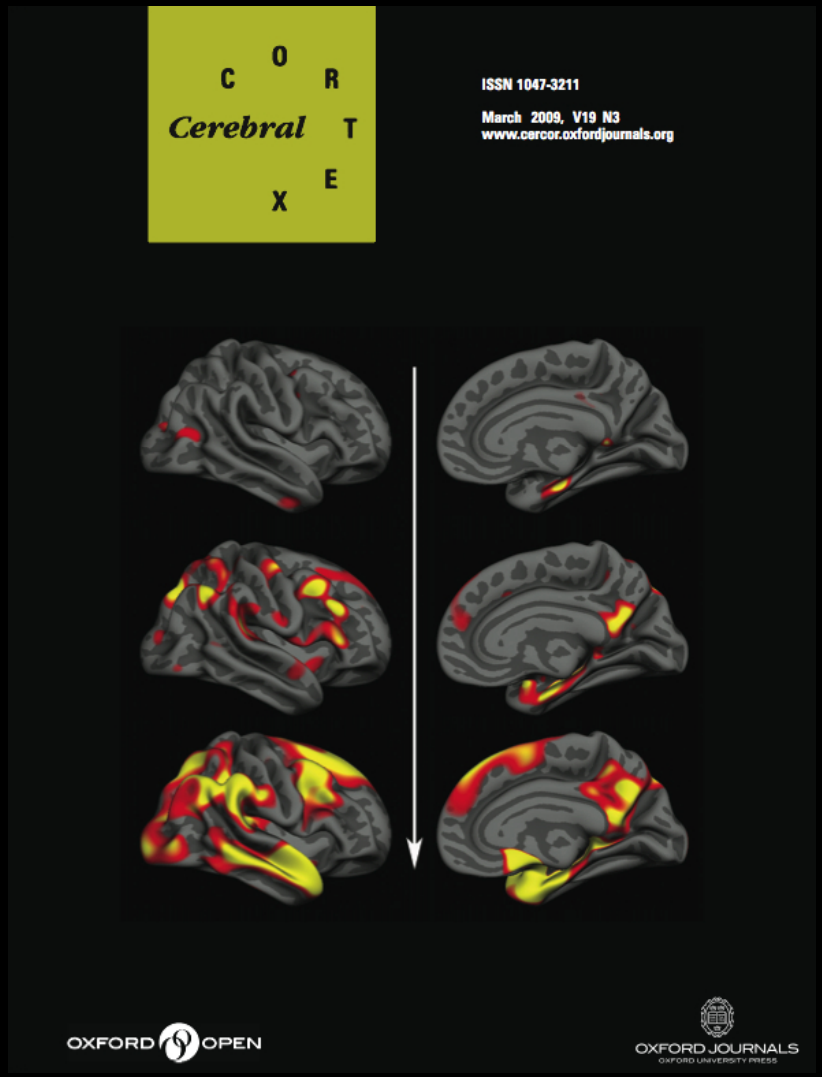

Dickerson et al, Cerebral Cortex 2009

Roles of biomarkers in dementia: Clinical practice, 2014

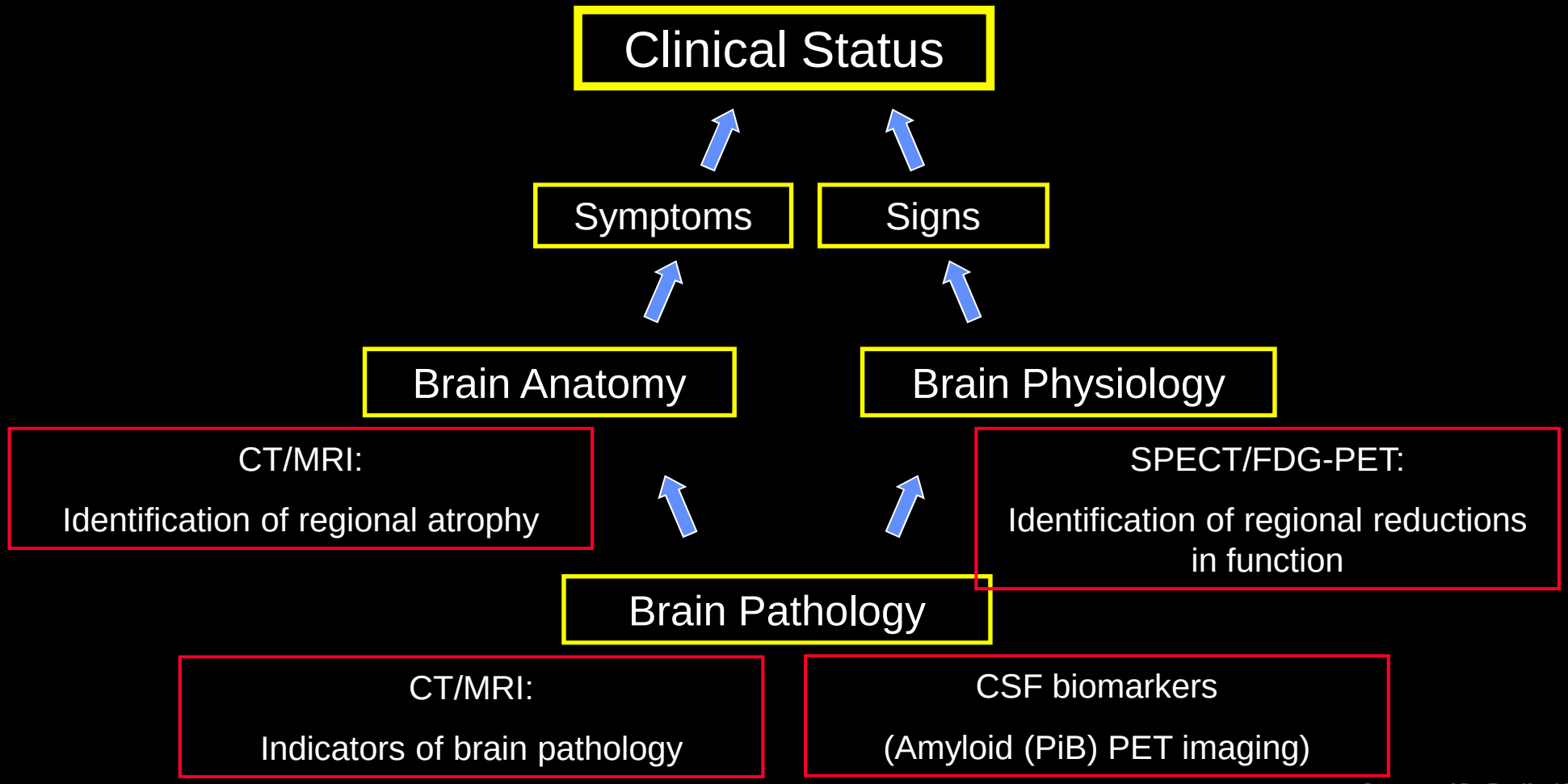

Courtesy of Dr. Bradford Dickerson

Plaque and Tangles

(Bielschowsky silver stain, association cortex of the temporal lobe)

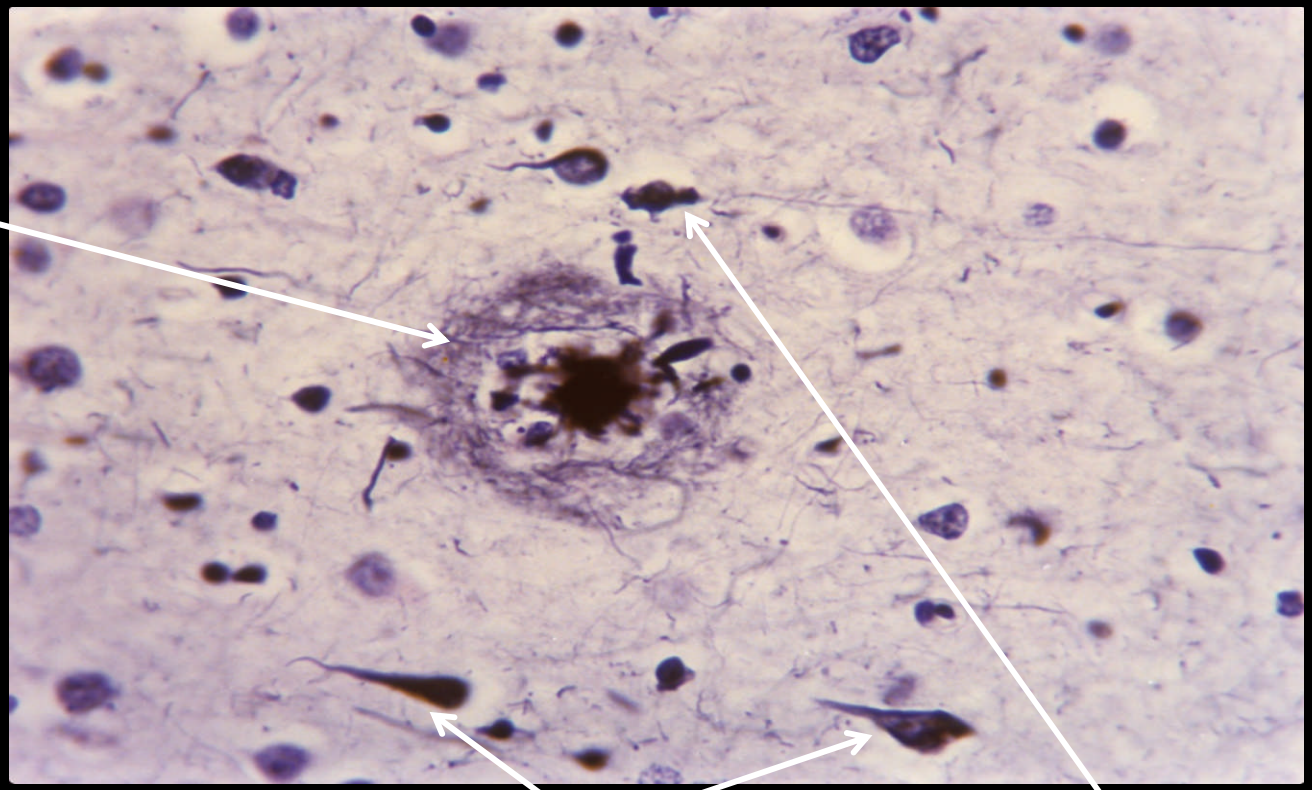

Only Post-Mortem Tau Pathology

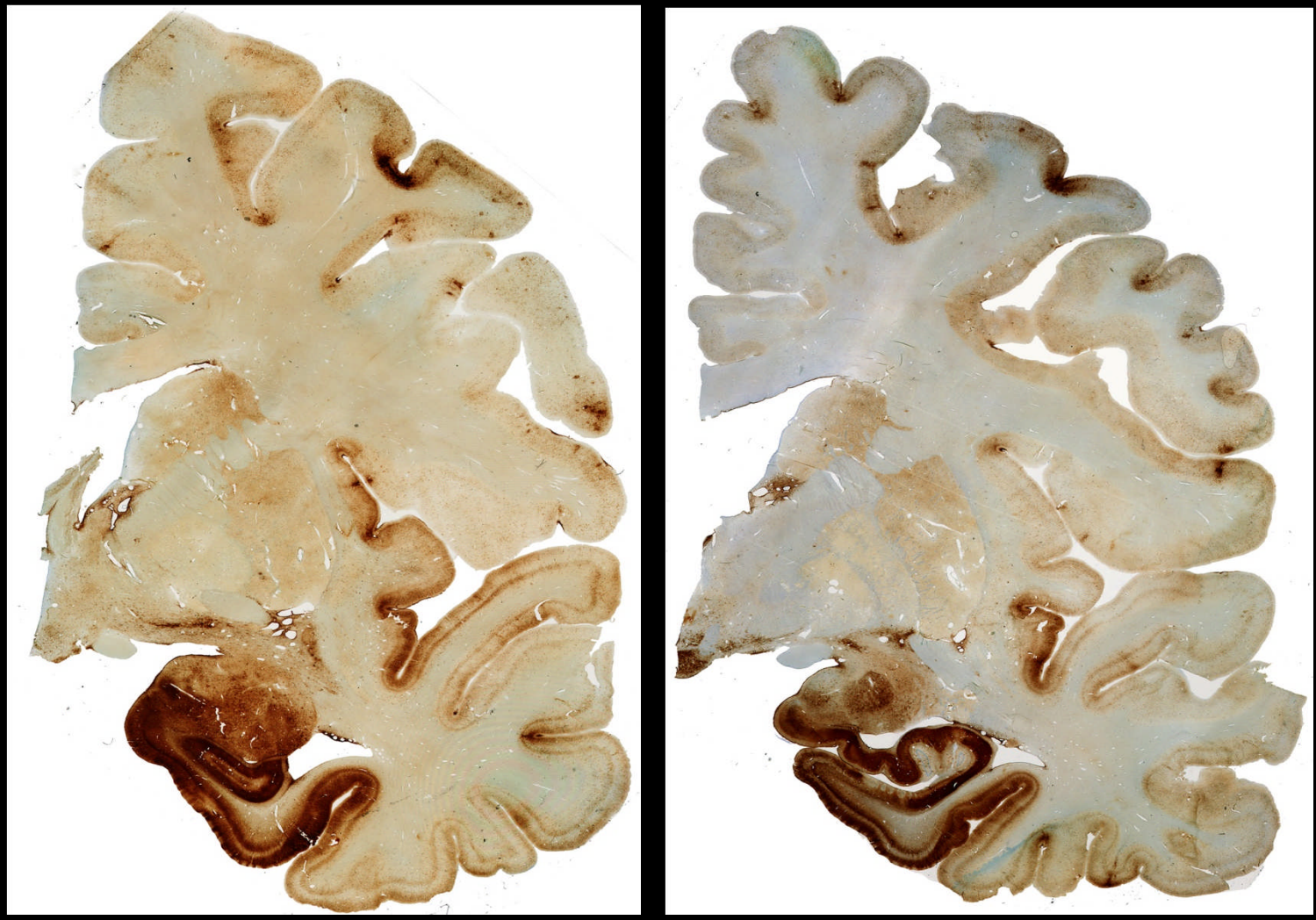

(McKee et al., 2009)

Amyloid imaging with PET

Pittsburgh Compound-B (PiB)

Alzheimer's disease

Normal aging

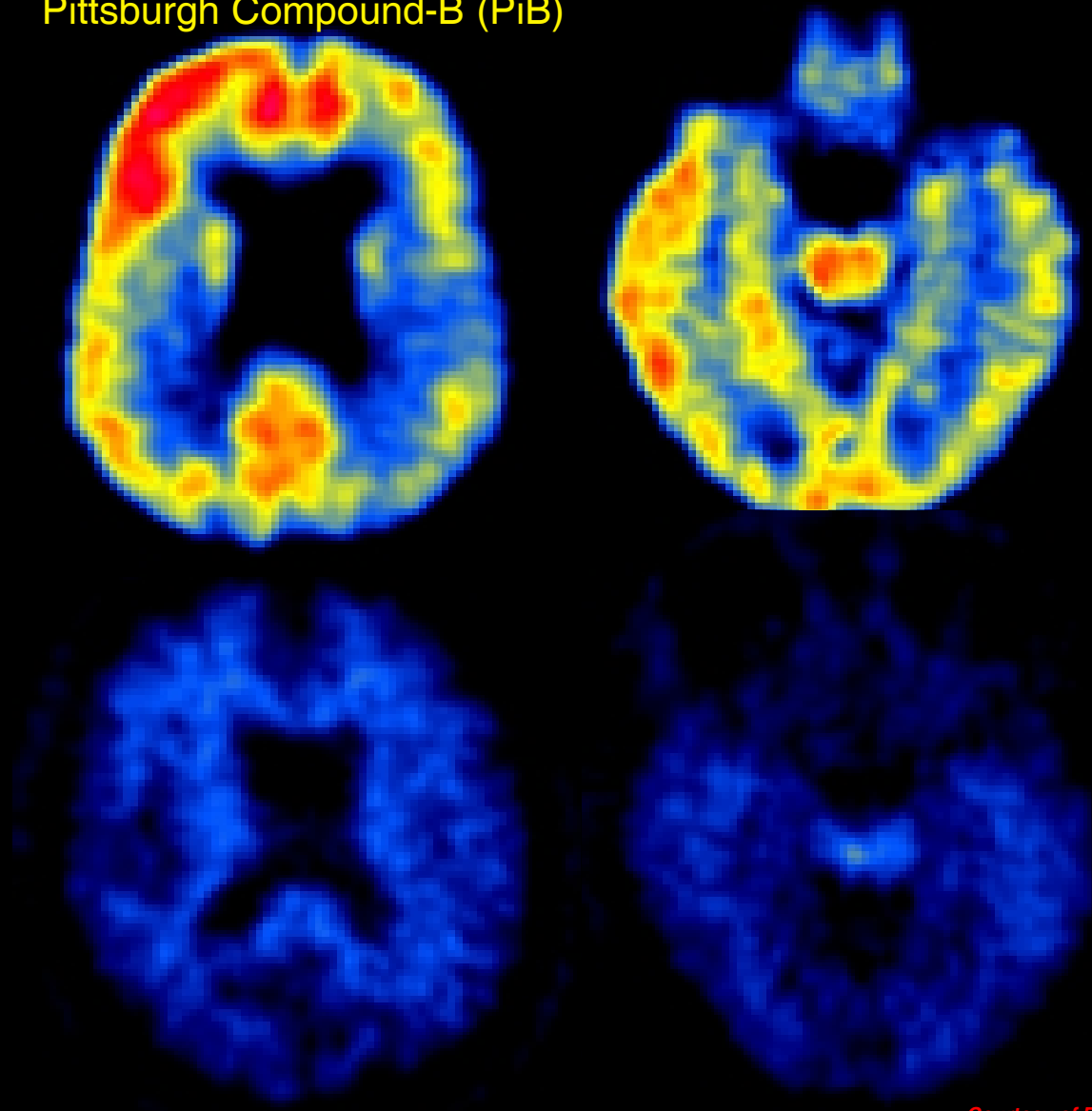

Courtesy of Dr. Bradford Dickerson

Aging, MCI, AD: FDG-PET

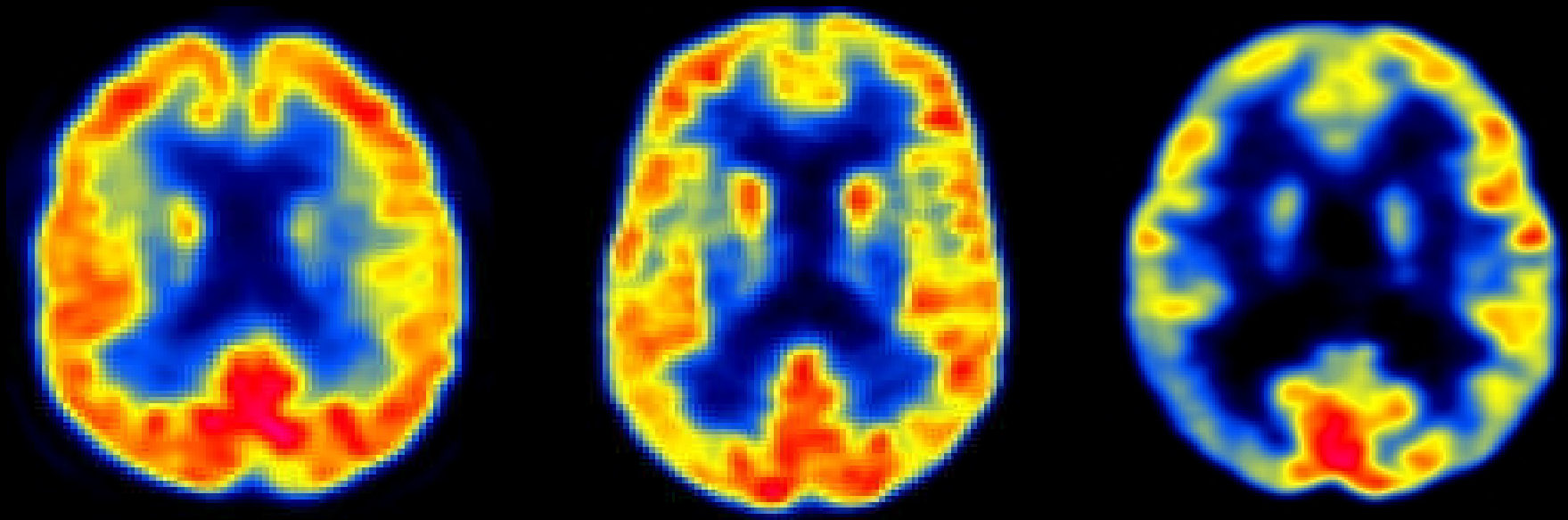

Cognitively intact older adult

Mild Cognitive Impairment

Alzheimer's Disease

Courtesy of Dr. Bradford Dickerson

Case 1

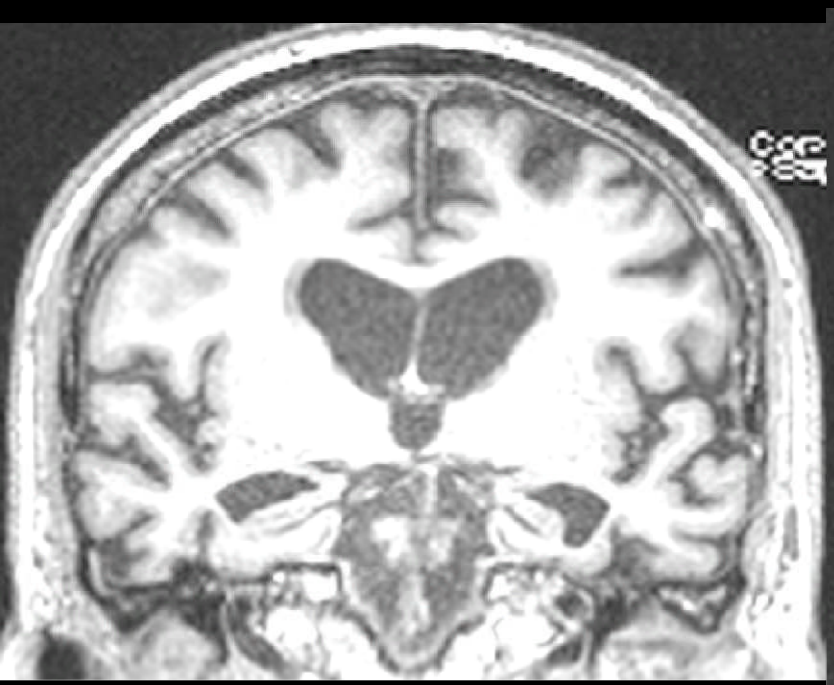

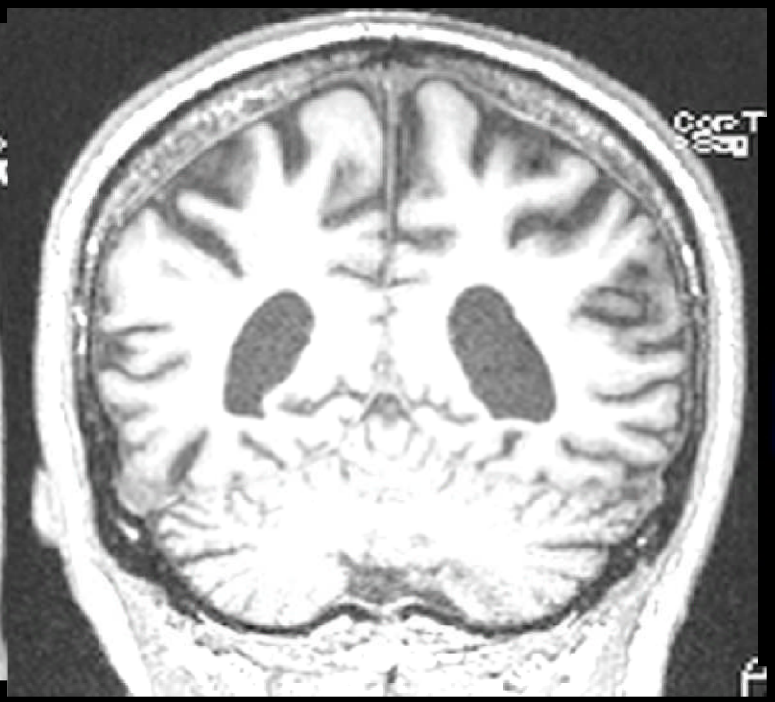

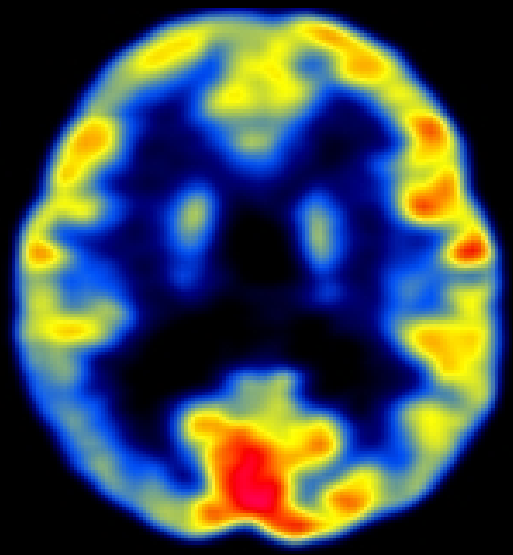

FDG-PET

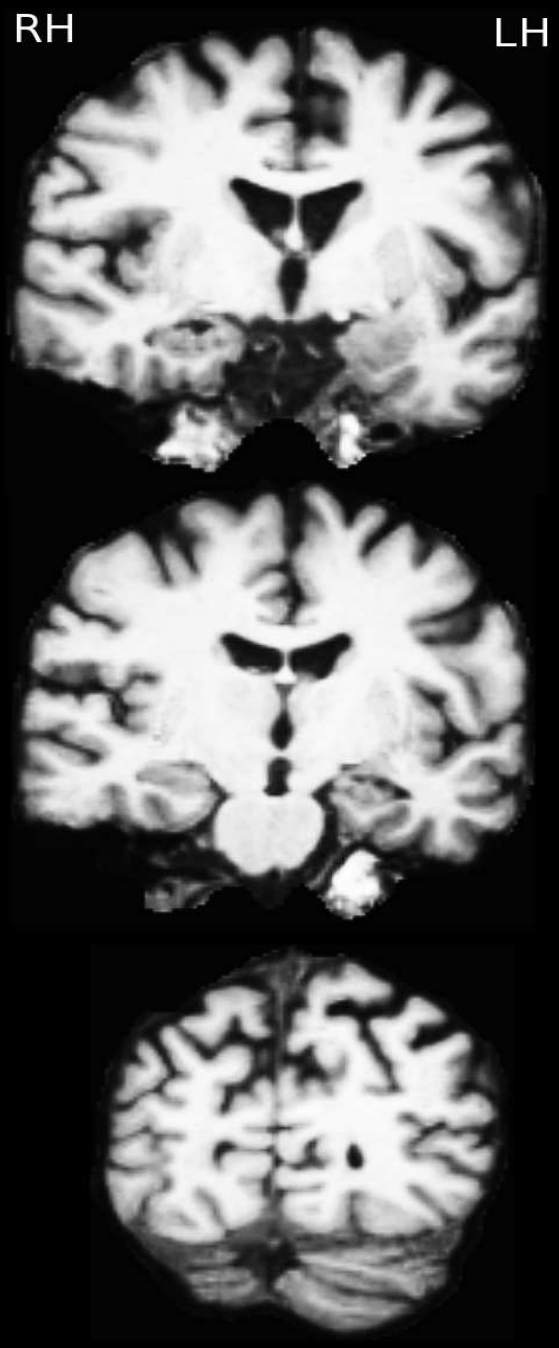

Case 2

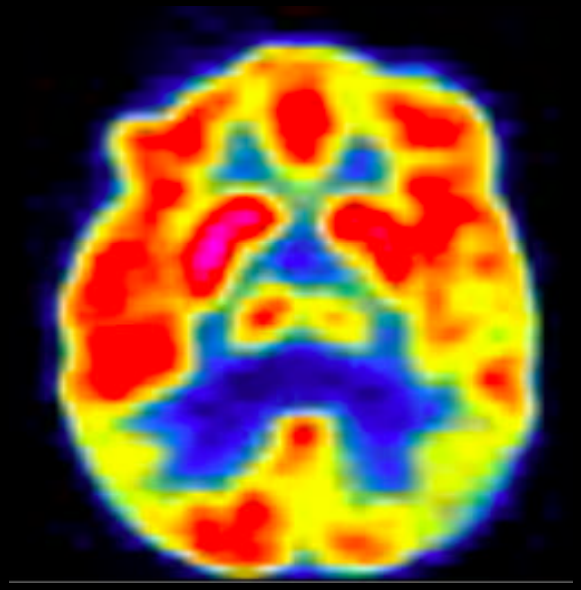

FDG-PET

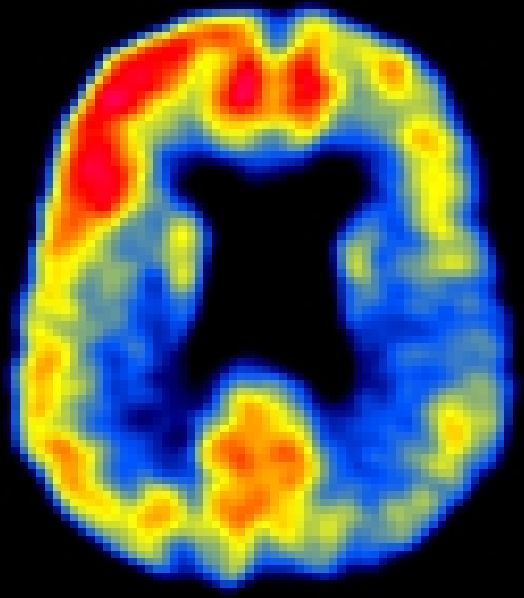

Amyloid (PiB)-PET

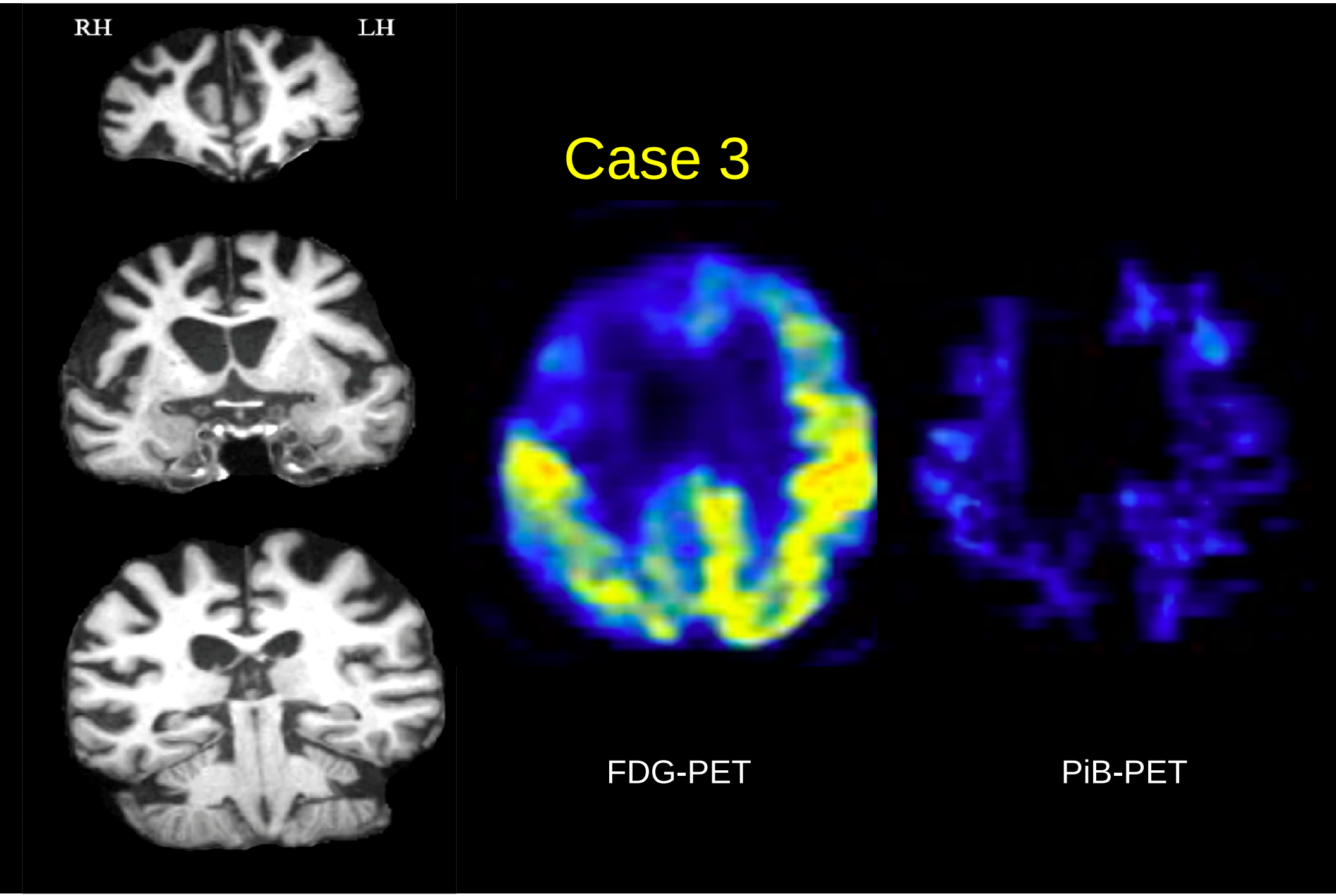
RH
LH
Case 3
FDG-PET
PiB-PET

Pre-Clinical PET Tracer Used in Animals

Journal of Alzheimer's Disease 31 (2012) 1–12
DOI 10.3233/JAD-2012-120712
IOS Press

A Highly Selective and Specific PET Tracer for Imaging of Tau Pathologies

Wei Zhang, Janna Arteaga, Daniel K. Cashion, Gang Chen, Umesh Gangadharmath, Luis F. Gomez, Dhanalakshmi Kasi, Chung Lam, Qianwa Liang, Changhui Liu, Vani P. Mocharla, Fanrong Mu, Anjana Sinha, A. Katrin Szardenings, Eric Wang, Joseph C. Walsh, Chunfang Xia, Chul Yu, Tieming Zhao and Hartmuth C. Kolb*
Siemens Molecular Imaging, Inc., Culver City, CA, USA

or Proof

Next Step PET in Humans

- Rule out Alzheimer's Disease (AD) in suspected CTE.

- Rule in Tauopathy in CTE – the Holy Grail. Positive *in vivo* tau imaging (paired helical filament Tau) using new PET Tau ligand from Siemens.

- Predictions: Amyloid-Beta retention in AD, but not CTE or controls (PiB), and Tau retention in AD and CTE but not controls (Tau; see table, below).

	AD	CTE	Control
PiB	+	-	-
Tau	+	+	-

Imaging technology is not just making pretty pictures or even simply increasing our scientific understanding of Alzheimer's and related diseases; it is in fact enabling new revolutions in testing treatments that may lead to real benefits for patients, possibly even forms of prevention.

e.g., anti-amyloid treatment with monoclonal antibodies in mildly symptomatic patients (MCI) or even asymptomatic individuals with brain amyloid.

Progression of neurodegenerative diseases

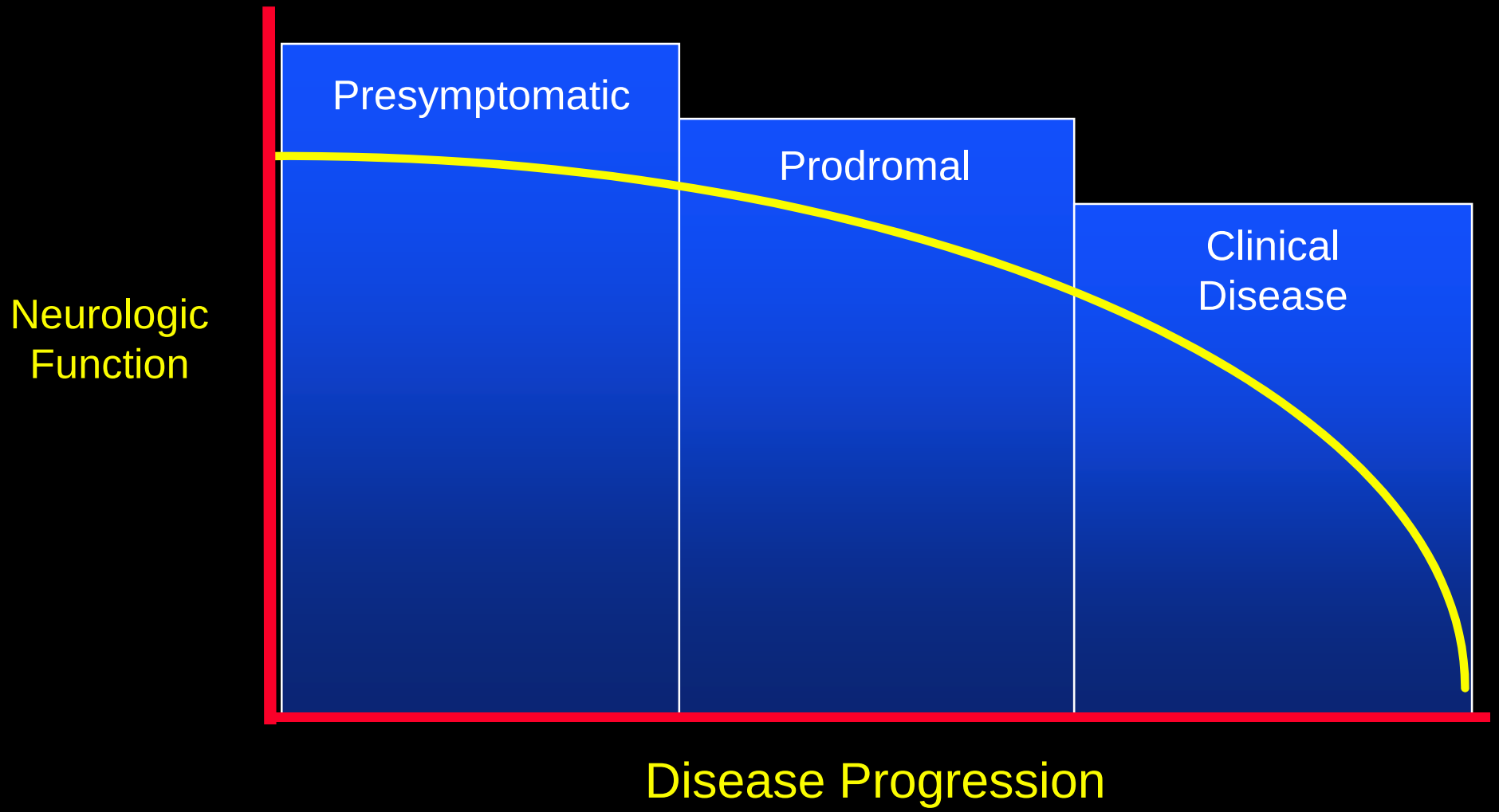

Courtesy of Dr. Bradford Dickerson

Progression of neurodegenerative diseases

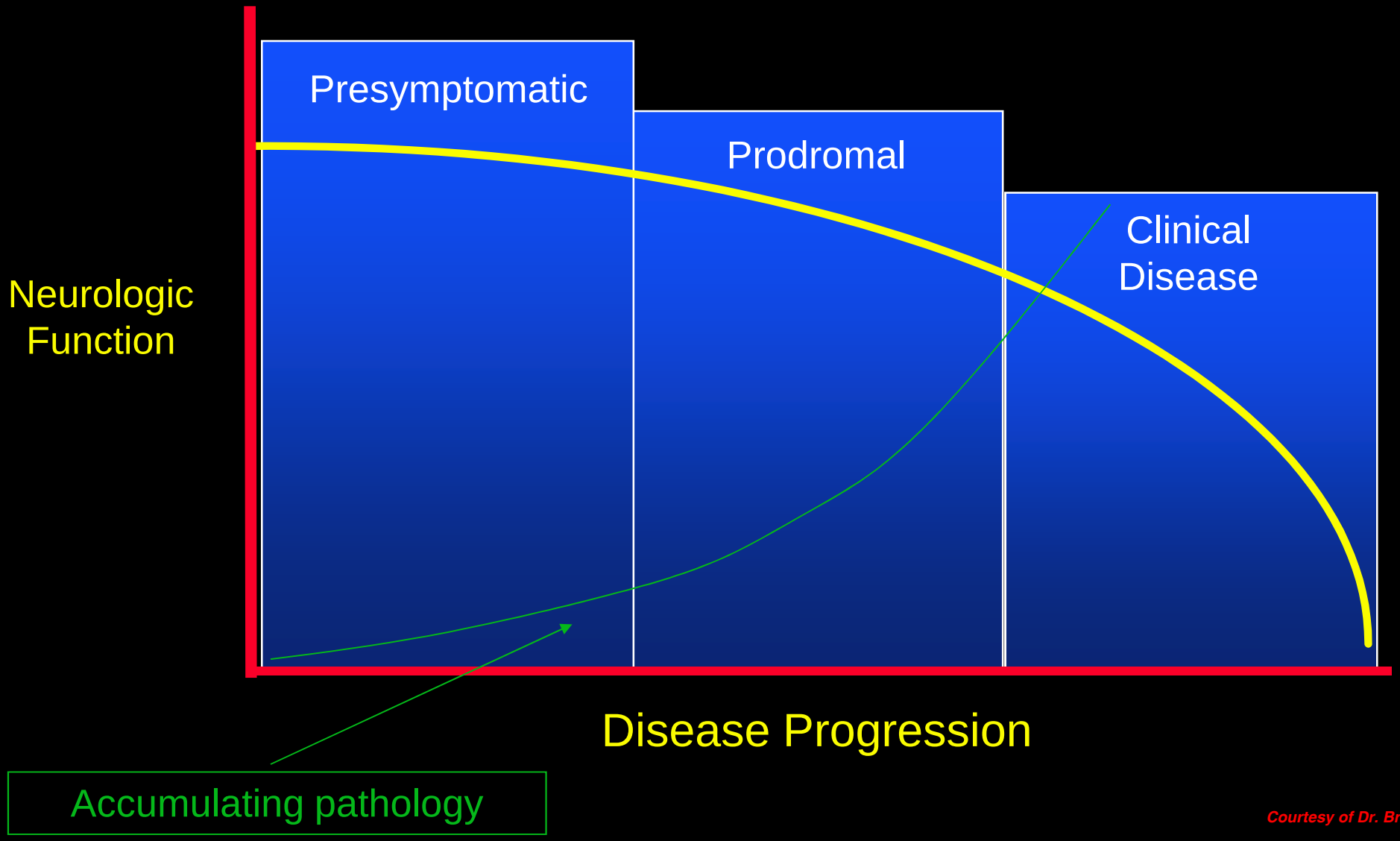

Courtesy of Dr. Bradford Dickerson

Progression of neurodegenerative diseases

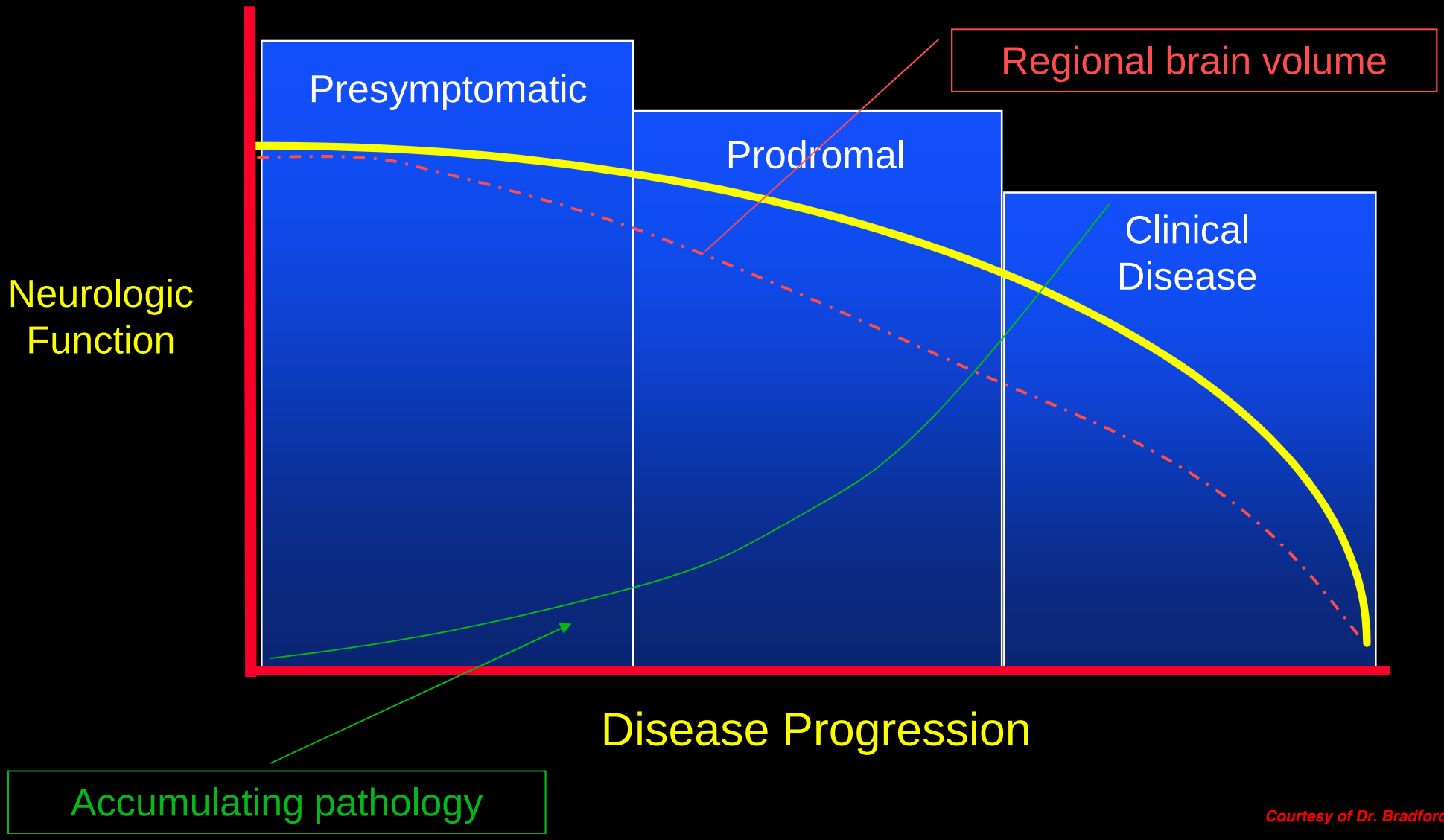

Courtesy of Dr. Bradford Dickerson

Progression of neurodegenerative diseases

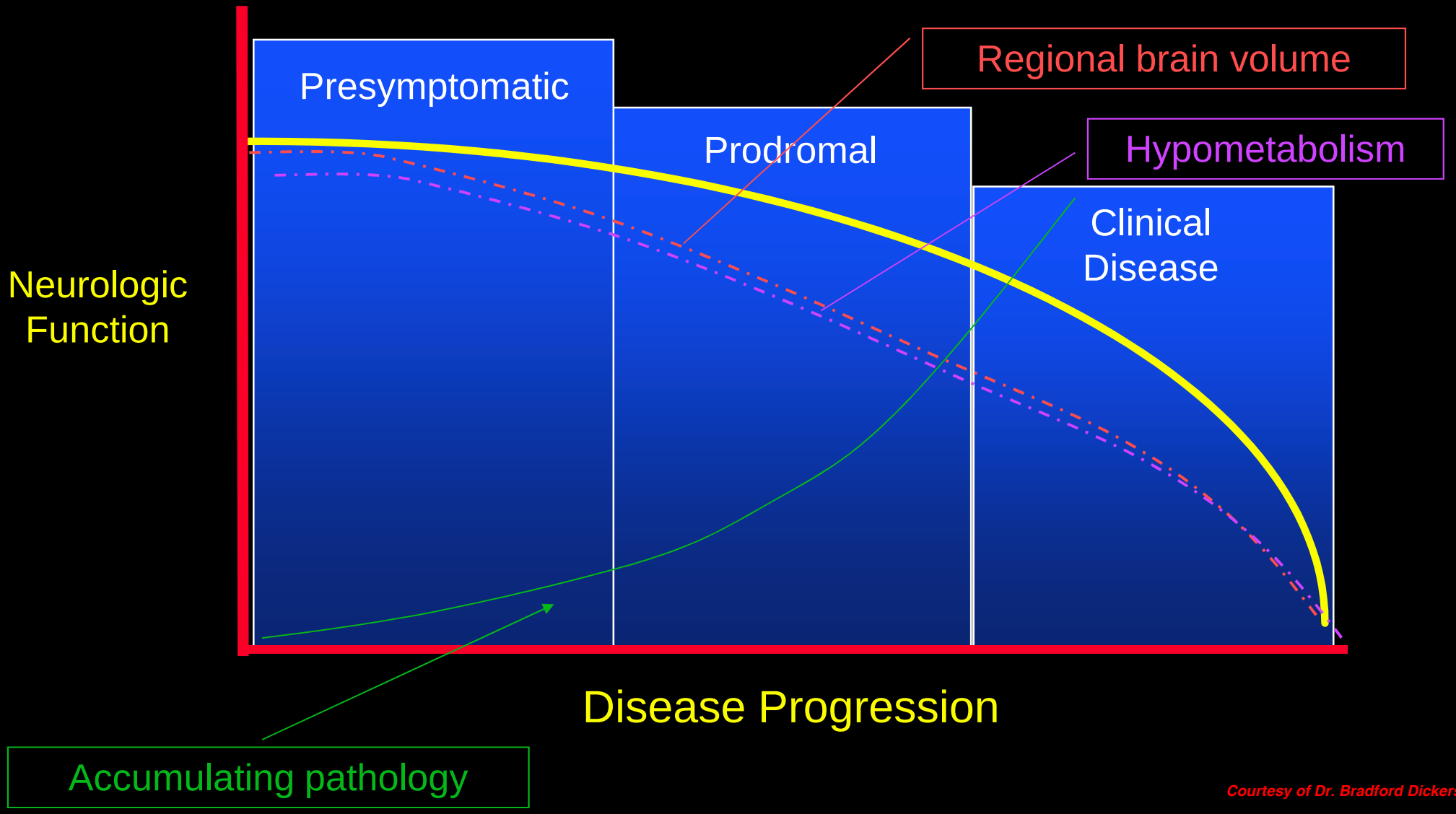

Courtesy of Dr. Bradford Dickerson

Progression of neurodegenerative diseases

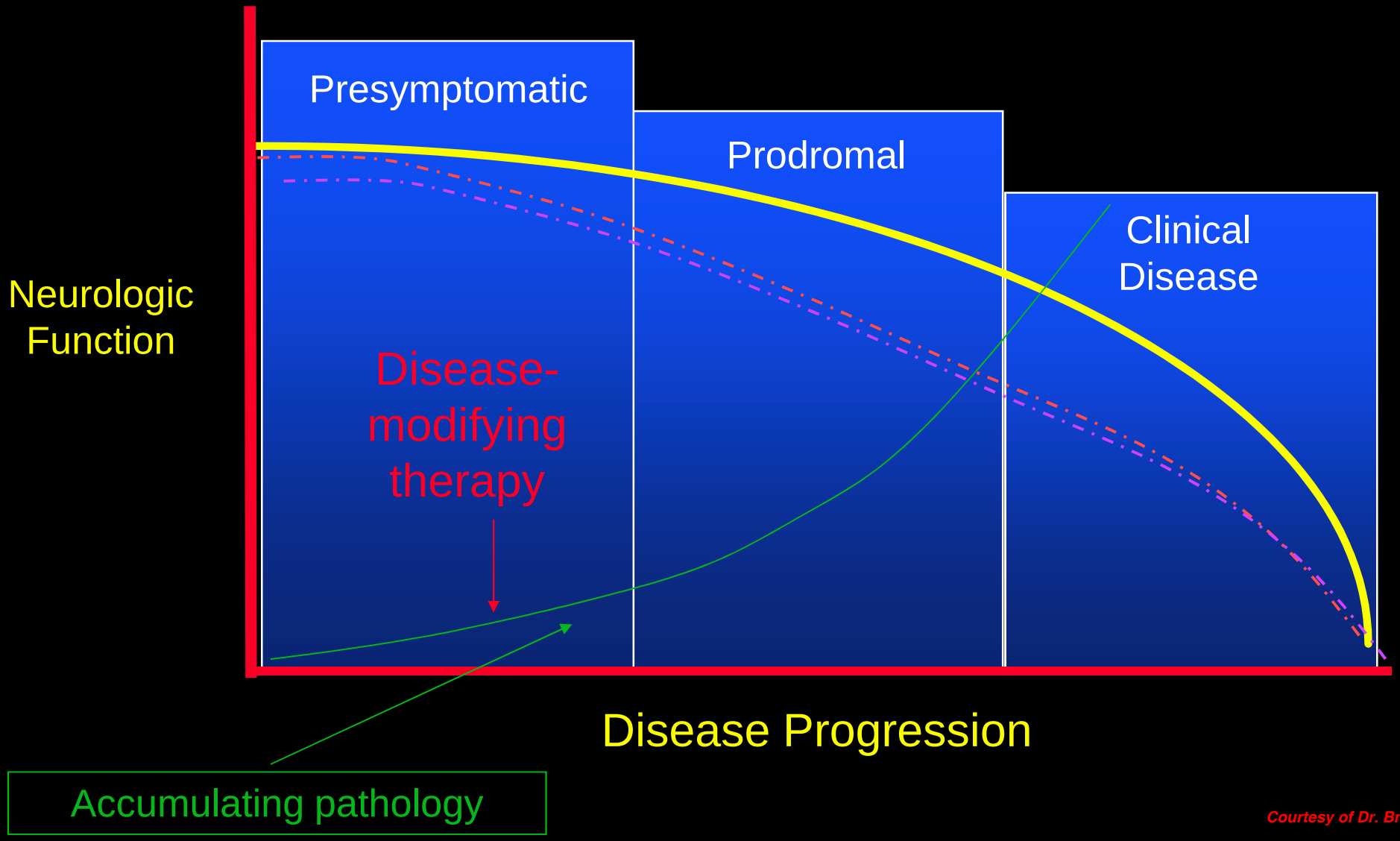

Courtesy of Dr. Bradford Dickerson

Progression of neurodegenerative diseases

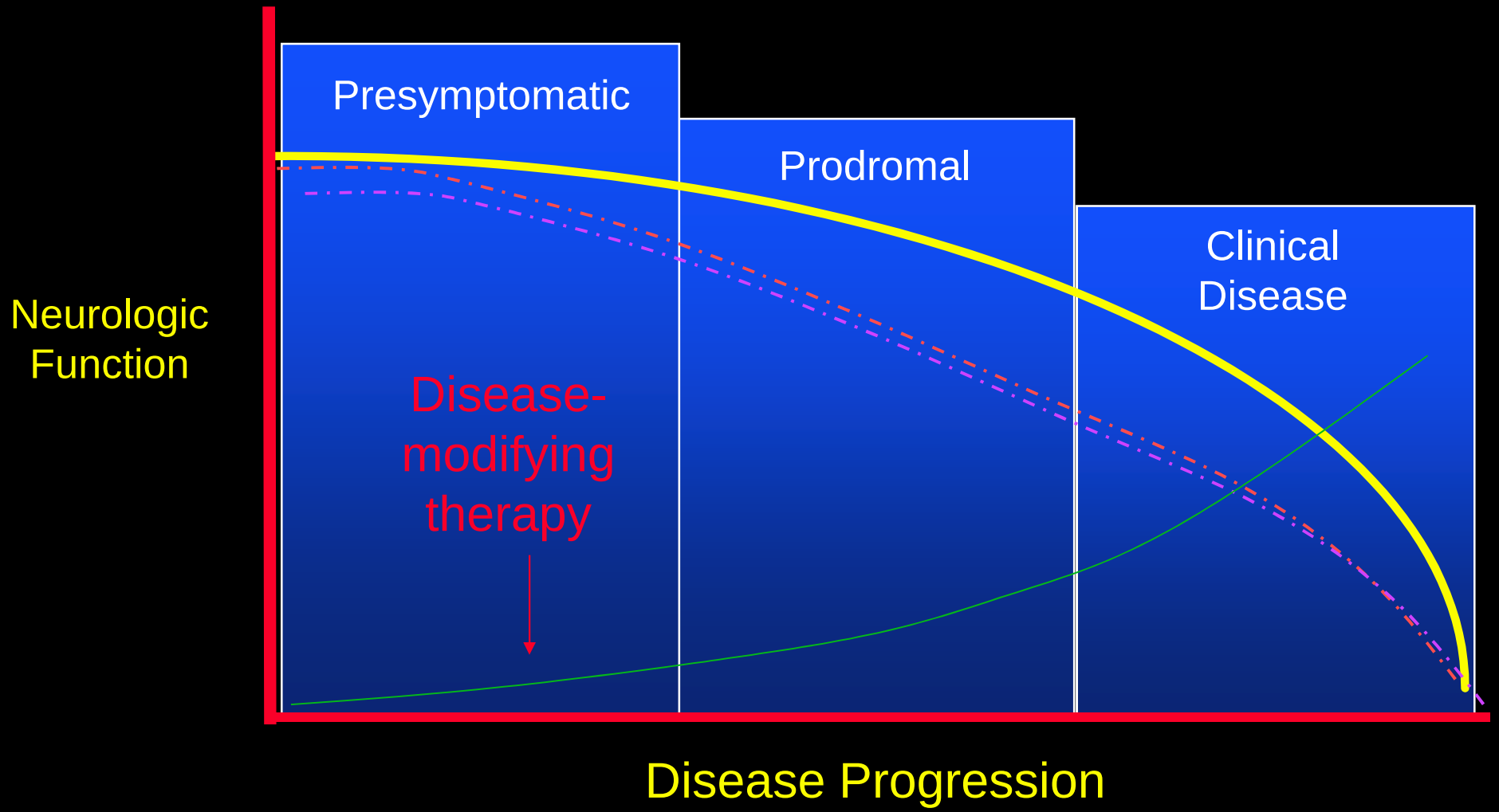

Courtesy of Dr. Bradford Dickerson

Progression of neurodegenerative diseases

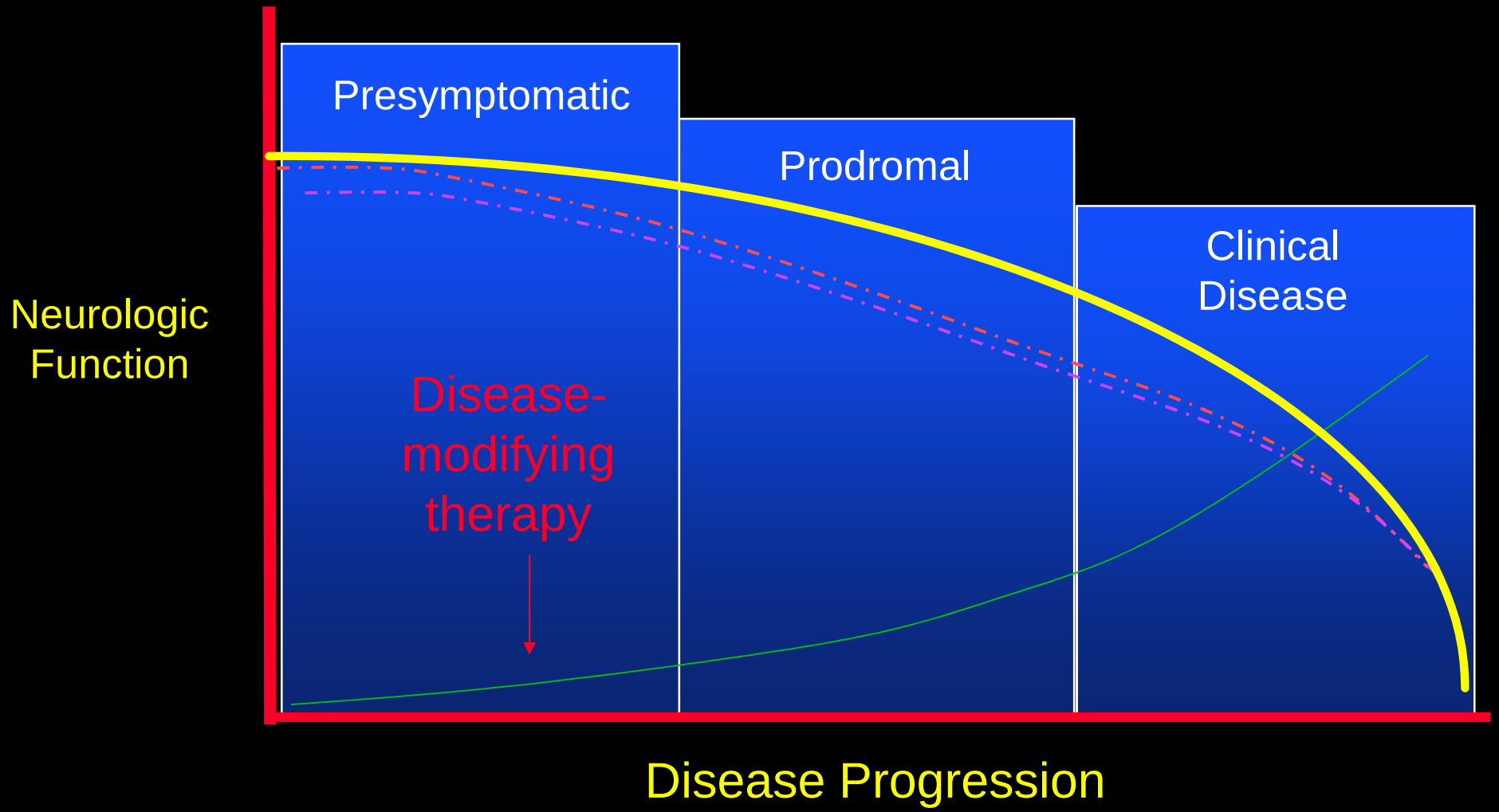

Courtesy of Dr. Bradford Dickerson

Progression of neurodegenerative diseases

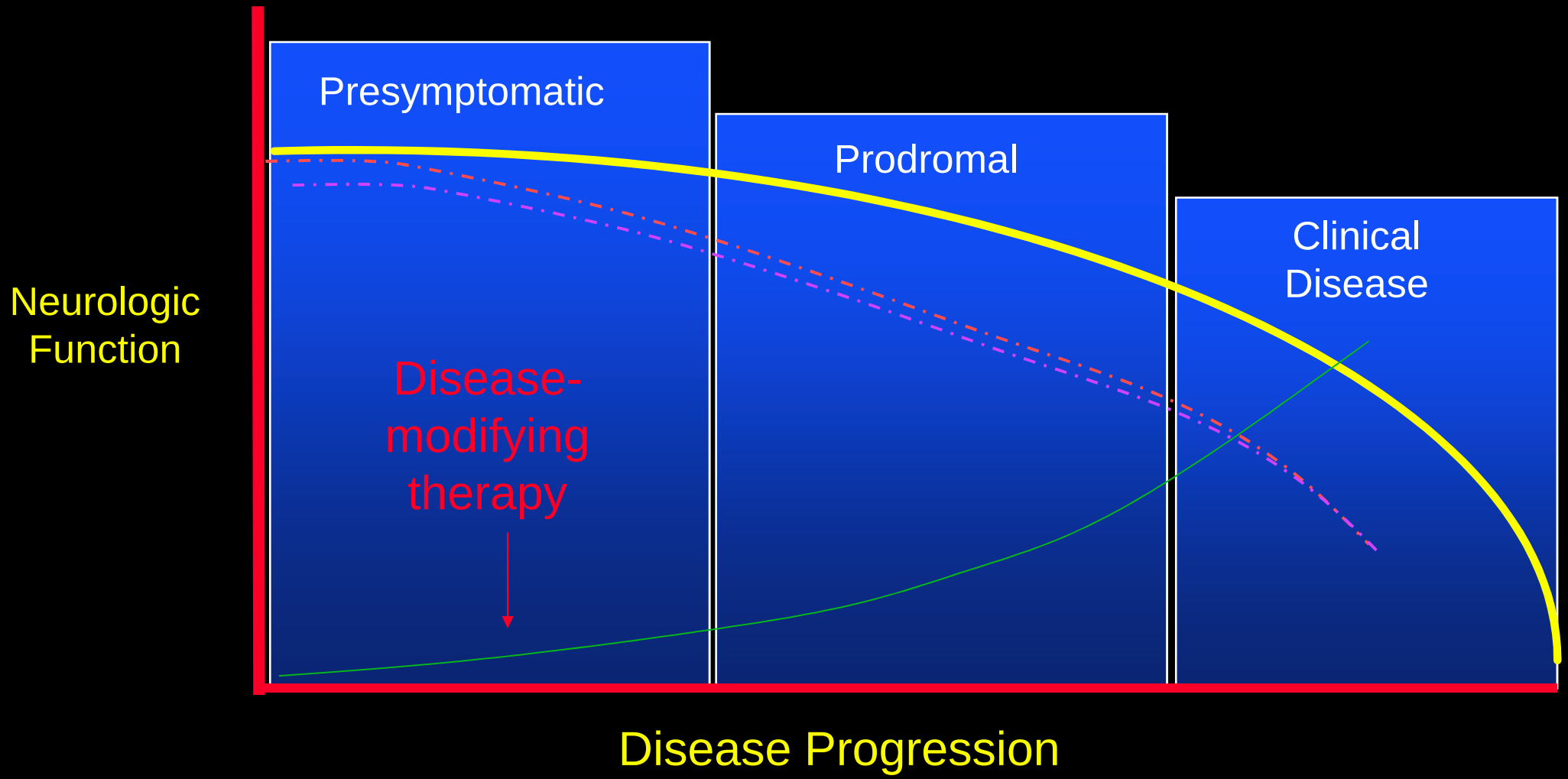

Courtesy of Dr. Bradford Dickerson

Imaging Research for Novel Diagnostics/therapeutics and Better Care

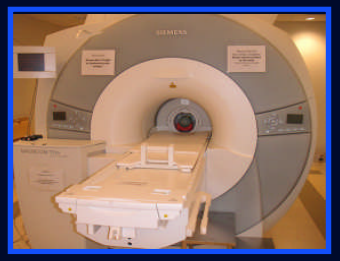

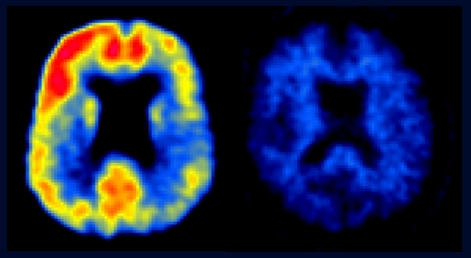

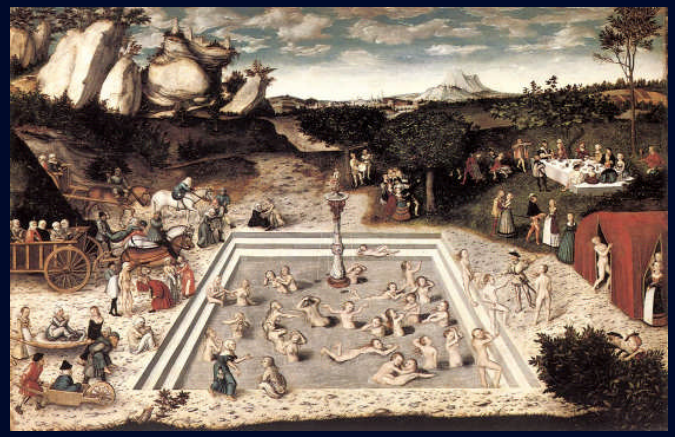

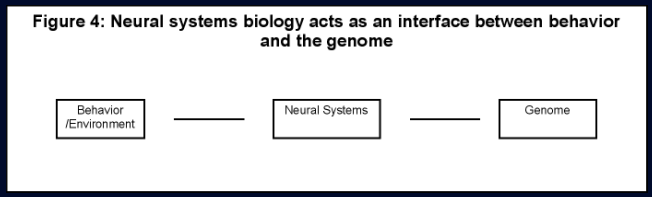

Automation and Databasing

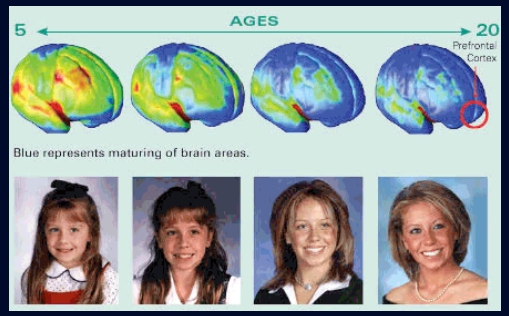

Translational (from bench to bedside)

Translational (from experimental animal to human)

THANK YOU!